

**VITOR JUSTE DOS SANTOS**

**IMPACTS OF LAND COVER CHANGES ON ENERGY FLOW AND THE WATER  
CYCLE IN THE BRAZILIAN SEMIARID REGION**

Thesis submitted to the Civil Engineering Program of the Universidade Federal de Viçosa in partial fulfillment of the requirements for the degree of *Doctor Scientiae*.

Adviser: Maria Lúcia Calijuri

Co-adviser: José Ivo Ribeiro Júnior

**VIÇOSA - MINAS GERAIS  
2021**

**Ficha catalográfica elaborada pela Biblioteca Central da Universidade  
Federal de Viçosa - Campus Viçosa**

T

S237i Santos, Vitor Juste dos, 1990-  
2021 Impactos das mudanças na cobertura do solo no fluxo de  
energia e no ciclo da água no semiárido brasileiro / Vitor Juste  
dos Santos. – Viçosa, MG, 2021.  
1 tese eletrônica (90 f.): il. (algumas color.).

Texto em inglês.

Orientador: Maria Lúcia Calijuri.

Tese (doutorado) - Universidade Federal de Viçosa,  
Departamento de Engenharia Civil, 2021.

Inclui bibliografia.

DOI: <https://doi.org/10.47328/ufvbbt.2021.276>

Modo de acesso: World Wide Web.

1. Mudanças climáticas - Regiões áridas - Brasil. 2. Secas.  
3. São Francisco, Rio. 4. Solo - Uso. I. Calijuri, Maria Lúcia,  
1955-. II. Universidade Federal de Viçosa. Departamento de  
Engenharia Civil. Programa de Pós-Graduação em Engenharia  
Civil. III. Título.

CDD 22. ed. 551.5253

Bibliotecário(a) responsável: Alice Regina Pinto CRB6 2523

**VITOR JUSTE DOS SANTOS**

**IMPACTS OF LAND COVER CHANGES ON ENERGY FLOW AND THE WATER  
CYCLE IN THE BRAZILIAN SEMIARID REGION**

Thesis submitted to the Civil Engineering  
Program of the Universidade Federal de  
Viçosa in partial fulfillment of the  
requirements for the degree of *Doctor  
Scientiae*.

APPROVED: September 30, 2021.

Assent:



---

Vitor Juste dos Santos

Author



---

Maria Lúcia Calijuri  
Adviser

*To my parents Ladio and Virginia;  
To my brothers Wagner and Vinícius;  
To my wife Letícia;  
To my daughter Cecilia;  
I dedicate.*

## **ACKNOWLEDGEMENTS**

To my parents, Ladio and Virgínia, for having dedicated their lives to my education and that of my siblings. Thanks for all your support and encouragement.

To Professor Maria Lúcia Calijuri for her guidance, both academic and professional. Thank you for your patience and encouragement for all these years.

To Professor José Ivo Ribeiro Júnior for his co-supervision. Thank you for contributing my research and academic background.

To the members of the board, for the contributions that certainly helped in the evolution and improvement of the research.

I would like to thank the friends at the SIGEOnPA Laboratory for the coexistence, companionship, exchange of knowledge and for making my walk lighter and more relaxed.

To Letícia, my wife, for all her support and patience throughout my academic training. With her support, everything was lighter and easier.

To my daughter Cecília, who hasn't even come to this world yet, but already fills me with joy.

To the funding agencies: FAPEMIG, CAPES and CNPq. This work was carried out with the support of the Coordination for the Improvement of Higher Education Personnel – Brazil (CAPES) – Financing Code 001.

*“Somewhere something amazing is waiting to be discovered “*

(Carl Sagan)

## ABSTRACT

SANTOS, Vitor Juste dos, D.Sc., Universidade Federal de Viçosa, September 2021. **Impacts of land cover changes on energy flow and the water cycle in the Brazilian Semiarid region.** Adviser: Maria Lúcia Calijuri. Co-adviser: José Ivo Ribeiro Júnior.

The São Francisco River is the most important water resource in the Northeast of Brazil, as it corresponds to 70% of the region's water availability, crossing the most populous semi-arid area on the planet. Its waters have multiple uses, for purposes of domestic consumption, irrigation, hydroelectric power generation, navigation, leisure, tourism, among others. Due to its significant strategic importance in the regional context, this river has undergone strong water stress over the last decade and, probably, this situation will continue, or even worsen, in the coming years. The reason for this is the strong demand for the withdrawal and consumption of its water, especially for the irrigation of agricultural crops. Such demand has increased even more, given the execution of the São Francisco River Integration Project (PISF), which already transposes part of its waters to the hydrographic basins of the Northern Northeast, territories that suffer from severe water shortages and have a high demand for water, both for domestic consumption and for carrying out productive activities. In addition, climate projections for the coming decades predict significant drops in rainfall volumes in the São Francisco River Basin, a situation that has already occurred between 2012 and 2018, and which resulted in a high decrease in flows, impacting various sectors, such as generation electricity and agricultural activities. Given this context, this research sought to assess the impacts of changes in land cover on the energy flow and on the hydrological cycle, especially for the estimation of precipitation and its effects on water availability in the Brazilian Semiarid Region. It was found that the São Francisco River Basin has undergone relevant changes in its land cover over the last four decades, with the deforestation of native vegetation in substitution for pastures and agricultural crops, and that these changes have significant relationships with reduction of water infiltration into the soil and subsurface runoff, in addition to the increase in surface runoff and evapotranspiration. Altogether, rainfall volumes have been decreasing since the 1990s, accompanied by reductions in the flow of the São Francisco River. The fall has been occurring more intensely since the last decade, in a strong event of drought

that hit the basin and the Brazilian Semiarid Region between 2012 and 2018. In this event, the long-term flows of the São Francisco were the lowest in the whole historical record, impacting the generation of hydroelectric energy in plants located in the Sub-Middle and Lower São Francisco hydrographic sub-regions, and enabling the intrusion of saline water from the Atlantic Ocean, reducing water quality kilometers inland from the continent in the São Francisco gutter.

Keywords: Climate Alterations. Drought. Land Use. São Francisco River.

## RESUMO

SANTOS, Vitor Juste dos, D.Sc., Universidade Federal de Viçosa, setembro de 2021. **Impactos das mudanças na cobertura do solo no fluxo de energia e no ciclo da água no Semiárido Brasileiro.** Orientador: Maria Lúcia Calijuri. Coorientador: José Ivo Ribeiro Júnior.

O rio São Francisco é o recurso hídrico mais importante do Nordeste do Brasil, pois corresponde a 70% da disponibilidade hídrica da região, atravessando a área semiárida mais populosa do planeta. Suas águas são de usos múltiplos, para fins de consumo doméstico, irrigação, geração de energia hidrelétrica, navegação, lazer, turismo, entre outros. Por ter uma importância estratégica expressiva no contexto regional, este rio passou por forte estresse hídrico ao longo da última década e, provavelmente, tal situação irá continuar, ou até mesmo se agravar, nos próximos anos. A razão disto é a forte demanda por retirada e consumo de suas águas, especialmente para a irrigação de culturas agrícolas. Tal demanda aumentou ainda mais, diante da execução do Projeto de Integração do Rio São Francisco (PISF), que já transpõe parte de suas águas para as bacias hidrográficas do Nordeste Setentrional, territórios que sofrem com forte escassez hídrica e possuem alta demanda por água, tanto para consumo doméstico quanto para exercer atividades produtivas. Além disso, as projeções climáticas para as próximas décadas preveem quedas expressivas nos volumes de chuvas na Bacia Hidrográfica do São Francisco, situação que já ocorreu entre 2012 e 2018, e que resultou em um alto decréscimo das vazões, impactando diversos setores, como a geração de energia elétrica e as atividades agrícolas. Diante deste contexto, a presente pesquisa buscou avaliar os impactos das mudanças na cobertura do solo no fluxo de energia e no ciclo hidrológico, especialmente para a estimativa da precipitação e seus efeitos na disponibilidade de água no Semiárido Brasileiro. Verificou-se que a Bacia Hidrográfica do Rio São Francisco passou por alterações relevantes de sua cobertura vegetal ao longo das últimas quatro décadas, com o desmatamento de vegetações nativas em substituição para as pastagens e culturas agrícolas, e que estas alterações tem significativas relações com a redução da infiltração de água no solo e no escoamento em subsuperfície, além do acréscimo do escoamento superficial e da evapotranspiração. Em conjunto, os volumes de chuvas vêm decrescendo desde a década de 1990, acompanhado das reduções das vazões do

rio São Francisco. Queda esta ocorrendo de forma mais intensa a partir da década passada, em um forte evento de seca que atingiu a bacia e o Semiárido Brasileiro entre 2012 e 2018. Neste evento, as vazões de longo prazo do São Francisco foram as mais baixas de todo o registro histórico, impactando a geração de energia hidrelétrica nas usinas localizadas nas sub-regiões hidrográficas do Submédio e Baixo São Francisco, e possibilitando a intrusão de água salina proveniente do oceano Atlântico, reduzindo a qualidade da água quilômetros adentro do continente na calha do São Francisco.

Palavras-chave: Alterações Climáticas. Seca. Rio São Francisco. Uso do Solo.

## LIST OF ILLUSTRATIONS

Figure 5.1 – Brazilian semiarid location .....	23
Figure 5.2 – Methodology Flowchart .....	25
Figure 5.3 – Performance of the different methods by NSE.....	32
Figure 5.4 – Performance of the different methods by R.....	33
Figure 5.5 – Performance of the different methods by RMSE .....	34
Figure 6.1 – Methodology Flowchart .....	53
Figure 6.2 – Study area location.....	54
Figure 6.3 – Trends in variables referring to energy flow and water cycle in SFB between January 1948 and December 2019.....	64
Figure 6.4 – Mann-Kendall, KPSS and Homogeneity tests (Pettitt and Buishand) for energy flow and water cycle variables in SFB between 1948 and 2019.....	66
Figure 6.5 – Changes in land use and land cover in SFB and its effects on the presence of tree and non-tree vegetation cover and bare soil.....	68
Figure 6.6 – Influence of rain dynamics and changes in land cover on the behavior of SFB flow rate in P1.....	71
Figure 6.7 – Influence of rain dynamics and changes in land cover on the behavior of SFB flow rate in P2.....	73
Figure 6.8 – Seasonal analysis of variables related to water cycle in the SFB.....	75
Figure 6.9 – Correlations between NDVI and water cycle variables in SFB. ....	77
Figure 6.10 – Correlations between average monthly flow rate with rainfall, surface and subsurface runoff data in SFB.....	79
Figure 6.11 – – Simplified water balance for the pre and post-1990s periods at SFB.....	80

## LIST OF TABLES

Table 5.1 – Database used in the research.....	24
Table 5.2 – Interpolation methods and characteristics .....	27
Table 5.3 – Geospatial rainfall and its characteristics .....	28
Table 5.4 – Statistics used in the assessment.....	30
Table 5.5 – Number of test stations, for each rain estimation method, according to the range of values of metrics used .....	35
Table 5.6 – Types of data used for rainfall estimates for each method .....	37
Table 6.1 – Database used .....	57
Table 6.2 – Trend (MK) range values and significance (p) analyze for energy flow variables in P1, between 1948 and 2019 .....	64
Table 6.3 – Trend (MK) range values and significance (p) analyze for energy flow variables in P2, between 1948 and 2019. ....	64
Table 6.4 – Absolute and relative variations of the variables related to the energy flow and water cycle in the SFB between 1948 and 2019. ....	64
Table 6.5 – Changes in tree and non-tree vegetable coverings and bare soil in the SFB .....	68
Table 6.6 – Changes in NDVI in SFB .....	68
Table 6.7 – Seasonal variation of water flow in SFB between 1951-1980 and 2001-2019 .....	75

## SUMMARY

1. PRESENTATION .....	14
2. INTRODUCTION.....	14
3. HYPOTHESES.....	16
4. GENERAL OBJECTIVE .....	16
4.1. Specific objectives.....	16
5. PAPER 1: RAINFALL ESTIMATION METHODS IN THE BRAZILIAN SEMIARID REGION: 30-YEAR EVALUATION ON A MONTHLY SCALE.....	17
5.1. Introduction .....	18
5.2. Study Area .....	20
5.3. Methodological Steps and Database.....	21
5.3.1. Database collection and standardization .....	23
5.3.2. Selection of training and test stations .....	24
5.3.3. Training data interpolation .....	24
5.3.4. Evaluation with test stations.....	27
5.3.5. Standardization of results .....	28
5.4. Results .....	28
5.5. Discussion.....	33
5.6. Conclusions.....	36
5.7. Acknowledgement.....	36
5.8. References.....	36
6. PAPER 2: LAND COVER CHANGES IMPLICATIONS IN ENERGY FLOW AND WATER CYCLE IN SÃO FRANCISCO BASIN, BRAZIL, OVER THE PAST SEVEN DECADES.....	46
6.1. Introduction.....	47
6.2. Materials and Methods .....	50
6.2.1. Study Area.....	50
6.2.2. Variables Definition.....	54
6.2.3. Statistical Analysis.....	57
6.2.3.1. Statistical analysis on variables related to energy and water cycles .....	57
6.2.3.2. Statistical analysis on variables related to LULC and MEaSUREs .....	58
6.2.3.3. Statistical analysis on variables related to São Francisco river flow rate.....	59
6.3. Results and Discussion .....	59
6.3.1. Spatiotemporal analysis of energy flow, water cycle and LULC variables.....	60
6.3.2. Impacts and changes in São Francisco river' flow rate dynamics .....	67

6.4. Conclusions.....	79
6.5. Acknowledgments, Samples, and Data.....	79
6.6. References .....	80
7. GENERAL CONCLUSIONS .....	88
8. REFERENCES .....	89

## **1. PRESENTATION**

This document is organized in the following structure: introduction (2); research hypotheses (3); objectives (general and specific) (4); presentation of articles one (5) and two (6), in addition to the general conclusions (7). Chapter five deals with an article that has already been published and chapter six is in the process of being evaluated in a journal. The Digital Object Identifier System (DOI) for each one was made available along with the footnote identified in the title of each chapter for easy consultation.

In the introduction (chapter 2) a brief presentation of the topics covered in the research and the areas of study was made, and the motivations for carrying out this thesis were also addressed, which guided the composition of the research hypothesis (chapter 3) and the objectives, general and specific (chapter 4).

In paper one (chapter 5) the performance of different methods for estimating the spatiotemporal dynamics of rainfall in the Brazilian Semiarid Region was evaluated. In the second (chapter 6), the energy flow and the hydrological cycle of the São Francisco basin were investigated in order to verify changes in them and whether there is a correlation with anthropic interventions in land use and land cover. Finally, a general conclusion was made (chapter 7), presenting the main results obtained by this research.

## **2. INTRODUCTION**

Researches which have the Northeast region of Brazil, the Brazilian Semiarid and the São Francisco basin as study areas, either together or separately, are recurrent in the scientific literature, due to the national importance that these territories have in terms socioeconomic, ecological, productive activities and natural resources. One of these resources, perhaps the most prominent one today, whether in Brazil or in the world, is water (BRITO et al., 2018; DE JONG et al., 2018; MARENGO et al., 2020; MARENGO; TORRES; ALVES, 2017; ROSSATO et al., 2017; SILVA et al., 2021a).

The three territories mentioned above have large spatiotemporal variations in the distribution of their water resources, which creates conflicts over their uses and, thus, makes planning and management of water essential for the quality of life of

populations and sustainable economic development. Therefore, the motivation for the study of water, in the aforementioned areas, attracted the attention of researchers in various scientific fields.

In the area of water resources, especially involving Geographic Information Systems (GIS) and water management, research mainly covers some topics, such as the development of methodologies for identifying and measuring water deficits and droughts (ALVALÁ et al., 2019; BARBOSA ; LAKSHMI KUMAR, 2016; BRITO et al., 2018; DANTAS; SILVA; SANTOS, 2020; MARENGO; BERNASCONI, 2015; MARENGO; TORRES; ALVES, 2017; TOMASELLA et al., 2018), or assessments of hydrological and climatic data to know the advantages and disadvantages of their uses (DA SILVA et al., 2020; SANTOS et al., 2021), in addition to the use of hydrological models that help identify changes in the hydrological cycle of river basins from anthropogenic interventions in the natural environment and ongoing climate change (CREECH et al., 2015; DE JONG et al., 2018; FREITAS, 2021; SILVA et al., 2021a). Other important studies, integrated into the human sciences, are the impact assessments caused by extreme events, whether due to excess or lack of water, in societies. In these, it is usual to investigate socioeconomic impacts, relating events to their consequences, such as losses in productive activities, unemployment, reduced quality of life, health impacts, among others (LINDOSO et al., 2014; LIRA AZEVÊDO et al., 2017; SILVA et al., 2021b).

Related topics were addressed in this research, such as the quality of databases, especially precipitation, human interventions in the environment, which interfere in the dynamics of energy flows and the planet's hydrological cycle, in addition to ongoing climate change, subject of paramount importance in research related to water, especially in quantitative terms.

All these themes were addressed having as study areas the Brazilian Semiarid and the São Francisco basin, as they are territories that historically coexist with conflicts over the use of water due to the spatio-temporal variations in their presence, whether in quantity or quality. Simultaneously, the choice of research areas came from concerns about the aggravation of such conflicts, which are intensified by the growth of water demands for anthropic uses, together with the climate changes already underway, which have resulted in a decrease in rainfall volumes, an increase in temperature and the potential for evapotranspiration, factors that interfere in the

hydrological cycle and in the water balance of river basins, estimating, even the end of the 21st century, the worsening of the water deficit.

### **3. HYPOTHESES**

From the context presented, this research has the following hypotheses:

- The best performance in estimating rainfall volumes for geospatial products, in addition to the methodological approach applied, is the incorporation of different information and data from different forms of data acquisition (in situ and remote);
- Changes in land use and land cover in the São Francisco basin have a direct influence on the energy balance and on the hydrological cycle of the watershed.

### **4. GENERAL OBJECTIVE**

Evaluate the impacts of land cover changes on the energy flow and hydrological cycle, especially for the estimation of precipitation and its effects on water availability in the Brazilian semiarid region.

#### **4.1. Specific objectives**

- Evaluate seven rain estimation methods, with different approaches, with the aid of statistical analysis of 30 years of monthly data, to verify their performance in the estimation of the spatiotemporal behavior of the rain against the information measured in situ;
- Identify and measure changes in energy flow and water cycle in the São Francisco basin in the second half of the 20th century and in the first two decades of the 21st century, and verify the implications of changes in land cover caused by human activities in the last four decades.

## 5. PAPER 1: RAINFALL ESTIMATION METHODS IN THE BRAZILIAN SEMIARID REGION: 30-YEAR EVALUATION ON A MONTHLY SCALE<sup>1</sup>

**Abstract:** Studies about evaluations of different rainfall estimation methods are important as they are usually applied in works related to water resources availability, public supply, watering, animal water supply, hydroelectric power generation, drought episodes' evaluation, among others. Studies that cover the entire area of the Brazilian semiarid within this scope are still scarce. In this context, the objective of this paper was to evaluate seven rain estimation methods, from different approaches, with the aid of statistical analysis. The focus was on the long term, using 30 years of data in monthly scale, in order to verify the methods performance in estimating the spatiotemporal behaviour of rainfall compared to data measured in situ, coming from rainfall and meteorological stations. The evaluation process was based on the random selection of training and testing stations, with the first being used to interpolate rainfall data using different methods, and the latter used to evaluate these estimates with the aid of statistical analysis. Finally, the results were standardized, interpreted and discussed. Of all the estimation methods evaluated, CHIRPS obtained the best performance when compared to field stations data used as test. From the results obtained, there is evidence that the best performance is due to the incorporation of several distinct data sources derived from in situ stations, geostationary satellite infrared sensor estimates and physiographic predictors. This information is not fully present in other evaluated methods. The worst estimation performances were in the eastern side of the Brazilian semiarid, an area that receives moisture from the Atlantic Ocean and has significant topographic variations, due to the set of the complex relief mountains present in the northeast coast of Brazil.

**Keywords:** CHELSA, CHIRPS, interpolation methods, complex terrain, PERSIANN, remote sensing.

---

<sup>1</sup> Published article:

dos Santos VJ, Calijuri ML, Ribeiro Júnior JI, de Assis LC. Rainfall estimation methods in the Brazilian semiarid region: 30-year evaluation on a monthly scale. *Int J Climatol*. 2021;41 (Suppl. 1):E752–E767. <https://doi.org/10.1002/joc.6723>.

## 5.1. Introduction

Several countries have difficulties in structuring rain stations networks that cover the whole territory and generate rainfall datasets that do not present significant failures in historical records, which hinders and undermines researches that needs extensive and consistent databases to study the spatial and time precipitation behaviour (Karaseva et al., 2012; Prasetia et al., 2013; Guofeng et al., 2017; Kumar et al., 2017; Duan et al., 2019). Even nations that have high station density in their territories, it is impossible to cover 100% of their limits.

To generate datasets that cover the entire territory boundaries, interpolation methods are applied. To estimate values of climate variables, such as precipitation, in areas where there is no monitoring, data interpolation is performed. Interpolation methods are based on the principle of autocorrelation or spatial dependence, which measure the relationship/dependence degree between near and far objects (Childs, 2004).

There are two categories of interpolation methods: deterministic and geostatistical. Deterministic methods create surfaces based on measured points or mathematical formulas. Geostatistical methods based on statistics and are used for advanced prediction surface modelling, which also includes some certainty measures or accuracy of predictions (Childs, 2004; Krivoruchko, 2012).

In addition to interpolation methods, to overcome the barriers of lack of rainfall data, several researches are using geospatial products from remote sensing or derivatives from algorithmic that help estimating rainfall volumes based on global circulation climate models. Some of those products are TRMM (Kumar et al., 2017; Duan et al., 2019), CHIRPS (Quesada-Montano et al., 2018; Zittis, 2018), WorldClim (Alves et al., 2013; Lyra et al., 2018), CRU (Li et al., 2013; Klutse et al., 2016), GPCC (Schneider et al., 2014; Sarmadi and Shokoohi, 2015), PRISM (Di Vittorio and Miller, 2013; Bernhardt and Carleton, 2018), CHELSA (Beck et al., 2018; Fang et al., 2018), PERSIANN (Ghajarnia et al., 2015; Bhardwaj et al., 2017; Katiraie-Boroujerdy et al., 2017), among others.

The quality of rainfall data has great importance for several studies, including those focusing on water-related issues such as public water supply (Rocha and Soares, 2015; Santos and Farias, 2017), watering (Araújo et al., 2004; Gondim et al., 2018), animal water supply (Lira et al., 2017), hydroelectric power generation (Jong et al., 2018), in addition to those that focus on drought episodes

analysis (de Azevedo et al., 2018; Mariano et al., 2018). In Brazil, such themes are exhaustively addressed within the limits of the Brazilian semi-arid, a region, as highlighted by the Northeast Development Superintendence (SUDENE, 2017), that has conflicts over water use due to its scarcity and densely populated.

Few studies were concerned with the evaluation of geospatial products and the results of interpolation methods for rainfall estimates throughout the Brazilian semi-arid. Research that has done so, efforts are focused on specific geospatial products such as CHIRPS (Paredes-Trejo et al., 2017; Costa et al., 2019) and TRMM (Franchito et al., 2009), besides another who evaluated the CHIRPS and the Ordinary kriging method (Santos et al., 2019). In addition, efforts were focused on specific areas or localities within the semi-arid, by assessing, in isolated way, sometimes some geospatial products (Soares et al., 2016; Anjos et al., 2017), sometimes interpolation methods (Barbalho et al., 2014; de Miranda et al., 2017; da Silva et al., 2019).

Of these few studies, Paredes-Trejo et al. (2017), evaluating the CHIRPS for the northeast region of Brazil, showed that estimates coming from the orbital images have a good overall correlation ( $r = 0.94$ ), but tend to underestimate the low rainfall values and overestimate the high ones ( $>100 \text{ mm-month}^{-1}$ ). They found that CHIRPS has better ability to estimate rainfall during rainy seasons and has poor performance to detect rain during drought seasons in the driest areas of the northeast, especially in the Sertão, which is the core area of the Brazilian semi-arid. They also concluded that the performance of CHIRPS depends on the characteristics of the terrain. In leeward areas, where there is less rainfall, has lower accuracy. Already near the coast, in windward areas where more rain occurs, has higher accuracy. Therefore, it has greater potential for assessment of drought events in windward, wetter areas, and less potential leeward, drier areas.

On this subject, due to the need to better understanding the spatial and temporal information generated by rain estimation methods, derived from different techniques, we proposed a different approach in relation to the mentioned studies. The evaluation covered the entire Brazilian semi-arid, considering geospatial products with different spatial resolutions and elaborated from differentiated methods, as well as interpolation methods from different categories. Thus, the objective was to evaluate seven rainfall estimation methods, with different approaches, with the aid of statistical analysis. The focus is on the long term, using

30 years of data in monthly scale, aiming to verify the performance of the methods in estimating the spatiotemporal behaviour of rainfall in face of information measured in situ.

## 5.2. Study Area

The study area is the current Brazilian Semiarid Official Limits (BSOL, unofficial acronym; Figure 5.1a), located between the latitudinal coordinates 2°41'12" S and 17°59'34" S and longitudinal coordinates 46°38'42" W and 35°18'38" W. It was updated in 2017 by the Northeast Development Superintendence, which belongs to the Ministry of Regional Development. It has approximately 28 million inhabitants living in 1,262 municipalities, with an area of 1,128,697 km<sup>2</sup> (SUDENE, 2017).

BSOL covers areas with intense solar radiation and low cloudiness and relative humidity (Tomasella et al., 2018). High temperatures (Figure 5.1d) make evapotranspiration high potential, in addition to low precipitation volumes (Figure 5.1d), which on average can reach values lower than 800 mm-year<sup>-1</sup>, especially in the core area (area where average annual rainfall is lower than 800 mm and average temperatures above 26°C; Conti, 2005). These characteristics make most of the official boundary classified in climatic terms as semiarid (Alvares et al., 2013; Vieira et al., 2015), according to the methodology that estimates the Aridity Index defined by the United Nations Environment and Food and Agriculture Organization of the United Nations (FAO, 2009).

Although the study area topography does not reach expressive altimetric values (Figure 5.1h), the relief significantly influences rain distribution, temperature discrepancies and winds directions and velocities (Figure 5.1 – f, g), therefore influencing the aridity levels throughout the BSOL. The orographic rain, caused by altimetric variations and irregularity of relief, results in wetter windward areas and more arid leeward areas, consolidating the topoclimatic characteristics of the study area (Conti, 2005).

The relief influence on the moisture distribution consequently affects the distribution of plant species (Figure 5.1e), of different sizes and vitalities, from Caatinga (smaller vegetation, from undergrowth to shrubs) in the core area of BSOL, to the transition areas to Cerrado and Atlantic Forest (larger vegetation, from shrubs to trees; Figure 5.1a) (Cunha et al., 2015; Barbosa and Lakshmi

Kumar, 2016; Tomasella et al., 2018).

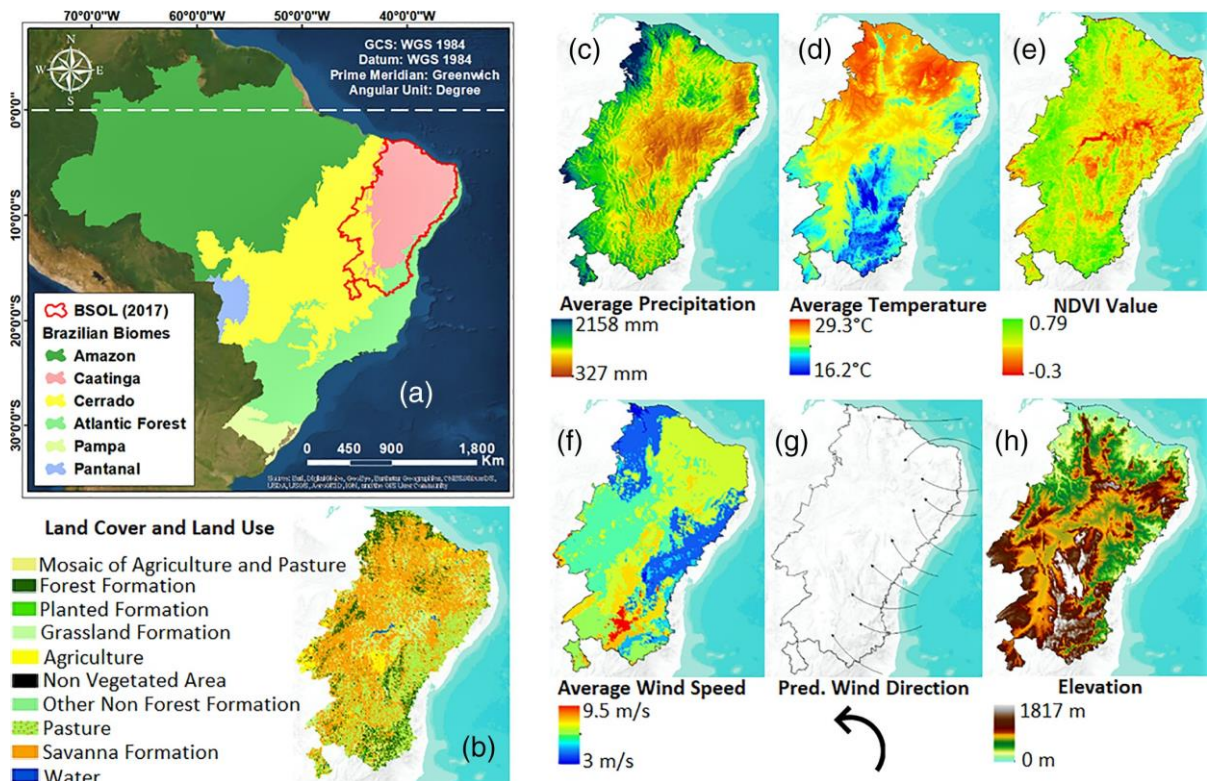


**Figure 5.1** - (a) Brazilian semiarid location (*source*: <http://mapas.mma.gov.br/i3geo/datadownload.htm> and <http://www.sudene.gov.br/delimitacao-do-semiarido>); (b) 2017 land use/land cover (*source*: [https://mapbiomas.org/downloads\\_colecoes](https://mapbiomas.org/downloads_colecoes)); (c) average annual rainfall between 1979 and 2013 (*source*: <http://chelsa-climate.org/downloads/>); (d) annual average temperature between 1979 and 2013 (*source*: <http://chelsa-climate.org/downloads/>); (e) NDVI average values between 1981 and 2014 (*source*: <https://e4ftl01.cr.usgs.gov/MEASURES/VIP30.004/>); (f) annual average wind speed (*source*: [http://www.cresesb.cepel.br/index.php?section=atlas\\_eolico](http://www.cresesb.cepel.br/index.php?section=atlas_eolico)); (g) predominant wind direction (*source*: [http://www.cresesb.cepel.br/index.php?section=atlas\\_eolico](http://www.cresesb.cepel.br/index.php?section=atlas_eolico)); (h) digital elevation model (*source*: <https://earthexplorer.usgs.gov/>)

In this physical-natural context, the predominant anthropic activities are plant extractivism and agriculture (Figure 5.1b), which are often exercised without proper land management. All these factors influence in land degradation and result in processes already occurring such as desertification (Marengo and Bernasconi, 2015; Vieira et al., 2015; Tomasella et al., 2018).

### 5.3. Methodological Steps and Database

Table 5.1 shows the database used in this research.

The methodology was divided into five steps (Figure 5.2): (a) collection and standardization of monthly rainfall data from January 1983 to December 2013 from different sources; (b) random selection of rainfall and meteorological stations for training and testing for further data evaluation; (c) performing interpolations using

different methods with the selected training stations; (d) interpolation results and geospatial products evaluation using specific statistical calculations, comparing with data from test stations; and (e) finally, standardization, interpretation and discussion of the results.

**Table 5.1** - Database used in the research

Data	Source	Description	References
Rainfall	INMET	Monthly data from January 1983 to December 2013 (360 months) from 102 meteorological stations located inside and around the study area	National Institute of meteorology <a href="http://www.inmet.gov.br/portal/">http://www.inmet.gov.br/portal/</a>
	ANA	Monthly data from January 1983 to December 2013 (360 months) from 458 rainfall stations located inside and around the study area	National water agency <a href="http://www.snirh.gov.br/hidroweb/">http://www.snirh.gov.br/hidroweb/</a>
	CHELSA	Monthly data from January 1983 to December 2013 (360 months), represented by 360 images with spatial resolution of 0.008°	Chelsa: Climatologies at high resolution for the earth's land surface <a href="http://chelsa-climate.org/">http://chelsa-climate.org/</a>
	CHIRPS	Monthly data from January 1983 to December 2013 (360 months), represented by 360 images with spatial resolution of 0.005°	Chirps: Rainfall estimates from rain gauge and satellite observations <a href="https://www.chc.ucsb.edu/data/chirps/">https://www.chc.ucsb.edu/data/chirps/</a>
	PERSIANN-CDR	Monthly data from January 1983 to December 2013 (360 months), represented by 360 images with spatial resolution of 0.25°	Persiann: Precipitation estimation from remotely sensed information using artificial neural networks <a href="https://chrsdata.eng.uci.edu/">https://chrsdata.eng.uci.edu/</a>

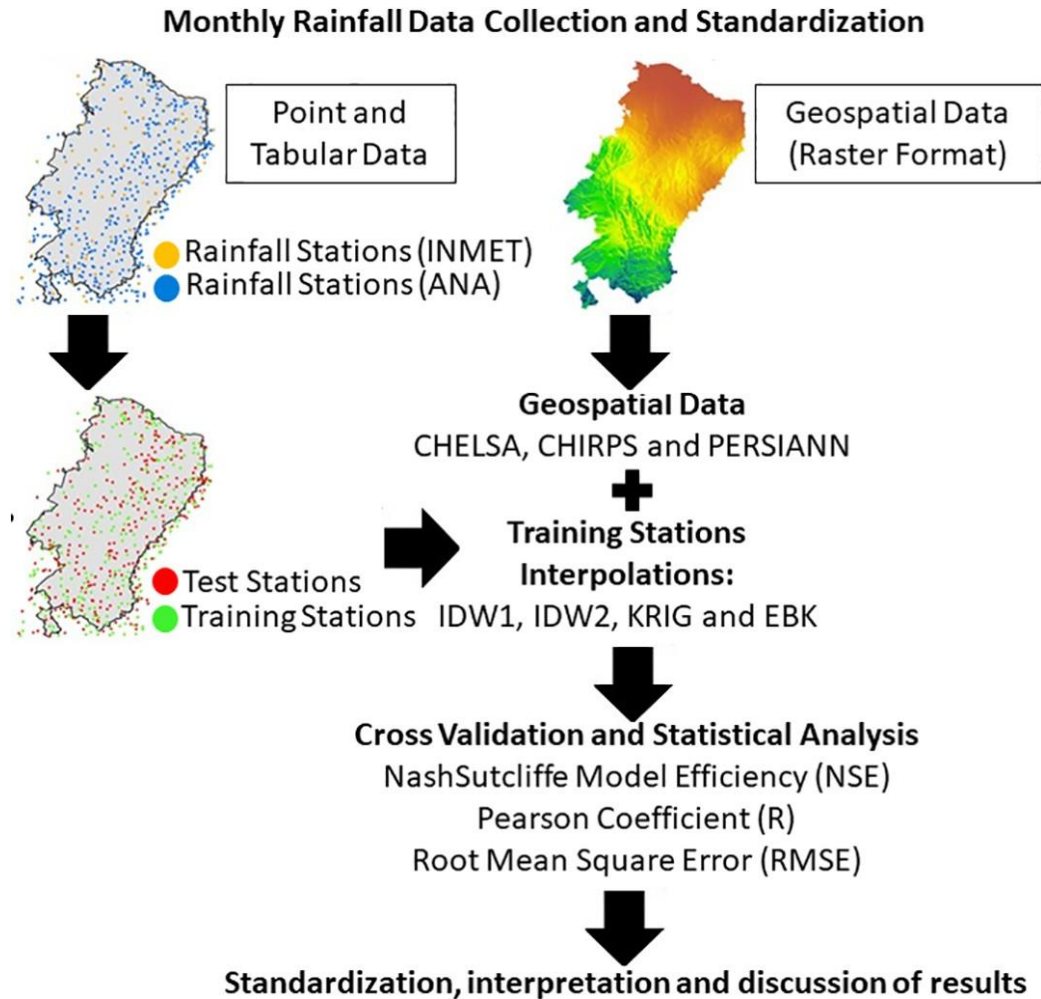


**Figure 5.2 – Methodology flowchart**

### 5.3.1. Database collection and standardization

The collected data containing information regarding rain volumes (mm), in monthly scale, between January 1983 and December 2013, from five distinct sources. Data from ANA and INMET, federal agencies, are tabulated data (CSV file formats) measured at meteorological or rainfall stations, thus come from punctual spatial distributions. The ones from CHELSA, CHIRPS and PERSIANN-CDR are raster data (files in GeoTiff format), consequently, from continuous spatial distributions.

The tabulated data were manipulated in Geographic Information System software using latitude and longitude information, in UTM format, present in the tables, allowing the spatial visualization of the stations inside and around the BSOL. The raster data have information of rain volumes for all continents, and for this study, the files were delimited as far as the stations are distributed.

The choice of these three geospatial products (raster data) was based on

the following premises: (a) ease of access and obtaining; (b) consistency in temporal frequency (monthly); (c) data with different spatial resolutions; (d) data estimated from different methodologies; (e) adherence and/or diffusion of use by the scientific community, from the most (CHIRPS and PERSIANN) to the least (CHELSA) frequent.

The tabulated data were spatialized from different interpolation methods. Four methods were used to estimate rainfall volumes, seeking to verify the performance of these regular interpolations in relation to the geospatial products mentioned above. The methods for preparing the three geospatial products will be detailed below.

To interpolation methods used in this study, no other variables were added, using only the location of the training stations and the rainfall volume data contained in them to estimate precipitation values for areas without information. The only products containing additional variables to make estimates were CHELSA and CHIRPS, such as information from digital terrain model and global climate circulation model (Funk et al., 2015; Karger et al., 2017).

### **5.3.2. Selection of training and test stations**

The original data set, the 560 stations selected for the study, were divided into two subsets, the training and the test sets. The first one was to model the spatial structure and produce a continuous surface, with spatial resolution of  $0.05^\circ$ , containing information of rain volumes from the interpolation methods. The second one was used to evaluate rain estimative, comparing the data measured in situ with those estimated by distinct methods. From those stations, 280 were selected for training and 280 for testing (50–50%). The selection was random with support of geoprocessing tools.

### **5.3.3. Training data interpolation**

The interpolation methods applied were: Empirical Bayesian Kriging (EBK), Ordinary Kriging (KRIG) and Inverse Distance Weighted (IDW). The training stations data were used. Table 5.2 describes precisely each method.

Two methods were used for Kriging, Ordinary and Bayesian. In the first one, the spherical function was chosen to fit the empirical semivariogram, as it is one of

the most used in climate variables interpolation (de Borges et al., 2016) and the one that showed the smallest estimation errors. The second is an interpolation method that explains the error in estimating the underlying semivariogram by repeated simulations. Unlike other kriging methods (which use weighted least squares), semivariogram parameters in EBK are estimated using restricted maximum likelihood (Krivoruchko, 2012).

**Table 5.2** – Interpolation methods and characteristics

Method	Characteristics	References
EBK	Geostatistical procedure that generates an estimated surface from a scattered set of points with Z values. It assumes that the distance or direction between the sample points reflects a spatial correlation that can be used to explain surface variation. Automates the most difficult aspects of building a valid kriging model. Automatically calculates parameters to receive accurate results and does not underestimate prediction standard errors by taking into accounting the uncertainties of estimates made by semivariograms	Krivoruchko (2012)
KRIG	Geostatistical procedure that generates an estimated surface from a scattered set of points with Z values. It assumes that the distance or direction between the sample points reflects a spatial correlation that can be used to explain surface variation. Unlike EBK, it is necessary to know the spatial behaviour of the phenomenon before selecting the best estimation method, because the semivariogram, calculated by Ordinary Kriging using known data, is used to make estimates in unknown locations, assuming it is true, not taking into account uncertainties in semivariogram estimates and underestimating standard errors	Krivoruchko (2012)
IDW	Deterministic interpolation that defines cell values using a linearly weighted combination of a set of sample points. This method assumes that the variable being mapped decreases in influence with the distance from its sampled location	Childs (2004)

IDW, a widely used method for interpolation of climate data, was applied using powers 1 and 2 (IDW1 and IDW2, respectively). The powers are inversely proportional to distance (between measured point data and the predicted location) increasing to the power value (p). As a result, according to distance increases, the weights decrease. The rate at which weights decrease depends on p value. If  $p = 0$ , there is no decrease with distance and, as each weight is the same, the prediction will be the average of all data values in the vicinity. According to p value increasing, the weights for distant points decrease rapidly. If the p value is too high, only the immediate surrounding points will influence the prediction.

Regarding the data from CHELSA, CHIRPS and PERSIANN-CDR, it was not necessary to apply the interpolation methods, since they are already spatially continuous data. Table 5.3 shows the description of each source aforementioned.

**Table 5.3** – Geospatial rainfall and its characteristics

Method	Characteristics	References
CHELSEA	Set of rainfall data that have estimates for all continents, generated from an algorithm (model output statistics) using data provided from the global climate circulation model reanalysis called European Center for Medium- Range Weather Forecast (ERA-Interim) together with interpolated data from meteorological stations around the world. Incorporated to rainfall information are orographic predictors as altitude, slope, and relief exposure that are considered to estimate precipitation volumes (orographic rainfall).	Karger et al. (2017) and (2018)
CHIRPS	Rainfall dataset estimated from three types of information: (a) monthly precipitation climate from CHPclim (climate hazard group precipitation climatology); (b) observations of thermal infrared sensor from Tropical Rainfall Measurement Mission (TRMM) geostationary satellite, specifically from product 3B42, from NOAA Climate Prediction Atmospheric Model; (c) in situ measurements of rainfall volumes from various stations, derived from national and regional meteorological services	Funk et al. (2015)
PERSIANN-CDR	An operating system that uses neural network function classification/ approximation procedures to calculate precipitation estimates of images from infrared longwave bands and visible colours provided by geostationary satellites. An adaptive training feature makes it easy to update network parameters whenever independent precipitation estimates are available. Does not use information from field stations	<a href="https://chrsdata.eng.uci.edu/">https://chrsdata.eng.uci.edu/</a>

CHIRPS uses different sources of information to estimate rainfall volumes, such as CHPclim, which is the monthly climatology for quasi-global rainfall, with a resolution of 0.05°. It is a raster product created using geospatial modelling based on moving window regressions and IDW interpolation method. This approach combines satellite data, physiographic indicators data contained in raster files and in situ weather conditions (meteorological stations) (Funk et al., 2015).

So far, CHELSA products are similarly generated using data from the ERA-Interim global climate circulation model in conjunction with interpolated data (Spline method) from meteorological stations around the world. It also incorporates information from orographic predictors, such as, altitude, slope, and exposure face of the relief to estimate precipitation values (orographic rain), producing raster data with a resolution of 0.008° (Karger et al., 2017).

However, CHIRPS has adding information from the thermal infrared sensor from the TRMM geostationary satellite. Although global climate information

generation combining field station observations and physiographic predictors such as latitude, longitude, elevation and slope are important for estimating from these products to generate data close to those observed in situ, reasonably dense station networks are required which is not the reality of many countries, especially developing ones. The relationship between physiographic variables and target climate variables, such as precipitation, can be indirect and spatially complex, making estimates difficult through this approach. Satellite observations with infrared and microwave sensors, on the other hand, directly monitor earth's energy emissions. These emissions generally correspond physically to the location and intensity of precipitation, indicating more accurately occurrence locations (Funk et al., 2015).

PERSIANN-CDR uses neural network function classification/approximation procedures to calculate precipitation estimates of longwave infrared bands and visible colour images provided by geostationary satellites, generating raster data containing rainfall volume information with a resolution of 0.25° ([http://chrs.web.uci.edu/SP\\_activities00.php](http://chrs.web.uci.edu/SP_activities00.php)). It also uses the infrared spectrum to estimate precipitation occurrences, but does not measure such estimates with field stations and does not enter physiographic information to improve estimates, such as CHELSA or CHIRPS.

#### **5.3.4. Evaluation with test stations**

Training stations interpolations (EBK, KRIG, IDW1 and IDW2) and geospatial products (CHELSA, CHIRPS and PERSIANN-CDR) were evaluated with data from test stations with aid of statistical methods. Table 5.4 shows the metrics used.

The use of NSE and R helps to interpret the modelled data fit level compared to the measured ones, that is, for both seasonal variations (intra-annual) and long-term changes (interannual). The RMSE assists in the measurement of rain volume deviations between the measurement point and the modelling. The fact that RMSE aggregates several magnitudes of errors and highlights larger errors of simulations (Chai and Draxler, 2014), led to its choice, in order to show discrepancies in precipitation volumes of geospatial products (grids) in relation to stations in the field.

**Table 5.4** – Statistics used in the assessment

Statistics	Description	References
Pearson coefficient (R)	It is a measure of the linear association between two variables. Correlation coefficient values range from $-1$ to $+1$ . Positive values indicate the tendency of one variable to increase or decrease together with another. Negative values indicate a tendency for increasing values of one variable to be associated with decreasing values of the other and vice versa. Values close to zero indicate low association between variables and values close to $-1$ or $+1$ indicate strong linear association between both	Kirch (2008)
Nash Sutcliffe Model Efficient Coefficient (NSE)	Normalized statistic that determines the relative magnitude of the residual variance compared to the measured data variance. Indicates how well the observed data is compatible with the simulated ones. $NSE = 1$ corresponds to a perfect model and observed data match; $NSE = 0$ indicates that the model predictions are as accurate as the observed data average; $-\infty < NSE < 0$ , indicates that the observed mean is a better predictor than the model	Nash and Sutcliffe (1970)
Root mean square error (RMSE)	Frequently used to measure the difference between the values predicted by a model and the values actually observed in situ. Such values are evaluated on absolute scales, in the same units used by the compared values. These individual differences are also called residuals, and RMSE serves to aggregate them into a single measure of predictive power. Briefly, it compares predicted to observed or known values. As closer as to 0, better it fits between the data	Chai and Draxler (2014)

### 5.3.5. Standardization of results

The results of the statistical analyses were standardized in graphical and map formats, seeking to show the difference in the results achieved for each method of estimating rainfall. The graphs show the averages of results for each metrics used considering all test stations, in addition to the standard deviations. On maps, results of the metrics are displayed for each test station, reclassified in certain value ranges, aiming to show the performance of each method in a spatial view.

We intended to show, in the first case (graphs), the results considering all stations, evaluating the methods, and, in the second case (maps), to check where the points (test stations) showed best and worse results for each method and then discuss why these spatial configurations.

## 5.4. Results

For each method used to estimate the spatiotemporal distribution of rainfall volumes, considering the 280 test stations, the one that presented the best results during the three statistical analyses used was the CHIRPS (Figures 5.3–5.5). This

method presented the smallest amplitudes between test stations for the three metrics used, showing lower variability and greater accuracy in relation to the other estimates, as shown by the standard deviations (red bars) in graphs.

The low standard deviations result from the high minimum and maximum values in NSE and R and the low maximum and minimum values in RMSE. This results in NSE and R averages closer to one, indicating that the estimated CHIRPS values have seasonal (intra- annual) and long-term (inter-annual) behaviours more compatible with those measured in situ by field stations (Figures 5.3 and 5.4). The same is true for the average RMSE closest to zero, indicating the smallest deviations from the observed data (Figure 5.5). CHIRPS was the method with largest number of test stations presenting the highest value ranges of the metrics used (Table 5.5).

In contrast, PERSIANN and CHELSA had the worst performances, respectively, with more test stations in lower ranges of values in NSE and R, and the highest ranges of values in RMSE (Table 5.5). Because of this, both have the lowest averages in NSE and R, and the highest in RMSE (Figures 5.3–5.5). Together with EBK, KRIG, IDW1 and IDW2, PERSIANN and CHELSA obtained performances with high variations between the test stations, as shown by the standard deviations, showing less spatial consistency in the results.

The CHIRPS demonstrated greater consistency in the results, with the exception of a few test stations, showing that it is a method little influenced in estimates of rainfall due to spatial variations caused, for example, by the relief, such as altimetric differences, slope orientation, among others.

On the contrary, the other methods of estimating rainfall performed differently over space. Regardless of the magnitude of inconsistencies in performance between test stations, from low to large (EBK, IDW2, KRIG, IDW1, CHELSA and PERSIANN, respectively), all these methods had greater difficulties in estimating in the eastern band of BSOL. CHIRPS also obtained lower performances in test stations located in this band; however, it was superior to the other methods.

The best performances of CHIRPS, including test stations located in the eastern band of BSOL, may be due to the characteristics of this rain estimation method, as will be discussed in the next session.

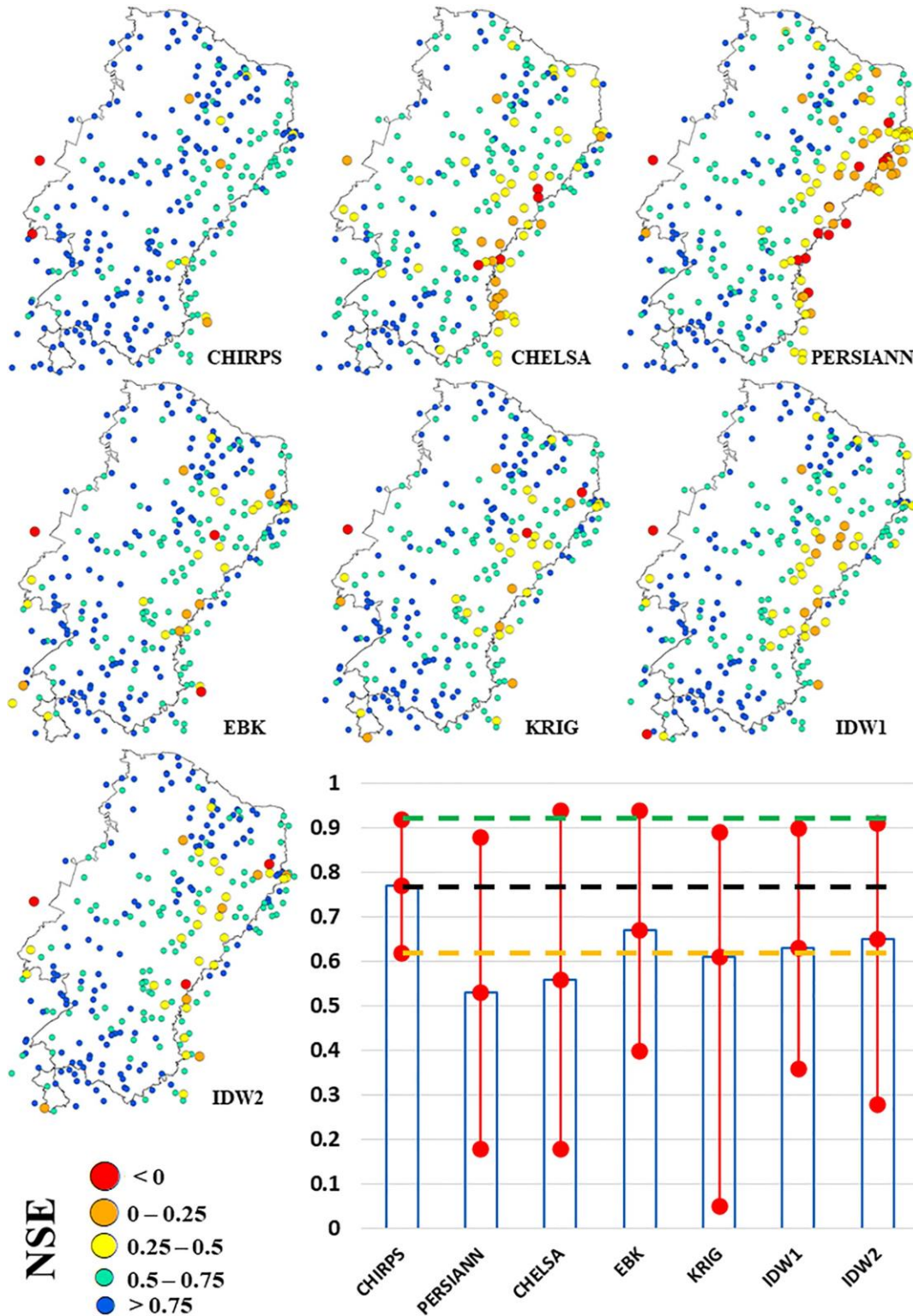


**Figure 5.3** - Performance of the different methods by NSE. The value ranges are represented by coloured circles, showing the performance of each method over the test stations at BSOL. The graph shows the average NSE values for the 280 test stations (blue bars) for the seven evaluated methods, in addition to the standard deviations (red bars). The dotted lines represent the mean value (black), the minimum standard deviation (orange) and the maximum standard deviation (green) for CHIRPS

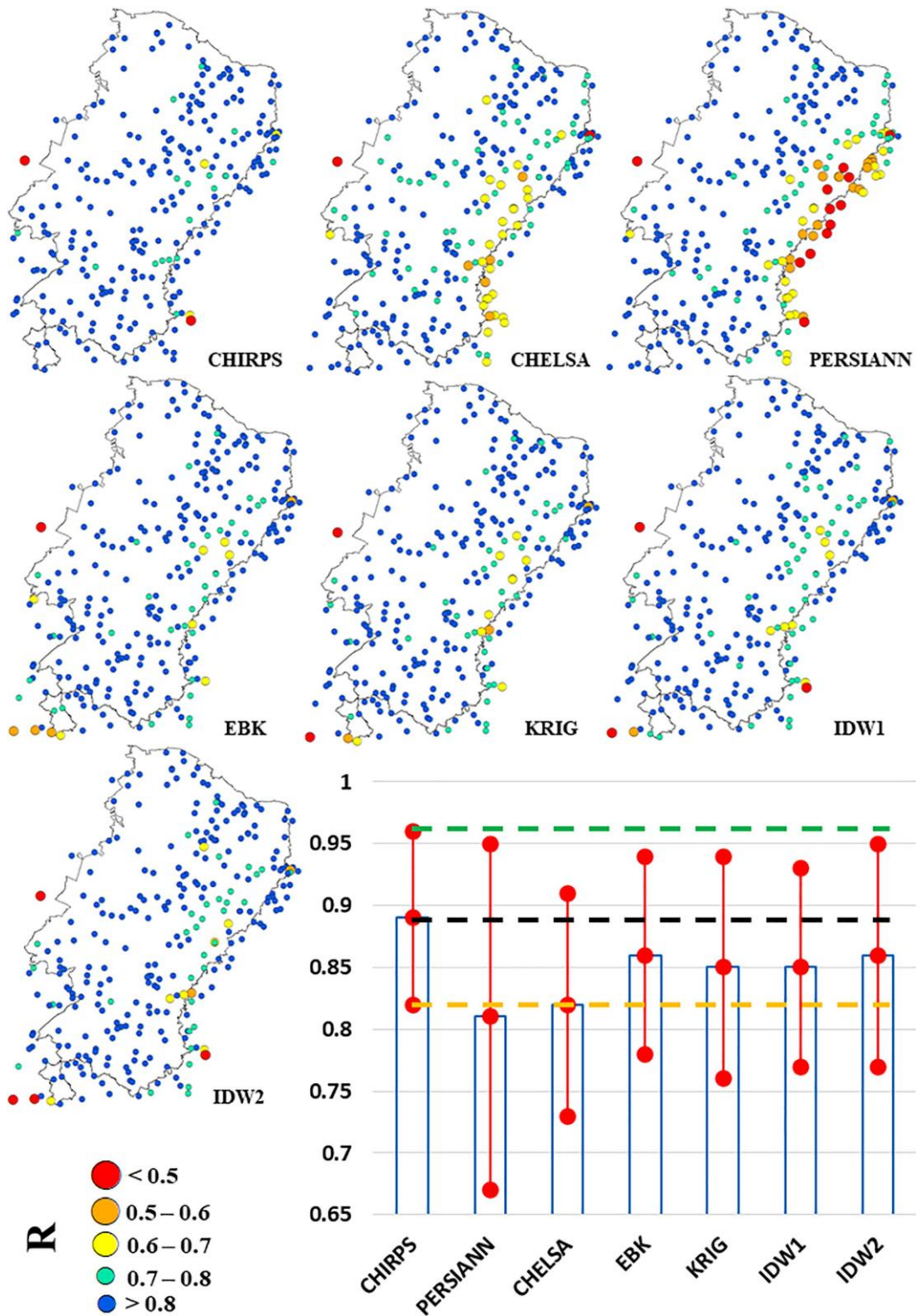


**Figure 5.4** - Performance of the different methods by  $R$ . The value ranges are represented by coloured circles, showing the performance of each method over the test stations at BSOL. The graph shows the average  $R$  values for the 280 test stations (blue bars) for the seven evaluated methods, in addition to the standard deviations (red bars). The dotted lines represent the mean value (black), the minimum standard deviation (orange) and the maximum standard deviation (green) for CHIRPS

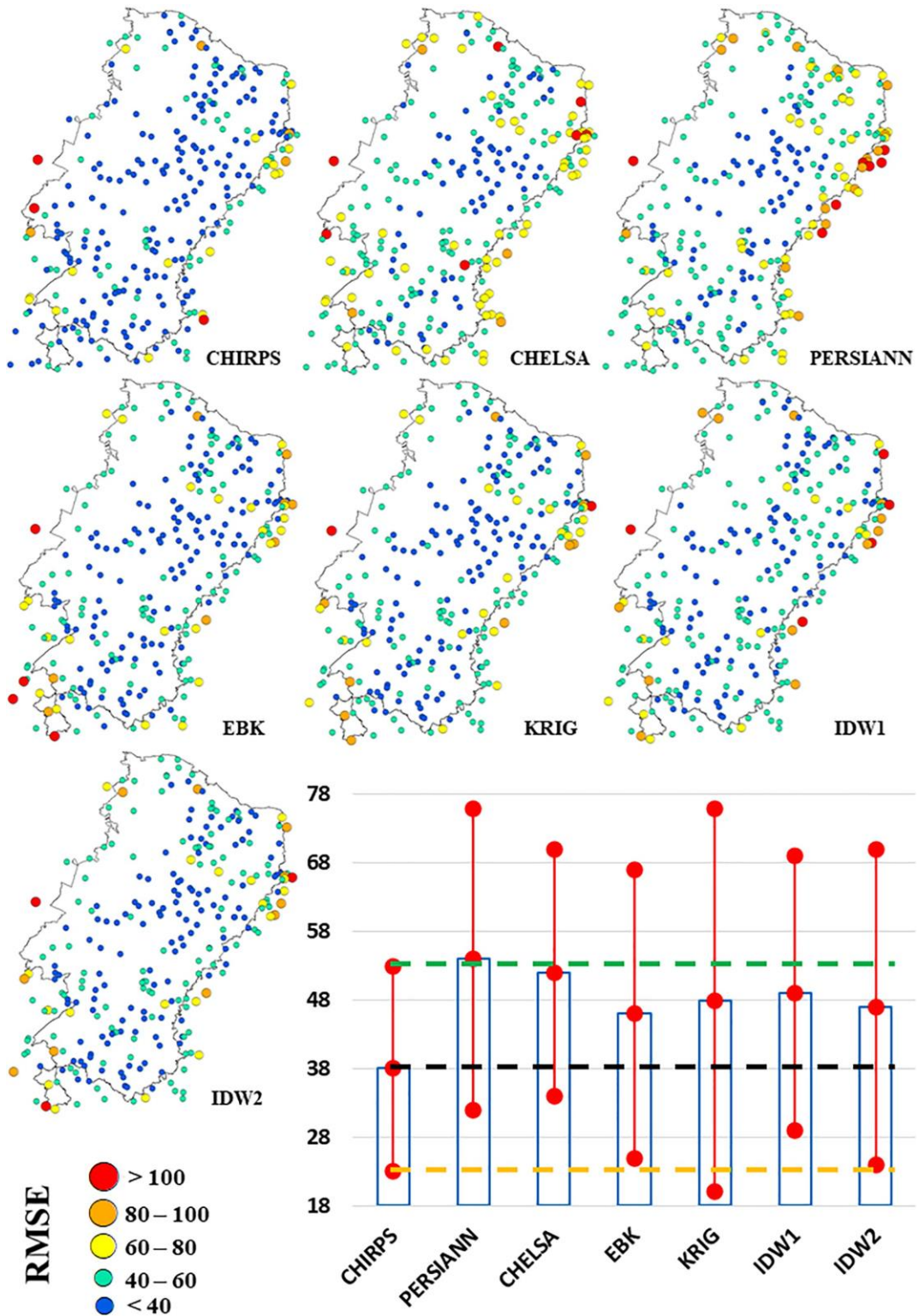


**Figure 5.5** - Performance of the different methods by RMSE (absolute values, in mm). The value ranges are represented by coloured circles, showing the performance of each method over the test stations at BSOL. The graph shows the average RMSE values for the 280 test stations (blue bars) for the seven evaluated methods, in addition to the standard deviations (red bars). The dotted lines represent the mean value (black), the minimum standard deviation (green) and the maximum standard deviation (orange) for CHIRPS

**Table 5.5** – Number of test stations, for each rain estimation method, according to the range of values of metrics used

Statistics	Range of values	Rain estimation methods						
		CHIRPS	CHELSEA	PERSIANN	EBK	KRIG	IDW1	IDW2
NSE	< 0	2	20	28	10	13	11	12
	0 – 0.25	3	14	23	7	7	8	7
	0.25 – 0.5	6	35	39	17	19	28	22
	0.5 – 0.75	78	124	23	101	108	123	98
	> 0.75	191	87	23	145	133	110	141
R	< 0.5	2	1	12	2	4	3	4
	0.5 – 0.6	0	5	16	2	2	2	1
	0.6 – 0.7	2	22	25	7	9	5	6
	0.7 – 0.8	14	54	33	25	31	40	31
	> 0.9	262	198	194	244	234	230	238
RMSE	> 100	3	9	14	9	7	9	7
	80 – 100	4	4	16	8	10	12	10
	60 – 80	16	53	41	22	21	14	18
	40 – 60	65	141	135	101	116	140	115
	< 40	192	73	74	140	126	105	130

## 5.5. Discussion

In the present study, was observed that the test stations located in the eastern band of the BSOL, near the coastal areas, had lower performance according to the statistical analysis results than those in the interior of the continent. In the eastern side, the topography is irregular from north to south, where the orientation of the relief slopes is mostly facing east (41%). In addition, the prevailing wind direction in this range comes from east to west (Silva et al., 2002; 2004), meeting the hillside of the north- east topographic complex. These winds, coming from the ocean and laden with moisture, when they meet in the higher areas near the shoreline, influence the formation of orographic windward rain, and, according to those winds enters in continental area, it loses moisture, resulting in drier leeward areas (Conti, 2005).

Test stations located in the eastern band, both wind- ward (more humidity) and leeward (lower humidity), obtained results in the statistical analyses lower than the ones located in the central and western bands. Therefore, unlike the results achieved by Paredes-Trejo et al. (2017), whether in dry or humid areas, the results indicate that rain estimation methods are less effective, suggesting that in areas where the topography is more complex, especially in the eastern BSOL band, the methods have higher difficulties in estimating rainfall volumes, regardless the stations are located at leeward or windward. Some studies have already demonstrated this fact, which has found that in areas where convec- tive orographic

rain, very cold surfaces and ice on mountain tops tend to result in disparate estimates of what happens in situ (Dinku et al., 2008; 2011; Rahman et al., 2009; Toté et al., 2015).

Rain estimates from interpolation methods also produce uneven results from those observed in situ in complex terrain areas, especially simpler methods, in which no other variables such as relief are added to the analysis. Methods that do so usually reach estimates closer to those measured by stations (Diodato, 2005; Diodato and Ceccarelli, 2005; Tobin et al., 2011).

Despite the addition of information, CHELSA did not perform better than other interpolation methods, whether geostatistical or deterministic. In general, the efficiency was lower than EBK, KRIG, IDW1 and IDW2, presenting worse performances in more test stations throughout the BSOL territory, mainly in the east.

Although all the methods in this study had worse performance in test stations located in complex topography areas, in east band of BSOL, CHIRPS was the one that presented the best results, even in places of greatest difficulty in estimating the rain volumes.

Thus, there is evidence from the results generated in this study that the differential of CHIRPS better performance, when compared to other geospatial products and regular interpolation methods, is the integration of various information sources, coming from field stations, physiographic predictors and satellite sensor estimates, sources not fully used in other precipitation estimation methods (Table 5.6).

Some studies show that CHIRPS has a better performance in semiarid areas when compared to other geospatial products. In Xinjiang, China, CHIRPS and PERSIANN-CDR were evaluated using data from 105 meteorological stations at various time and space scales (Gao et al., 2018). Although both products have similar correlations, the first one's BIAS and RMSE are better than the second one, with smaller deviations. In terms of long evaluation periods, CHIRPS presents higher accuracy with observations measured monthly and annual frequency, while PERSIANN-CDR tends to overestimate rainfall in rainy seasons. In addition, compared to PERSIANN-CDR, the results show that CHIRPS is more accurate in reflecting the spatial distribution of monthly and annual average rainfall.

**Table 5.6** – Types of data used for rainfall estimates for each method

Method	Use of field station data	Use of satellite infrared sensors	Use of physiographic predictors
CHIRPS	✓	✓	✓
CHELSEA	✓		✓
PERSIANN-CDR		✓	
EBK	✓		
KRIG	✓		
IDW1	✓		
IDW2	✓		

In another study (Babaousmail et al., 2019), CHIRPS was evaluated with NOAA CPC Morphing Technique (CMORPH) in Algeria. The evaluation was conducted over a 19-year period, ranging from 1998 to 2016, using 20 rainfall data sets. The study area was divided into five regions (zones) according to the Köppen climate classification. In monthly time scale, CHIRPS had the best performance ( $r = .9$ ), while CMORPH had a relatively weaker but good correlation ( $r = .83$ ). On an annual timescale, CHIRPS perform better in some regions, and CMORPH shows better results in others.

In Ethiopia (Bayissa et al., 2017), CHIRPS was evaluated with four other products, including PERSIANN-CDR, between 1998 and 2015 using data from 10 meteorological stations. Evaluation results of these satellite precipitation products shows that there is a good correlation ( $r > .7$ ) of CHIRPS and African Rainfall Climatology and Time-Series (TARCAT) products with in situ observations at most meteorological stations for all the time scales evaluated. TARCAT showed a higher correlation coefficient ( $r > 0.70$ ) in seven meteorological stations on a decadal time scale (10 days), while CHIRPS showed a higher correlation coefficient ( $r > .84$ ) in nine meteorological stations on monthly time scale. TARCAT performed well near CHIRPS, while PERSIANN-CDR performed poorly on all criteria.

CHELSEA is a geospatial product that still not commonly used in scientific studies, being the focus of biogeographic research (Castro-Pena et al., 2017; Dvorský et al., 2017; Maria and Udo, 2017; Guo et al., 2018; Moradi and Oldeland, 2019). Comparative or evaluative studies of other products to CHELSEA are difficult to find, being Karger et al. (2017) the only one found so far and structured by the database organizers themselves.

There are other geospatial products, generated from different rainfall estimation methods that could be evaluated for BSOL that were not considered in

this research. In addition, other time scales, such as daily, could also be evaluated. But our research is not intended to close the discussion about the best method to estimate rainfall to the BSOL region in all circumstances.

What was done in this work was an effort to understand how different methods perform in rainfall estimates, and how different sources of information can make a difference in these estimates. Therefore, the focus on three geospatial products elaborated in different ways and the inclusion of regular interpolation methods usually used in rainfall spatialization data, to verify whether the inclusion of new sources of information really makes a difference in estimates, improving them. Consequently, we recommend CHIRPS as a method to estimate monthly rainfall to almost the entire BSOL area, only excluding the region near the coast.

## **5.6. Conclusions**

Overall, CHIRPS had the best performance in estimating rainfall volumes when compared to data from field stations used as a test for product evaluation. From the results obtained there is evidence that the best performance is due to incorporation of several distinct data sources from field stations, geostationary satellite infrared sensor estimates and physiographic predictors. Information not fully present in other products. Thus, CHIRPS, for studies that use long-term monthly data, would be the best information choice on rainfall volumes for the Brazilian semiarid, although further studies are needed to assess other data and scales.

All methods had worse performance in the eastern band of BSOL, an area that receives moisture from the Atlantic Ocean and has complex terrain, due to the set of mountains located on the topographic complex of the northeast coast of Brazil. There is no novelty, as previous studies show. Rainfall estimation methods tend to be less effective in areas of complex topography, such as the Swiss Alps and mountainous regions in Italy.

## **5.7. Acknowledgement**

This work was carried out with the support of CAPES – Financing Code 001.

## **5.8. References**

Alvares, C.A., Stape, J.L., Sentelhas, P.C., de Moraes Gonçalves, J.L. and

Sparovek, G. (2013) Köppen's climate classification map for Brazil. *Meteorologische Zeitschrift*, 22(6), 711–728. <https://doi.org/10.1127/0941-2948/2013/0507>.

Alves, M.C., Carvalho, L.G., Vianello, R.L., Sedyama, G.C., de Oliveira, M.S. and de Sá Junior, A. (2013) Geostatistical improvements of evapotranspiration spatial information using satellite land surface and weather stations data. *Theoretical and Applied Climatology*, 113(1–2), 155–174. <https://doi.org/10.1007/s00704-012-0772-1>.

Anjos, R.S., Nóbrega, R.S. and Candeias, A.L.B. (2017) Possíveis causas para os erros das estimativas do satélite TRMM—estudo de caso na Microrregião de Itaparica-PE. *Revista Brasileira de Climatologia*, 21, 509–528. <https://doi.org/10.5380/abclima.v21i0.53241>.

Araújo, J.C., Döll, P., Güntner, A., Krol, M., Abreu, C.B.R., Hauschild, M. and Mendiondo, E.M. (2004) Water scarcity under scenarios for global climate change and regional development in semiarid northeastern Brazil. *Water International*, 29 (2), 209–220. <https://doi.org/10.1080/02508060408691770>.

Babaousmail, H., Hou, R., Ayugi, B. and Gnitou, G.T. (2019) Evaluation of satellite-based precipitation estimates over Algeria during 1998–2016. *Journal of Atmospheric and Solar-Terrestrial Physics*, 195, 105139. <https://doi.org/10.1016/j.jastp.2019.105139>.

Barbalho, F.D., Silva, G.F.N. and da Formiga, K.T.M. (2014) Average rainfall estimation: methods performance comparison in the Brazilian semi-arid. *Journal of Water Resource and Protection*, 6(2), 97–103. <https://doi.org/10.4236/jwarp.2014.62014>.

Barbosa, H.A. and Lakshmi Kumar, T.V. (2016) Influence of rainfall variability on the vegetation dynamics over northeastern Brazil. *Journal of Arid Environments*, 124, 377–387. <https://doi.org/10.1016/J.JARIDENV.2015.08.015>.

Bayissa, Y., Tadesse, T., Demisse, G. and Shiferaw, A. (2017) Evaluation of satellite-based rainfall estimates and application to monitor meteorological drought for the Upper Blue Nile Basin, Ethiopia. *Remote Sensing*, 9(7), 669. <https://doi.org/10.3390/rs9070669>.

Beck, H.E., Zimmermann, N.E., TR, M.V., Vergopolan, N., Berg, A. and Wood,

E.F. (2018) Present and future Köppen–Geiger climate classification maps at 1-km resolution. *Scientific Data*, 5, 180214. <https://doi.org/10.1038/sdata.2018.214>.

Bernhardt, J. and Carleton, A.M. (2018) Comparing daily temperature averaging methods: the role of surface and atmosphere variables in determining spatial and seasonal variability. *Theoretical and Applied Climatology*, 136, 499–512. <https://doi.org/10.1007/s00704-018-2504-7>.

Bhardwaj, A., Ziegler, A.D., Wasson, R.J. and Chow, W.T.L. (2017) Accuracy of rainfall estimates at high altitude in the Garhwal Himalaya (India): a comparison of secondary precipitation products and station rainfall measurements. *Atmospheric Research*, 188, 30–38. <https://doi.org/10.1016/j.atmosres.2017.01.005>.

Castro-Pena, J.C., Goulart, F., Wilson Fernandes, G., Hoffmann, D., Leite, F.S.F., Britto dos Santos, N., Soares-Filho, B., Sobral-Souza, T., Humberto Vancine, M. and Rodrigues, M. (2017) Impacts of mining activities on the potential geographic distribution of eastern Brazil mountaintop endemic species. *Perspectives in Ecology and Conservation*, 15(3), 172–178. <https://doi.org/10.1016/J.PECON.2017.07.005>.

Chai, T. and Draxler, R.R. (2014) Root mean square error (RMSE) or mean absolute error (MAE)? — arguments against avoiding RMSE in the literature. *Geoscientific Model Development*, 7(3), 1247–1250. <https://doi.org/10.5194/gmd-7-1247-2014>.

Childs, C. (2004) Interpolating surfaces in ArcGIS spatial analyst. *ArcUser Online*, pp. 32–35.

Conti, J.B. (2005) A Questão Climática do Nordeste Brasileiro e os Processos de Desertificação. *Revista Brasileira de Climatologia*, 1(1), 7–14. <https://doi.org/10.5380/abclima.v1i1.25226>.

Costa, J.C., Pereira, G., Siqueira, M.E., da Cardozo, F.S. and da Silva, V.V. (2019) Validação dos dados de precipitação estimados pelo CHIRPS para o Brasil. *Revista Brasileira de Climatologia*, 24, 228–243. <https://doi.org/10.5380/abclima.v24i0.60237>.

Cunha, A.P.M., Alvalá, R.C., Nobre, C.A. and Carvalho, M.A. (2015) Monitoring vegetative drought dynamics in the Brazilian semiarid region. *Agricultural and Forest Meteorology*, 214–215, 494–505.

<https://doi.org/10.1016/J.AGRFORMET.2015.09.010>.

da Silva, A.S.A., Stosic, B., Menezes, R.S.C. and Singh, V.P. (2019) Comparison of interpolation methods for spatial distribution of monthly precipitation in the state of Pernambuco, Brazil. *Journal of Hydrologic Engineering*, 24(3), 04018068. [https://doi.org/10.1061/\(ASCE\)HE.1943-5584.0001743](https://doi.org/10.1061/(ASCE)HE.1943-5584.0001743).

de Azevedo, S.C., Cardim, G.P., Puga, F., Singh, R.P. and da Silva, E.A. (2018) Analysis of the 2012-2016 drought in the northeast Brazil and its impacts on the Sobradinho water reservoir. *Remote Sensing Letters*, 9(5), 438–446. <https://doi.org/10.1080/2150704X.2018.1437290>.

de Borges, P.A., Franke, J., da Anunciação, Y.M.T., Weiss, H. and Bernhofer, C. (2016) Comparison of spatial interpolation methods for the estimation of precipitation distribution in Distrito Federal, Brazil. *Theoretical and Applied Climatology*, 123 (1–2), 335–348. <https://doi.org/10.1007/s00704-014-1359-9>.

de Miranda, R.Q., Dos, H., Ferreira, S., Cristiano, Y., Moraes, B., Galvíncio, J.D. and de Moura, M.S.B. (2017) Avaliação de dez métodos diferentes de interpolação sobre dados meteorológicos em Petrolina, Pernambuco.

Di Vittorio, A.V. and Miller, N.L. (2013) Evaluating a modified point-based method to downscale cell-based climate variable data to high-resolution grids. *Theoretical and Applied Climatology*, 112(3–4), 495–519. <https://doi.org/10.1007/s00704-012-0740-9>.

Dinku, T., Ceccato, P. and Connor, S.J. (2011) Challenges of satellite rainfall estimation over mountainous and arid parts of East Africa. *International Journal of Remote Sensing*, 32(21), 5965–5979. <https://doi.org/10.1080/01431161.2010.499381>.

Dinku, T., Chidzambwa, S., Ceccato, P., Connor, S.J. and Ropelewski, C.F. (2008) Validation of high-resolution satellite rainfall products over complex terrain. *International Journal of Remote Sensing*, 29(14), 4097–4110. <https://doi.org/10.1080/01431160701772526>.

Diodato, N. (2005) The influence of topographic co-variables on the spatial variability of precipitation over small regions of complex terrain. *International Journal of Climatology*, 25(3), 351–363. <https://doi.org/10.1002/joc.1131>.

Diodato, N. and Ceccarelli, M. (2005) Interpolation processes using multivariate geostatistics for mapping of climatological precipitation mean in the Sannio Mountains (southern Italy). *Earth Surface Processes and Landforms*, 30(3), 259–268. <https://doi.org/10.1002/esp.1126>.

Duan, L., Fan, K., Li, W. and Liu, T. (2019) Spatial downscaling algorithm of TRMM precipitation based on multiple high-resolution satellite data for Inner Mongolia, China. *Theoretical and Applied Climatology*, 135(1–2), 45–59. <https://doi.org/10.1007/s00704-017-2347-7>.

Dvorský, M., Macek, M., Kopecký, M., Wild, J. and Doležal, J. (2017) Niche asymmetry of vascular plants increases with elevation. *Journal of Biogeography*, 44(6), 1418–1425. <https://doi.org/10.1111/jbi.13001>.

Fang, L., Tao, S., Zhu, J. and Liu, Y. (2018) Impacts of climate change and irrigation on lakes in arid northwest China. *Journal of Arid Environments*, 154, 34–39. <https://doi.org/10.1016/j.jaridenv.2018.03.008>.

FAO (2009). Global map of aridity. FAO.

Franchito, S.H., Rao, V.B., Vasques, A.C., Santo, C.M.E. and Conforte, J.C. (2009) Validation of TRMM precipitation radar monthly rainfall estimates over Brazil. *Journal of Geophysical Research*, 114(D2), D02105. <https://doi.org/10.1029/2007JD009580>.

Funk, C., Peterson, P., Landsfeld, M., Pedreros, D., Verdin, J., Shukla, S., Husak, G., Rowland, J., Harrison, L., Hoell, A. and Michaelsen, J. (2015) The climate hazards infrared precipitation with stations — a new environmental record for monitoring extremes. *Scientific Data*, 2, 150066. <https://doi.org/10.1038/sdata.2015.66>.

Gao, F., Zhang, Y., Chen, Q., Wang, P., Yang, H., Yao, Y. and Cai, W. (2018) Comparison of two long-term and high-resolution satellite precipitation datasets in Xinjiang, China. *Atmospheric Research*, 212, 150–157. <https://doi.org/10.1016/j.atmosres.2018.05.016>.

Ghajarnia, N., Liaghat, A. and Daneshkar, A.P. (2015) Comparison and evaluation of high-resolution precipitation estimation products in Urmia Basin-Iran. *Atmospheric Research*, 158–159, 50–65.

<https://doi.org/10.1016/j.atmosres.2015.02.010>.

Gondim, R., Silveira, C., de Souza, F.F., Vasconcelos, F. and Cid, D. (2018) Climate change impacts on water demand and availability using CMIP5 models in the Jaguaribe basin, semi-arid Brazil. *Environmental Earth Sciences*, 77(15), 550. <https://doi.org/10.1007/s12665-018-7723-9>.

Guo, F., Lenoir, J. and Bonebrake, T.C. (2018) Land-use change interacts with climate to determine elevational species redistribution. *Nature Communications*, 9(1), 1315. [1038/s41467-018-03786-9](https://doi.org/10.1038/s41467-018-03786-9).

Guofeng, Z., Dahe, Q., Yuanfeng, L., Fenli, C., Pengfei, H., Dongdong, C. and Kai, W. (2017) Accuracy of TRMM precipitation data in the southwest monsoon region of China. *Theoretical and Applied Climatology*, 129(1–2), 353–362. <https://doi.org/10.1007/s00704-016-1791-0>.

Jong, P., Tanajura, C.A.S., Sánchez, A.S., Dargaville, R., Kiperstok, A. and Torres, E.A. (2018) Hydroelectric production from Brazil's São Francisco River could cease due to climate change and inter-annual variability. *Science of the Total Environment*, 634, 1540–1553. <https://doi.org/10.1016/j.scitotenv.2018.03.256>.

Karaseva, M.O., Prakash, S. and Gairola, R.M. (2012) Validation of high-resolution TRMM-3B43 precipitation product using rain gauge measurements over Kyrgyzstan. *Theoretical and Applied Climatology*, 108(1–2), 147–157. <https://doi.org/10.1007/s00704-011-0509-6>.

Karger, D.N., Conrad, O., Böhrer, J., Kawohl, T., Kreft, H., Soria-auza, R.W., Zimmermann, N.E., Linder, H.P. and Kessler, M. (2017) Data descriptor: climatologies at high resolution for the earth's land surface areas. *Nature*, 4, 1–20. <https://doi.org/10.1038/sdata.2017.122>.

Katiraie-Boroujerdy, P.S., Akbari Asanjan, A., Hsu, K. and Sorooshian, S. (2017) Intercomparison of PERSIANN-CDR and TRMM-3B42V7 precipitation estimates at monthly and daily time scales. *Atmospheric Research*, 193, 36–49. <https://doi.org/10.1016/j.atmosres.2017.04.005>.

Kirch, W. (2008) Pearson's Correlation Coefficient. *Encyclopedia of Public Health*. Dordrecht: Springer.

Klutse, N.A.B., Abiodun, B.J., Hewitson, B.C., Gutowski, W.J. and Tadross, M.A.

(2016) Evaluation of two GCMs in simulating rainfall inter-annual variability over southern Africa. *Theoretical and Applied Climatology*, 123(3–4), 415–436. <https://doi.org/10.1007/s00704-014-1356-z>.

Krivoruchko, K. (2012) Empirical Bayesian kriging: implemented in ArcGIS Geostatistical Analyst. *ArcUser*, pp. 6–10.

Kumar, D., Gautam, A.K., Palmate, S.S., Pandey, A., Suryavanshi, S., Rathore, N. and Sharma, N. (2017) Evaluation of TRMM multi-satellite precipitation analysis (TMPA) against terrestrial measurement over a humid sub-tropical basin, India. *Theoretical and Applied Climatology*, 129(3–4), 783–799. <https://doi.org/10.1007/s00704-016-1807-9>.

Li, X., Li, L., Wang, X. and Jiang, F. (2013) Reconstruction of hydro-meteorological time series and its uncertainties for the Kaidu River basin using multiple data sources. *Theoretical and Applied Climatology*, 113(1–2), 45–62. <https://doi.org/10.1007/s00704-012-0771-2>.

Lira, E.A., Alves, R.R.N., Dias, T.L.P. and Molozzi, J. (2017) How do people gain access to water resources in the Brazilian semiarid (Caatinga) in times of climate change? *Environmental Monitoring and Assessment*, 189(8), 375. <https://doi.org/10.1007/s10661-017-6087-z>.

Lyra, A., Tavares, P., Chou, S.C., Sueiro, G., Dereczynski, C., Sondermann, M., Silva, A., Marengo, J. and Giarolla, A. (2018) Climate change projections over three metropolitan regions in southeast Brazil using the non-hydrostatic Eta regional climate model at 5-km resolution. *Theoretical and Applied Climatology*, 132(1–2), 663–682. <https://doi.org/10.1007/s00704-017-2067-z>.

Marengo, J.A. and Bernasconi, M. (2015) Regional differences in aridity/drought conditions over northeast Brazil: present state and future projections. *Climatic Change*, 129(1–2), 103–115. <https://doi.org/10.1007/s10584-014-1310-1>.

Maria, B. and Udo, S. (2017) Why input matters: selection of climate data sets for modelling the potential distribution of a treeline species in the Himalayan region. *Ecological Modelling*, 359, 92–102. <https://doi.org/10.1016/J.ECOLMODEL.2017.05.021>.

Mariano, D.A., do Santos, C.A.C., Wardlow, B.D., Anderson, M.C., Schiltmeyer,

A.V., Tadesse, T. and Svoboda, M.D. (2018) Use of remote sensing indicators to assess effects of drought and human-induced land degradation on ecosystem health in northeastern Brazil. *Remote Sensing of Environment*, 213, 129–143. <https://doi.org/10.1016/j.rse.2018.04.048>.

Moradi, H. and Oldeland, J. (2019) Climatic stress drives plant functional diversity in the Alborz Mountains, Iran. *Ecological Research*, 34(1), 171–181. <https://doi.org/10.1111/1440-1703.1015>.

Nash, J.E. and Sutcliffe, J.V. (1970) River flow forecasting through conceptual models part I - A discussion of principles. *Journal of Hydrology*, 10(3), 282–290. [https://doi.org/10.1016/0022-1694\(70\)90255-6](https://doi.org/10.1016/0022-1694(70)90255-6).

Paredes-Trejo, F.J., Barbosa, H.A. and Lakshmi Kumar, T.V. (2017) Validating CHIRPS-based satellite precipitation estimates in northeast Brazil. *Journal of Arid Environments*, 139, 26–40. <https://doi.org/10.1016/j.jaridenv.2016.12.009>.

Prasetia, R., Assyakur, A.R. and Osawa, T. (2013) Validation of TRMM precipitation radar satellite data over Indonesian region. *Theoretical and Applied Climatology*, 112(3–4), 575–587. <https://doi.org/10.1007/s00704-012-0756-1>.

Quesada-Montano, B., Wetterhall, F., Westerberg, I.K., Hidalgo, H.G. and Halldin, S. (2018) Characterising droughts in Central America with uncertain hydro-meteorological data. *Theoretical and Applied Climatology*, 137, 2125–2138. <https://doi.org/10.1007/s00704-018-2730-z>.

Rahman, S.H., Sengupta, D. and Ravichandran, M. (2009) Variability of Indian summer monsoon rainfall in daily data from gauge and satellite. *Journal of Geophysical Research*, 114(D17), D17113. <https://doi.org/10.1029/2008JD011694>.

Rocha, R. and Soares, R.R. (2015) Water scarcity and birth outcomes in the Brazilian semiarid. *Journal of Development Economics*, 112, 72–91. <https://doi.org/10.1016/j.jdeveco.2014.10.003>.

Santos, S.M. and Farias, M.M.M.W.E.C. (2017) Potential for rainwater harvesting in a dry climate: assessments in a semiarid region in northeast Brazil. *Journal of Cleaner Production*, 164, 1007–1015. <https://doi.org/10.1016/j.jclepro.2017.06.251>.

Santos, S.R.Q., do Cunha, A.P.M.A. and Ribeiro-Neto, G.G. (2019) Avaliação de

dados de precipitação para o monitoramento do padrão espaço-temporal da seca no Nordeste do Brasil. *Revista Brasileira de Climatologia*, 25, 80–100. <https://doi.org/10.5380/abclima.v25i0.62018>.

Sarmadi, F. and Shokoohi, A. (2015) Regionalizing precipitation in Iran using GPCP gridded data via multivariate analysis and L- moment methods. *Theoretical and Applied Climatology*, 122 (1–2), 121–128. <https://doi.org/10.1007/s00704-014-1292-y>.

Schneider, U., Becker, A., Finger, P., Meyer-Christoffer, A., Ziese, M. and Rudolf, B. (2014) GPCP's new land surface precipitation climatology based on quality-controlled in situ data and its role in quantifying the global water cycle. *Theoretical and Applied Climatology*, 115(1–2), 15–40. <https://doi.org/10.1007/s00704-013-0860-x>.

Silva, B.B., Alves, J.J.A., Cavalcanti, E.P. and Dantas, R.T. (2002) Potencial Eólico na Direção Predominante do Vento no Nordeste Brasileiro. *Revista Brasileira de Engenharia Agrícola e Ambiental*, 6(3), 431–439. <https://doi.org/10.1590/S1415-43662002000300009>.

Silva, B.B., Alves, J.J.A., Cavalcanti, E.P. and Ventura, E.D. (2004) Variabilidade Espacial e Temporal do Potencial Eólico da Direção Predominante do Vento no Nordeste do Brasil. *Revista Brasileira de Meteorologia*, 19(2), 189–202.

Soares, A.S.D., da Paz, A.R. and Picilli, D.G.A. (2016). Avaliação das estimativas de chuva do satélite TRMM no Estado da Paraíba. *Revista Brasileira de Recursos Hídricos*, 21(2), 288–299. <https://doi.org/10.21168/rbrh.v21n2.p288-299>.

SUDENE. (2017) Delimitação do semiárido. SUDENE. <http://www.sudene.gov.br/delimitacao-do-semiarido>.

Tobin, C., Nicotina, L., Parlange, M.B., Berne, A. and Rinaldo, A. (2011) Improved interpolation of meteorological forcings for hydrologic applications in a Swiss Alpine region. *Journal of Hydrology*, 401(1–2), 77–89. <https://doi.org/10.1016/j.jhydrol.2011.02.010>.

Tomasella, J., Silva Pinto Vieira, R.M., Barbosa, A.A., Rodriguez, D. A., Oliveira Santana, M. and de Sestini, M.F. (2018) Desertification trends in the northeast of Brazil over the period 2000–2016. *International Journal of Applied Earth Observation*

and Geoinformation, 73, 197–206. <https://doi.org/10.1016/J. JAG.2018.06.012>.

Toté, C., Patricio, D., Boogaard, H., van der Wijngaart, R., Tarnavsky, E. and Funk, C. (2015) Evaluation of satellite rainfall estimates for drought and flood monitoring in Mozambique. *Remote Sensing*, 7 (2), 1758–1776. <https://doi.org/10.3390/rs70201758>.

Vieira, R.M.S.P., Tomasella, J., Alvalá, R.C.S., Sestini, M.F., Affonso, A.G., Rodriguez, D.A., Barbosa, A.A., Cunha, A.P.M.A., Valles, G.F., Crepani, E., de Oliveira, S.B.P., de Souza, M.S. B., Calil, P.M., de Carvalho, M.A., Valeriano, D.M., Campello, F.C.B. and Santana, M.O. (2015) Identifying areas susceptible to desertification in the Brazilian northeast. *Solid Earth*, 6(1), 347–360. <https://doi.org/10.5194/se-6-347-2015>.

Zittis, G. (2018) Observed rainfall trends and precipitation uncertainty in the vicinity of the Mediterranean, Middle East and North Africa. *Theoretical and Applied Climatology*, 134(3–4), 1207–1230. <https://doi.org/10.1007/s00704-017-2333-0>.

## 6. PAPER 2: LAND COVER CHANGES IMPLICATIONS IN ENERGY FLOW AND WATER CYCLE IN SÃO FRANCISCO BASIN, BRAZIL, OVER THE PAST SEVEN DECADES<sup>2</sup>

**Abstract:** This research aimed to quantify and qualify alterations in land cover and verify the implications of these modifications for variables related to energy flows and water cycle in São Francisco basin (SFB), located entirely in Brazilian territory, in the second half of the 20th century and beginning of the 21st. For this, statistical analyzes (descriptive, trends, seasonal and correlations) were used to quantify changes in the variables of land cover and energy/water flows, in addition to relating them. As a result, it was found that the SFB lost 65,680 km<sup>2</sup> of native vegetation (10.4% of basin area) to crops and pastures, reducing water infiltration (-52%) while the rains remained stable (-2%). Water loss increased through evapotranspiration (+5%) and surface runoff (+225%). Such changes in the water cycle have entailed an 11% reduction in São Francisco River long term flow rate (Q95), comparing pre and post-1990s period. In SFB, the activities that required water, such as farming activities, are those that promote hydric loss.

**Keywords:** Correlation; Flow Rate; Rainfall; Trend Analysis; Water Balance; Water Loss.

---

<sup>2</sup> Under review by the journal Environmental Earth Sciences.  
DOI: <https://doi.org/10.21203/rs.3.rs-444119/v1>

## 6.1. Introduction

Investigating Earth's energy and water cycles is essential to understand global climate dynamics and how it impacts and is influenced by human actions (Seyoum and Milewski, 2017; Umair et al., 2019). The terrestrial climate is susceptible to radiation flows, both those of short-wave originating from solar activities and those of long-wave from solar rays' irradiation on the planet's surface (Mokhtari et al., 2018; Yan et al., 2020; Yang et al., 2017).

In addition to the intensity of solar activities, the balance of terrestrial radiation will depend on atmosphere composition, land cover, relief, and the amount of surface water present in the upper lithosphere (Jiang et al., 2021; Mokhtari et al., 2018; Yan et al., 2020). It is already known, therefore, that the energy flux on Earth will depend on the interaction between its various spheres (Atmosphere, Lithosphere, Hydrosphere and Biosphere). It is also known that man, nowadays, can influence these different spheres, changing energy and water flows among them, with their actions that change land cover and atmosphere chemical composition (Rodell et al., 2004; Umair et al., 2019).

Precipitated water will be distinguished into two main categories (Umair et al., 2019): i) first is the demand for water required by the atmosphere, called potential evapotranspiration, which will convert part of the water present in the lithosphere, hydrosphere and biosphere into real evapotranspiration, not always reaching the total potential demand, as there is dependence on the amount of water present in the environment (Jiang et al., 2021); ii) second is the surface and subsurface runoff, which the balance between these will depend on relief, soils type, land cover, human activities and atmospheric water demand (Ala-aho et al., 2017; Umair et al., 2019). About 67% of the precipitated water across the globe is converted to moisture into the atmosphere by evapotranspiration (Umair et al., 2019).

Although the planet has its dynamics in terms of energy and water flows, human beings, mainly after the industrial revolution (Lindsey, 2009), begin to participate in these complex cycles more significantly. Its activities, such as deforestation, irrigation, urbanization, mining, among others, are vectors of changes in terrestrial land cover and atmospheric chemical composition. In turn, they directly influence energy flows, altering the radiation balance and, consequently, the heat flow (sensitive and latent), which in turn will influence and modify the planet's surface

temperature and cause changes in water exchanges between surface and atmosphere (Das et al., 2018; Umair et al., 2019).

To understand these complex interactions between the terrestrial spheres, initiatives emerged, such as the Land Data Assimilation System (LDAS) (<https://ldas.gsfc.nasa.gov/>). This is developed by the Hydrological Sciences Laboratory of the Goddard Space Flight Center belonging to the National Aeronautics and Space Administration (NASA). With numerical models use, physical processes inherent in the interactions between Earth's surface and atmosphere are modeled from data collected in the field and by orbital images.

From the results, several LDAS projects were developed, which are the Global Land Data Assimilation System (GLDAS), the North American Land Data Assimilation System (NLDAS), the National Climate Assessment - Land Data Assimilation System (NCA-LDAS) and the Famine Early Warning System Network (FEWS NET) Land Data Assimilation System (FLDAS). All of these projects have in common the study and understanding of energy and water terrestrial fluxes, but with different areas and technical specifications with the database used, according to the regional reality.

The use of information generated by models like as LDAS program helps in water resources management, as it is possible to carry out monitoring of drought events, numerical studies of the weather forecast and scientific investigations of water and energy flows (Rodell et al., 2004). Without the application of such models, it would be even more difficult and costly to monitor energy and humidity dynamics with frequent periodicity and adequate geographic scale (Mokhtari et al., 2018; Yang et al., 2017).

Several studies have been carried out based on data generated by LDAS, as the impacts caused by changes in land use and land cover on surface runoff and energy flows, under different climatic conditions, in East Asia (Umair et al., 2019), or to measure water consumption in irrigating crops in agricultural areas in China (Yin et al., 2020). In addition to these, others used data from LDAS to investigate what are the climatic forces associated with occurrences of droughts and wet periods across the planet (Yuan et al., 2019). There are several other examples of studies, which can be found on LDAS website.

In this context, the objective of this research is to identify and measure changes in the energy flow and water cycle in São Francisco Basin (SFB) in the

second half of the 20th century and the first two decades of the 21st, and verifying the implications of land cover modifications, caused by human activities in the last four decades, in changes caused in these cycles' dynamics. Although studies have already been carried out for the basin in this sense, there are still certain gaps concerning changes in the inlet and outlet of water and energy, alterations that have been influenced by human activities.

The most recent SFB studies dealing with the water cycle focus on issues related to water availability and demand. Sun et al. (2016) identified a loss rate of 3.3 km<sup>3</sup> of water per year over 13 years of assessment (between 2002 and 2015), caused mainly by the drought that started in 2012 and ended in 2017, which resulted in a loss rate of 27.63 km<sup>3</sup> between 2012 and 2015. In this study, data on precipitation and stored water present on the earth's surface were used, and the influence of the *El Niño* phenomenon on drought period occurrence.

In another research, by Koch et al. (2015), water availability and demand were assessed under two scenarios: i) a regionalized world with slow economic development, high population growth and little awareness of environmental problems; ii) a globalized world with low population growth, high growth in Gross National Product (GNP) and environmental sustainability, also adding climate change scenarios to both. As a result, they found that between 2021 and 2050 the basin will be wetter, with more intense rainy and dry periods, and increased water availability for irrigation and a drop in electricity generation.

In addition to these, some other studies highlight that hydroelectric energy production may cease in this first half of the 21st century in drought periods (de Jong et al., 2018). Also the prices of agricultural products generated in SFB will be affected, which will depend on climate change, the production location, variety of products and production technology (Torres et al., 2012). It is as well estimated that economic values of water for use in irrigation tend to increase in the coming decades (Alcoforado de Moraes et al., 2018).

Although they are important researches, none of them deal with implications that changes in land cover, having as vectors the anthropic activities, cause in the energy flows and water cycle in SFB, a theme that will be the focus of this research.

## 6.2. Materials and Methods

The stages of this research were organized as follows (Figure 1): i) study area determination; ii) definition of variables to be studied; iii) statistical analysis of the variables defined in study area over the available historical series; iv) spatiotemporal analysis of the studied variables; v) evaluation of impacts on the water availability in São Francisco River caused by changes in the studied variables.

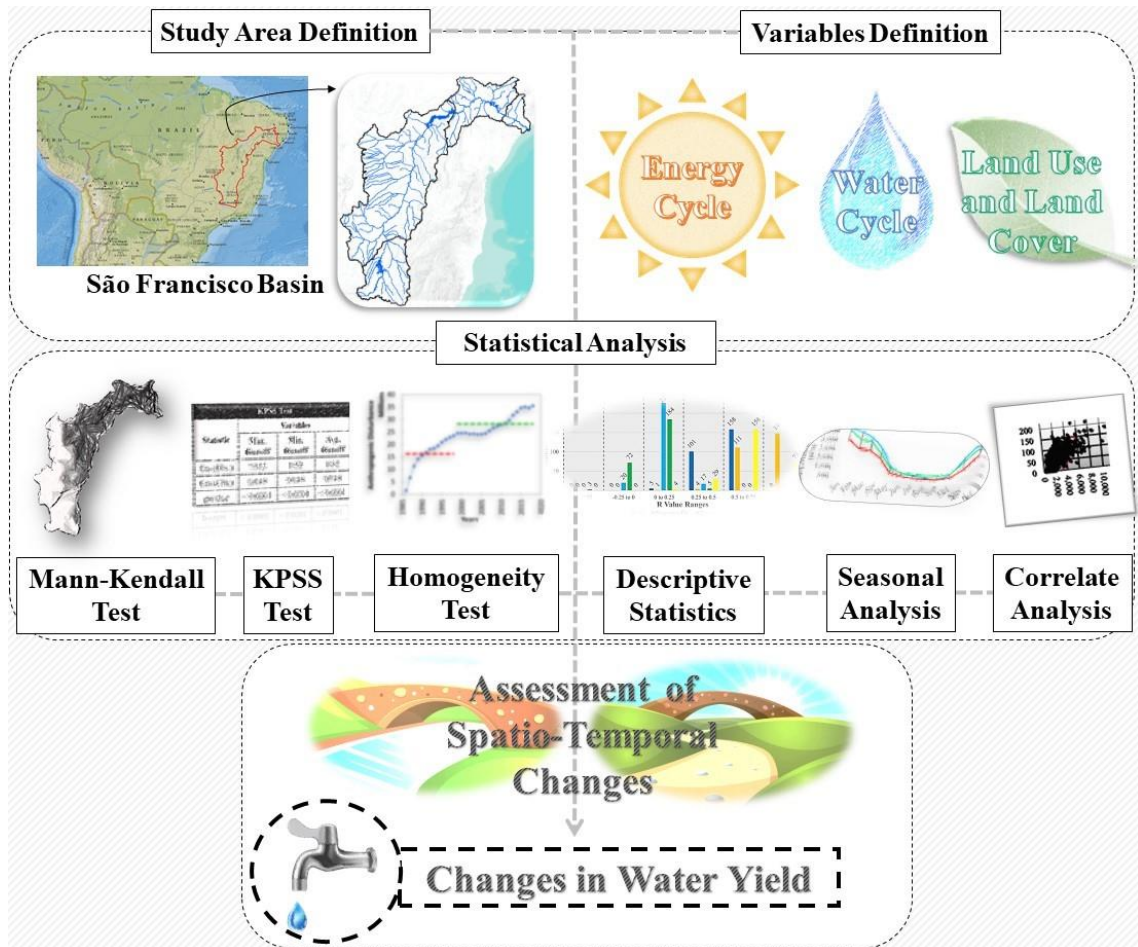


Figure 6.1 – Methodological flowchart

### 6.2.1. Study Area

The São Francisco Basin (SFB) (Figure 2) is located in the Northeast and North of the Southeast of Brazil, with an area of 630,000 km<sup>2</sup> and with its main river running 3,200 km from the source, in the State of Minas Gerais, at its mouth, on the border of the States of Alagoas and Sergipe, flowing into South Atlantic Ocean (Bezerra et al., 2019; de Jong et al., 2018). It is between the latitudes of 21° and 7° South, with climatic characteristics, according to the revised classification of Thornthwaite (Feddema, 2005), ranging from humid and wet sub-humid types

between latitudes 21° and 10° South (29% of basin area), until dry sub-humid, semi-arid and arid types between latitudes 17° and 7° South (71%).

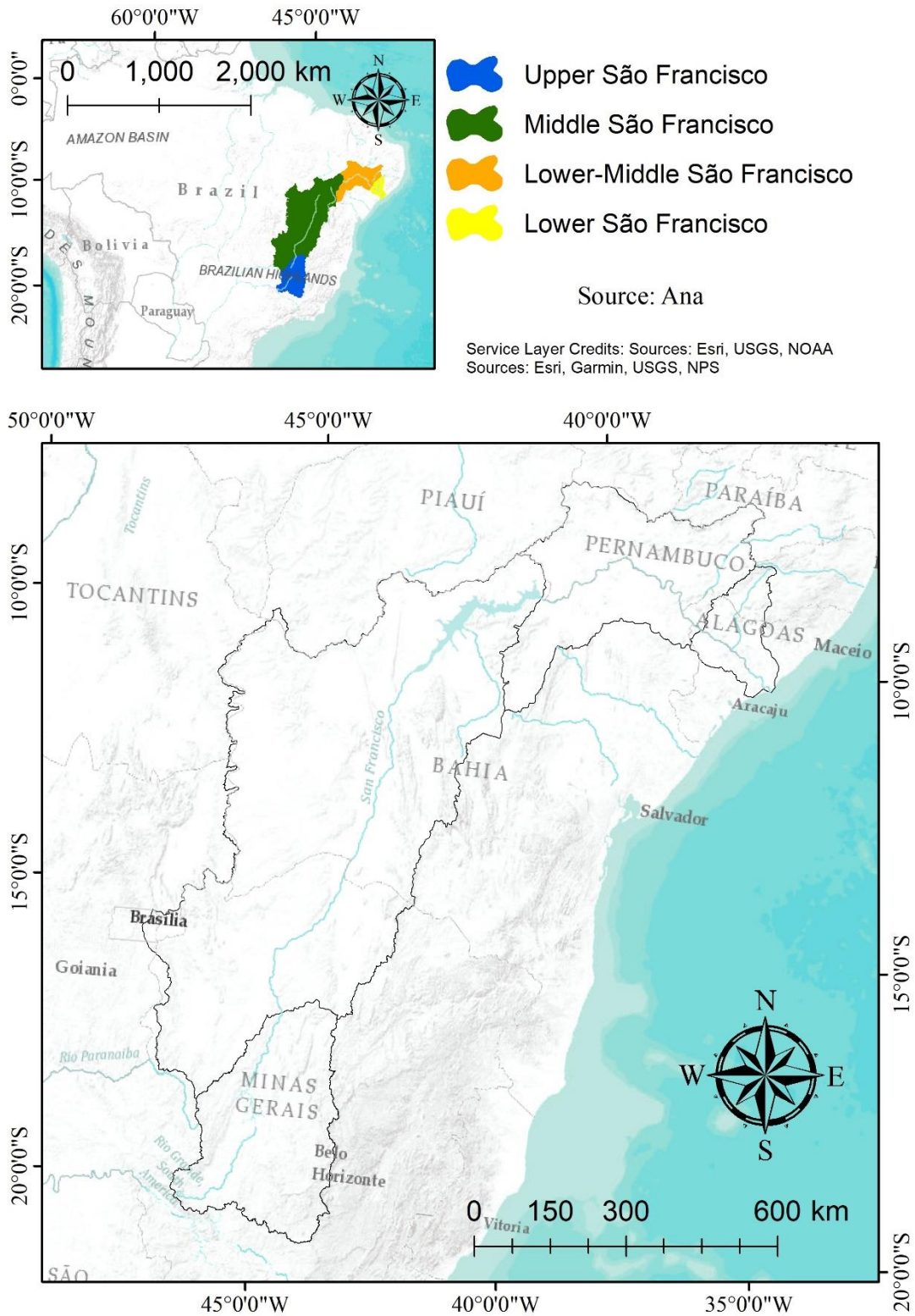


Figure 6.2 – Study area location

In humid and wet sub-humid areas, south and southwest of basin, temperatures reach an average of 20°C (Torres et al., 2012), with potential evapotranspiration ranging from 1,241 to 4,344 mm/year, with an average of 2,300 mm/year (Beaudoin and Rodell, 2019), and rains precipitate an average of 1,500 to 2,000 mm/year (Koch et al., 2015; Sun et al., 2016). In dry sub-humid, semi-arid and arid areas, north and northeast of basin, temperatures reach an average of 26.5°C (Torres et al., 2012), with potential evapotranspiration ranging from 1,533 to 5,110 mm/year, with an average of 2,884 mm/year (Beaudoin and Rodell, 2019), and rainfall precipitates an average of 350 mm/year (Koch et al., 2015; Sun et al., 2016).

Precipitation in humid and wet sub-humid areas is mainly associated with the South Atlantic Convergence Zone (SACZ) that operates in the southeastern region of Brazil and southwestern Bahia during the summer (between October and March) (Torres et al., 2012). In the dry sub-humid, semi-arid and arid areas, rains are concentrated during the months of March and April, caused mainly by action of the Intertropical Convergence Zone (ITCZ), which acts more intensely in this period due to weakening of the inter-hemispheric south gradient of sea surface temperature, which allows ITCZ to reach regions further south. In the rest of the year, there is a strong presence of a high-level cyclone over the Amazon, which inhibits rains formations in the region and favors dry weather conditions, which is often enhanced by strong *El Niño* events.

The humid and wet sub-humid areas cover almost all the sub-regions of Upper São Francisco and western part of the Middle. The main river has its contribution mainly from these areas, which were responsible for 93%, between 1951 and 1999, of total permanence flow curves ( $Q_{95}$ ). That is, approximately 43% of basin was responsible for maintaining flow rate that flowed through the riverbed 95% of the time. The other 57%, corresponding to the sub-regions of Low, Lower-Middle, and eastern part of the Middle São Francisco, which are mostly covered by dry sub-humid, semi-arid and arid areas, contributed with remaining 7% of  $Q_{95}$  (Pereira et al., 2007; Pruski et al., 2004). This showing the importance of the areas closest to its source for maintenance of main river.

São Francisco has an average flow rate of 2,850 m<sup>3</sup>/s, ranging from 1,077 to 5,290 m<sup>3</sup>/s (Bezerra et al., 2019), with a permanence flow curve ( $Q_{95}$ ) of 800.4 m<sup>3</sup>/s (Pereira et al., 2007; Pruski et al., 2004). It comes from 70% of the surface waters of entire Northeast region of Brazil (Torres et al., 2012), which has a population of over

53 million people, approximately a quarter of the Brazilian population. Besides, hydroelectric system of this river normally meets 70% of the demand for electricity in Northeast region (de Jong et al., 2018).

In relation to groundwater, the Urucua Aquifer System (UAS) is the most important for the SFB, responsible for approximately 35% of the São Francisco average flow recharge. During dry periods, the UAS is responsible for 80 to 90% of the São Francisco recharge, that is, it is essential to streamflow maintenance (Gonçalves et al., 2020).

The SFB has several geological formations, with a wide range of ages, from older rocks (Eoarchean – 3.6 billion years) occurring in a localized manner, to more recent ones (less than 65 million years), covering the entire basin area. Outcrops of sedimentary rocks predominate (69% of the territory), and in 26% of the basin there are outcrops of metamorphic, metasedimentary and metaigneous rocks, and 5% correspond to igneous rocks (CBHSF, 2016).

In the detrital and carbonated sedimentary lands there is high hydrogeological favorability (17% of the basin), highlighting the sedimentary lands of the Urucua Group. In 47% of the SFB there are variable favorabilities, associated with the significant diversity of terrains and their respective permeability conditions, acquiring particular expression in the Upper and Middle São Francisco (CBHSF, 2016).

In terms of geomorphology, approximately half of the basin is the morphostructural domain of the Neoproterozoic Cratons, in particular the São Francisco Craton, in which the Phanerozoic basins and sedimentary covers are developed over the crystalline basement rocks. The only region of the SFB that does not cover the Neoproterozoic Cratons is the Lower São Francisco, where the Neoproterozoic Mobile Belts are predominant (CBHSF, 2016; Donzé et al., 2020).

Added to these hydrological and geological conditions, the basin has vegetations of Cerrado types (Savannah Formation) with a great diversity of tree vegetations (Forest Formation) in Upper and western sub-region of Middle São Francisco, as well as the vegetation of Caatinga biome, which is widely spaced and smaller, associated with drier and hotter climate in Low, Lower-Middle and east of Middle São Francisco (Creech et al., 2015).

Land use is predominantly agricultural, with crops (46%) and pastures (41%) dominating the land cover in basin. Aside from, there are remnants of large and medium-sized tree vegetation, urban areas, mining, among others. The main

agricultural production is soy, with other major crops such as corn, wheat and cotton, in addition to important fruit centers (Juazeiro and Petrolina) (Correia et al., 2001) and family farming throughout the basin. Vegetations, crops and pastures are on soils of latosol (41% of the basin), podzols (11%), sandy soils (10%) and cambisols (7%) (Alcoforado de Moraes et al., 2018; Creech et al., 2015; Torres et al., 2012).

Covering approximately 7.5% of the Brazilian territory, SFB has a population of over 17 million people (8% of Brazilian population), 21% of which are considered poor by the country's standards (Sun et al., 2016). Due to population growth and the demand for food, water, jobs and services, the municipalities in basin have had satisfactory socio-economic development in recent decades, but at the cost of natural resources, mainly native vegetation, soil and water, relative with deforestation problems, desertification, water scarcity, pollution and water bodies silting up (Creech et al., 2015; de Jong et al., 2018; Koch et al., 2015).

From the above, it is clear that SFB has significant physical-natural and socioeconomic diversity, which are dynamic in space and time. Due to these factors, the basin was defined as a study area precisely because of its dynamics and diversity related to environmental and human aspects, which interfere with each other. The choice focused on dynamics pertinent to energy and water cycles, which are affected by the basin's socio-economic activities, but also affect them. The option for the area is also linked to the fact that the basin has one of the main rivers in Brazil, entirely within the national territory, which passes through the driest region and one of the poorest in the country. The river has great national importance due to its strong potential for economic use, mainly linked to agricultural activities, irrigation, public supply, navigation and generation of electric energy, but has been under strong pressure exactly by exploration of these same activities.

### **6.2.2. Variables Definition**

The variables defined in this research were those related to the energy flow and water cycle in SFB, as well as those that can interfere in these cycles, referring to land use and land cover (LULC), in addition to the minimum, average and maximum flows rate of São Francisco river (Table 1). The Global Land Data Assimilation System (GLDAS) database units have been converted, as suggested on Land Data Assimilation System website (<https://ldas.gsfc.nasa.gov/faq/ldas>), for better comparison between variables.

Table 6.1 - Database used

<b>GLDAS (1948 - 2019)</b> <b>[<a href="https://das.gsfc.nasa.gov/gldas">https://das.gsfc.nasa.gov/gldas</a>]</b>			<b>Dataset Units</b>	<b>Converted Units</b>
<b>Swnet</b>	Shortwave Radiation Flow		W/m <sup>2</sup>	W/m <sup>2</sup>
<b>Lwnet</b>	Long Wave Radiation Flow		W/m <sup>2</sup>	W/m <sup>2</sup>
<b>Qh</b>	Sensitive Heat Flow		W/m <sup>2</sup>	W/m <sup>2</sup>
<b>Qle</b>	Latent Heat Flow		W/m <sup>2</sup>	W/m <sup>2</sup>
<b>Rainf</b>	Rainfall Rate		Kg/m <sup>2</sup> /s	mm
<b>AvgSurfT</b>	Average Surface Temperature		K	°C
<b>PotEvap</b>	Potential Evapotranspiration		W/m <sup>2</sup>	mm
<b>Evap</b>	Real Evapotranspiration		Kg/m <sup>2</sup> /s	mm
<b>Tveg</b>	Vegetation Transpiration		W/m <sup>2</sup>	mm
<b>Ecanop</b>	Direct Evaporation of Plants Canopy		W/m <sup>2</sup>	mm
<b>Esoil</b>	Direct Evaporation of Bare Soil		W/m <sup>2</sup>	mm
<b>Canint</b>	Moisture in Plants Canopy		Kg/m <sup>2</sup>	mm
<b>RootMoist</b>	Root Zone Soil Moisture		Kg/m <sup>2</sup>	mm
<b>Qs</b>	Surface Runoff		Kg/m <sup>2</sup> /3h	mm
<b>Qsb</b>	Subsurface Runoff		Kg/m <sup>2</sup> /3h	mm
<b>MapBiomias (1985 - 2018)</b> <b>[<a href="https://mapbiomas.org/">https://mapbiomas.org/</a>]</b>			<b>Dataset Units</b>	<b>Converted Units</b>
<b>LULC</b>	Lan Use and Land Cover		-	-
<b>MEaSURES</b> <b>[<a href="https://lpdaac.usgs.gov/data/get-started-data/collection-overview/measures/">https://lpdaac.usgs.gov/data/get-started-data/collection-overview/measures/</a>]</b>			<b>Dataset Units</b>	<b>Converted Units</b>
<b>VCF</b>	<b>Tree Cover</b>	Percent Tree Cover (1982 - 2014)	%	%
	<b>Non- Tree Cover</b>	Percent Non-Tree Cover (1982 - 2014)	%	%
	<b>Bare Ground</b>	Percent Bare Ground (1982 - 2014)	%	%
<b>VIP</b>	<b>NDVI</b>	Normalized Difference Vegetation Index (1981 - 2019)	-	-
<b>ANA (1928 - 2019)</b> <b>[<a href="http://www.snirh.gov.br/hidroweb/">http://www.snirh.gov.br/hidroweb/</a>]</b>			<b>Dataset Units</b>	<b>Converted Units</b>
<b>Flow Rate</b>	Minimum, Average and Maximum Flows Rate		m <sup>3</sup> /s	m <sup>3</sup> /s

GLDAS is a program from the National Aeronautics and Space Administration (NASA) in which observational data from orbital images and information collected in the field are used to model the dynamics of terrestrial phenomena linked to energy flow and the water cycle of the planet Earth. Produces results almost in real-time, with resolutions that vary between 2.5° and 1 km, with historical series between 1948 until today with periodic update (Beaudoing and Rodell, 2019; Rodell et al., 2004).

The data used in GLDAS contains relief information, soil types, vegetation and atmospheric variables such as rain and radiation flows. Data assimilation techniques are employed to incorporate hydrological products based on satellite sensor imaging that include snow cover and water equivalent, soil moisture, surface temperature and leaf area indexes (Beaudoin and Rodell, 2019; Rodell et al., 2004).

Although the use of this database is still scarce for hydrological studies in the SFB, those that used it (Paredes-Trejo et al., 2021; Sun et al., 2016) obtained results consistent with other databases from remote sensing already validated, such as the Tropical Rainfall Measuring Mission (TRMM). Both studies identified similar trends related to hydrological dynamics, consistent with meteorological events related to such trends.

The Annual Mapping of Land Use and Land Cover in Brazil (MapBiomas) (Souza et al., 2020) is a collaborative network with specialists in Brazilian biomes, land uses, remote sensing, geographic information systems and computer science, which uses cloud processing and automatic classifiers (Random Forest) developed and operated from Google Earth Engine platform. Since its foundation (2015) it has been generating an annual historical series of LULC maps for the whole of Brazil (1985 to 2018 - Collection 4.1), with a spatial resolution of 30 meters using the series of images from Landsat sensors.

The program Making Earth System Data Records for Use in Research Environments (MEaSUREs), from NASA's Land Processes Distributed Active Archive Center (LP DAAC), is dedicated to the advancement of remote sensing and the scientific use of measurements from satellite sensors to expand the understanding of terrestrial system, with production and recording of consistent, high quality and long-term data. Among several databases, those used in this research were the Vegetation Continuous Fields (VCF) (Hansen and Song, 2018) and the Vegetation Index and Phenology (VIP) (Didan and Barreto, 2016). The first is a collection that provides global vegetation information from the Advanced Very High-Resolution Radiometer (AVHRR) long-term records between 1982 and 2014, annually, with a spatial resolution of 5,600 m containing information on the percentage of tree vegetation cover, non-tree vegetation cover and bare ground. The second is another collection containing a monthly historical series from 1981 to 2019, of vegetation and landscape phenology indexes, based on data from the Moderate-Resolution Imaging

Spectroradiometer (MODIS), AVHRR and *Satellite Pour l'Observation de la Terre* (SPOT), also with a spatial resolution of 5,600 m.

The Hidroweb Portal (<http://www.snirh.gov.br/hidroweb/>) is a Brazilian tool that is part of the National Water Resources Information System (SNIRH, acronym in Portuguese) and offers access to database that contains all information collected by the National Hydrometeorological Network (RHN, acronym in Portuguese), which gathers data on flows rate, river height, rainfall, climatology, sediment and water quality. The data used come from conventional fluviometric stations with codes 45298000 (14.3° S and 43.76° W) and 49705000 (10.21 S and 38.82 W), with historical series of daily and monthly frequencies between 1928-2019 and 1959-2019, respectively. The use of these two stations is better detailed in item 3.1, as the choice of both was defined based on some results of this research.

### **6.2.3. Statistical Analysis**

The statistical procedures were broken down into three stages: i) first performed on variables related to energy flow and water cycle; ii) later on variables related to LULC; iii) and, finally, in the variables related to São Francisco river flow rate and its correlations with the analysis of the previous data.

#### **6.2.3.1. Statistical analysis on variables related to energy and water cycles**

First, the Mann-Kendall test (MK tau) was performed on variables related to energy flow and water cycle, from GLDAS database, monthly, between January 1948 and December 2019.

This first analysis aimed to verify the spatiotemporal behavior of the variables and to search for different trend patterns throughout SFB in the mappings made by the test, pixel by pixel, using the Series Trend tool of the Earth Trend Modeler module available by Idrisi Selva 17.0 software (Eastman, 2016). With the identification of patterns, it was decided to divide the study area into two parts (P1 and P2). This decision is explained in results.

MK tau is a non-parametric trend indicator that measures the degree to which a trend is increasing or decreasing consistently. It was first proposed by Mann (1945) and later studied by Kendall (1975), then enhanced by Hirsch et al. (1982) and Hirsch & Slack (1984), which made it possible to take seasonality into account. It has a range of -1 to +1. A value of +1 indicates a trend that continually increases and

never decreases. The opposite is true when it has a value of -1. The zero value indicates that there is no consistent trend. All combinations of pair values over time are evaluated at each pixel and a count is made of the number that is increasing or decreasing over time. It is simply the relative frequency of increases minus the relative frequency of decreases (Eastman, 2016).

With P1 and P2 discriminated, descriptive statistics were made to verify variations of the average values of each variable in both areas, checking if in general there was an increase, stability or decrease in each one of them. Stationarity (KPSS) and homogeneity (Pettitt and Buishand) tests were also performed.

The stationarity test used was the KPSS (Kwiatkowski et al., 1992), which allows to check whether a series is stationary or not. The test result varies from zero to  $\infty$  (Eta Observed Value), in which the higher the critical value (Eta Critical Value), greater the tendency for the series not to be stationary, and the opposite being also true, that is, as closer to zero and below the critical value, greater the tendency to stationarity.

The homogeneity tests used were those by Buishand (1982) and Pettitt (1979), that check if a series is homogeneous over time, or if there is a moment when a change or break in that homogeneity occurs. Such tests were selected based on different sensitivities they present for identification at the change time and because they are widely used to test homogeneity in environmental data series (Bickici Arikan and Kahya, 2019; Rougé et al., 2013; Serinaldi et al., 2018; Serinaldi and Kilsby, 2015; Yozgatligil and Yazici, 2016).

### **6.2.3.2. Statistical analysis on variables related to LULC and MEaSURES**

To measure changes in LULC in SFB, the Change Analysis tool of Land Change Modeler module, from Idrisi Selva 17.0 software, was used (Eastman, 2016). In this tool, it was possible to verify the main changes between the years 1985 and 2018.

In addition to measuring changes in LULC using MapBiomass data, the MEaSURES database was also used, which contains data on the percentage of tree cover, non-tree cover and bare ground (VCF) between 1982 and 2014, and NDVI (VIP) between 1981 and 2019, respectively (Didan and Barreto, 2016; Hansen and Song, 2018).

For MapBiomas LULC data, from the measurements generated in Land Change Modeler module, all classes related to human actions (Farming, Mining, Planted Forest and Urban Areas) were grouped into a single class called Anthropogenic Disorders. In this, Mann-Kendall and homogeneity tests (Pettitt and Buishand) were performed.

In the MEaSURES data, Mann-Kendall test was used to identify differences spatiotemporal trends in the SFB with Series Trend tool of Earth Trend Modeler module from Idrisi Selva 17.0 software aid (Eastman, 2016).

#### **6.2.3.3. Statistical analysis on variables related to São Francisco river flow rate**

The data series on the minimum, average and maximum flows rate of São Francisco river was analysed in two river stations, one located in P1 (code 45298000) and another in P2 (code 49705000).

Mann-Kendall, stationarity and homogeneity tests were also applied. After the application of this tests and results obtained, these were compared to the results of tests related to the variables of previous topics. This was performed to verify possible implications of changes in land cover, in energy flows and, consequently, in water cycle basin, and the impacts of these processes on flow rate dynamics of São Francisco river at P1 and P2.

To reinforce possible influences of changes in land cover in water cycle basin, correlation analyzes between NDVI and variations related to water cycle were performed, with the aid of Correlate module of Idrisi Selva 17.0 software (Eastman, 2016). The main application of the module is to identify areas that correlate with a specific temporal pattern of interest, calculating the correlation coefficient R between one or more predictors (independent) with a time series of images (dependent) for each pixel. In addition, such analyzes were also performed between historical series of average flows rate in P1 and P2 with rainfall, surface and subsurface runoff data, using Pearson's correlation (Barber et al., 2020).

### **6.3. Results and Discussion**

This topic is divided into two subtopics, which are results and discussion 1) related to spatiotemporal analysis of energy flow, water cycle and LULC variables; and 2) referring to consequences on the dynamics of São Francisco river flow rate resulting from changes in the variables evaluated in the previous subtopic.

### 6.3.1. Spatiotemporal analysis of energy flow, water cycle and LULC variables

Mann-Kendall tests carried out for energy flow variables showed that there were different intensities in trends, positive and negative, of radiation (short and long waves) and heat (sensitive and latent) fluxes, in specific areas in SFB between January 1948 and December 2019 (Figure 3).

Due to this distinctions, the basin was segmented into two parts, P1 and P2 (Figure 3). Such segmentation was based on trends of radiation flux (short and long waves) (Tables 2 and 3), which will influence the dynamics of other variables, such as heat flux (sensitive and latent), evapotranspiration and presence of moisture in the canopies and plants' root zones. These results also guided the choice for used fluviometric stations locations, aiming to relate the changes in trends of the variables evaluated in GLDAS database with flow rate dynamics. The definition of the fluviometric stations followed two conditions: i) close to the place further downstream from P1 and P2, seeking to cover the entire contribution basin and; ii) with sufficient historical series to satisfactorily cover the period of GLDAS and MEaSURES data.

Although, on average, the latent heat flux is more stable at P2 and in the Lower SF there is a more significant drop in precipitation, the results in Mann-Kendall test, for the entire SFB, show that there were increases in radiation and heat fluxes, in addition to stability in rainfall indexes (Figures 3, 4 and Table 4). The KPSS test confirms such trends, showing that rainfall has a stationary behavior, both in P1 and P2, over time, whereas for radiation and heat fluxes the critical value has been reaching, mainly for specific heat and short-wave radiation, showing a tendency towards non-stationarity throughout the series.

As a consequence of increase in radiation and heat fluxes, trends in potential and real evapotranspiration are positive, except for real evapotranspiration in P2, tending to stationarity. This is probably due to the fact that in P1 there is more moisture availability to be lost to the atmosphere by evapotranspiration than in P2 (in addition to less radiation and heat fluxes) since the potential evapotranspiration in P1 is three times greater than the real one, while in P2 it is five times. Although actual evapotranspiration did not keep up with the increase in potential, it was positive due to the plant transpiration growth, as the water evaporation directly from plants' canopies reduced, and evaporation directly from bare soils was stable.

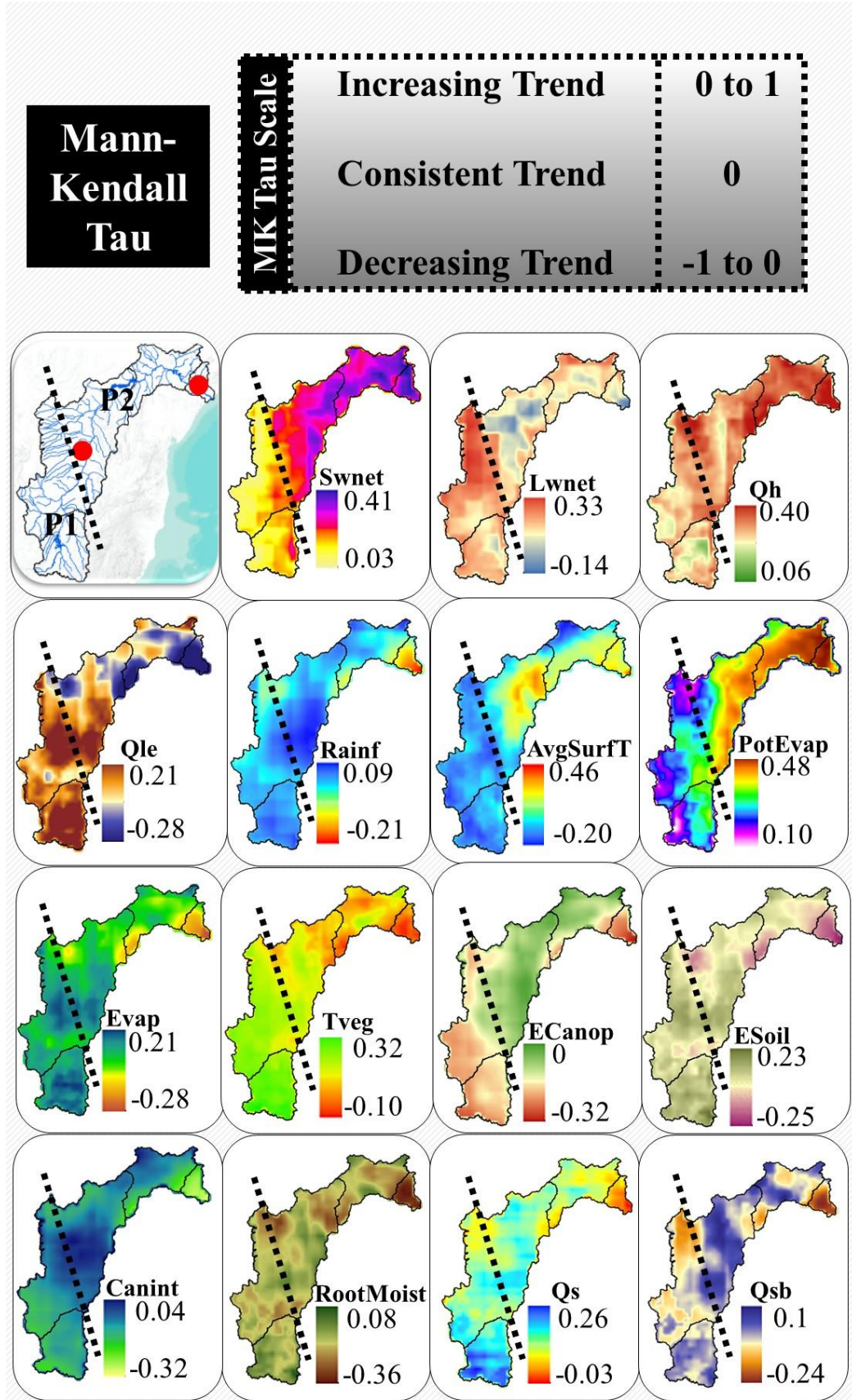


**Figure 6.3** - Trends in variables referring to energy flow and water cycle in SFB between January 1948 and December 2019. The red dots are the fluviometric stations locations with codes 45298000 (P1) and 49705000 (P2).

**Table 6.2** - Trend (MK) range values and significance (p) analyze for energy flow variables in P1, between 1948 and 2019.

Variable	MK Tau	Area (%)	p-value	Area (%)
Swnet	0.03 to 0.18	95	0	89
	0.18 to 0.41	5	> 0	11
Lwnet	0 to 0.1	10	0	98
	0.1 to 0.33	90	> 0	2
Qh	0.06 to 0.1	2	0	100
	0.1 to 0.4	98	> 0	0
Qle	-0.04 to 0.1	54	0	79
	0.1 to 0.21	46	> 0	21

**Table 6.3** - Trend (MK) range values and significance (p) analyze for energy flow variables in P2, between 1948 and 2019.

Variable	MK Tau	Area (%)	p-value	Area (%)
Swnet	0.13 to 0.18	9	0	100
	0.18 to 0.41	91	> 0	0
Lwnet	-0.14 to 0.1	42	0	79
	0.1 to 0.33	58	> 0	21
Qh	0.14 to 0.18	4	0	100
	0.18 to 0.4	96	> 0	0
Qle	-0.28 to 0.1	81	0	54
	0.1 to 0.21	19	> 0	46

**Table 6.4** – Absolute and relative variations of the variables related to the energy flow and water cycle in the SFB between 1948 and 2019.

Variable	Average Variation - P1		Average Variation - P2	
	Absolute	Relative	Absolute	Relative
Swnet	+ 10 W/m <sup>2</sup>	+ 5%	+ 23 W/m <sup>2</sup>	+ 12%
Lwnet	+ 6 W/m <sup>2</sup>	+ 9%	+ 3 W/m <sup>2</sup>	+ 4%
Qh	+ 14 W/m <sup>2</sup>	+ 29%	+ 26 W/m <sup>2</sup>	+ 40%
Qle	+ 5 W/m <sup>2</sup>	+ 12%	+ 2 W/m <sup>2</sup>	+ 4%
Rainf	-63 mm/year	- 5%	0 mm/year	0%
PotEvap	+ 467 mm/year	+ 23%	+ 1072 mm/year	+ 45%
Evap	+ 66 mm/year	+ 8%	+ 31 mm/year	+ 5%
Tveg	+ 176 mm/year	+ 66%	+ 76 mm/year	+ 26%
Ecanop	- 127 mm/year	- 37%	- 63 mm/year	- 28%
Esoil	+ 13 mm/year	+ 6%	0 mm/year	0%
CanopInt	- 0.07 mm	- 37%	- 0.04 mm	- 36%
RootMoinst	- 16 mm	- 7%	- 31 mm	- 15%
Qs	+ 64 mm/year	+ 400%	+37.6 mm/year	+ 4,700%
Qsb	- 162.4 mm/year	- 36%	- 88 mm/year	- 70%

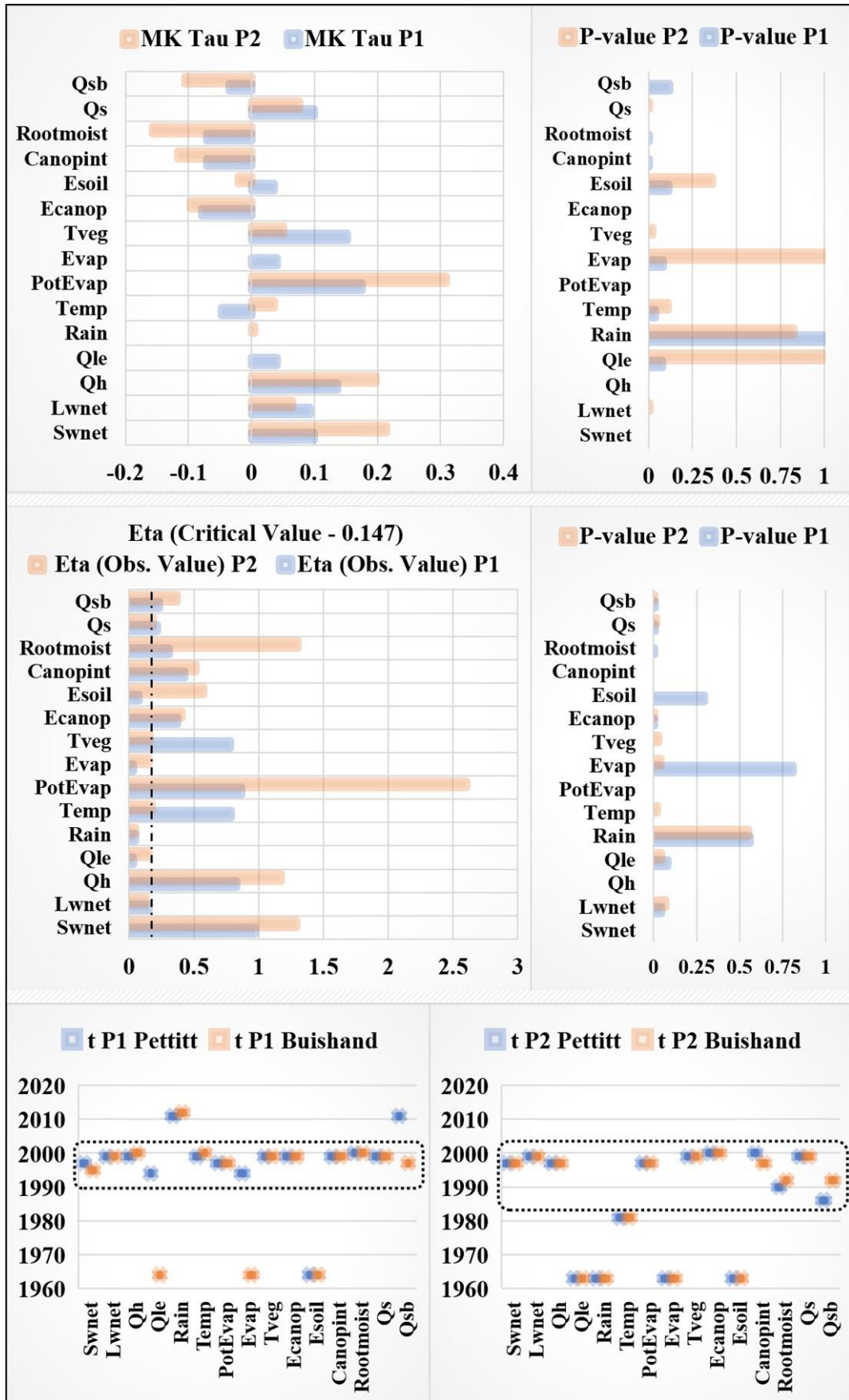


Figure 6.4 – Mann-Kendall, KPSS and Homogeneity tests (Pettitt and Buishand) for energy flow and water cycle variables in SFB between 1948 and 2019.

The trends for the presence of moisture in plants' canopies and their root zones are decreasing, ratified by non-stationarity in KPSS test. The reduction in humidity in these places is probably due to the increase in evapotranspiration, but, mainly, to the rise in surface runoff, which has a positive tendency, and to subsurface runoff reduction, which has a downward trend. This shows less water infiltration in the soil, providing less moisture to plants' roots, and less water containment by vegetation, reflected by less water maintenance in their canopies and increase in water loss due to surface runoff.

These results are reinforced from the analysis of LULC changes, which show that between 1985 and 2018 at SFB there was a reduction of 68,631 km<sup>2</sup> of native vegetation formations, equivalent to 10.8% of the basin total area. From this reduction, 95.7% was caused by agricultural activities (perennial and semi-perennial crops, planted forests and pastures), and the remainder, 2,951 km<sup>2</sup> (4.3%), due to the advance of urban areas, mining and other uses (Figure 5). The most degraded vegetation formations were savannas and grasslands, medium and small sizes vegetations from Cerrado and Caatinga biomes and transition between them. The third most affected were forests, of medium and large size, originating mainly in Atlantic Forest biome, but also present in transition areas between these, Cerrado and Caatinga.

This reduction in native vegetation formations and their substitution by areas for agricultural use caused a fall in tree cover (Table 5), both in P1 and P2. As for the non-tree cover, in P1 and P2 there was an increase, reflecting the pasture and crop expansion in detriment of forest and savanna areas, medium to large vegetation. The bare soil, at the same time, was reduced in P1, even with native vegetation degradation, due to territorial growth of agricultural cover. Although there were dynamics similar to P1 in P2, that is, the replacement of native vegetation with pastures and crops, there was a significant increase in bare soil, in contrast to what happened in P1.

Between 1982 and 2014, in P1, tree cover reduced, on average, from 18.5% to 15%, and non-tree cover increased from 77.1% to 81.3%. Bare soil fell from 5.8% to 4%. In P2, tree cover dropped, on average, from 22% to 13.3%, and non-tree cover increased from 72.7% to 76.8%. Bare soil rose from 5.3% to 9.9%.

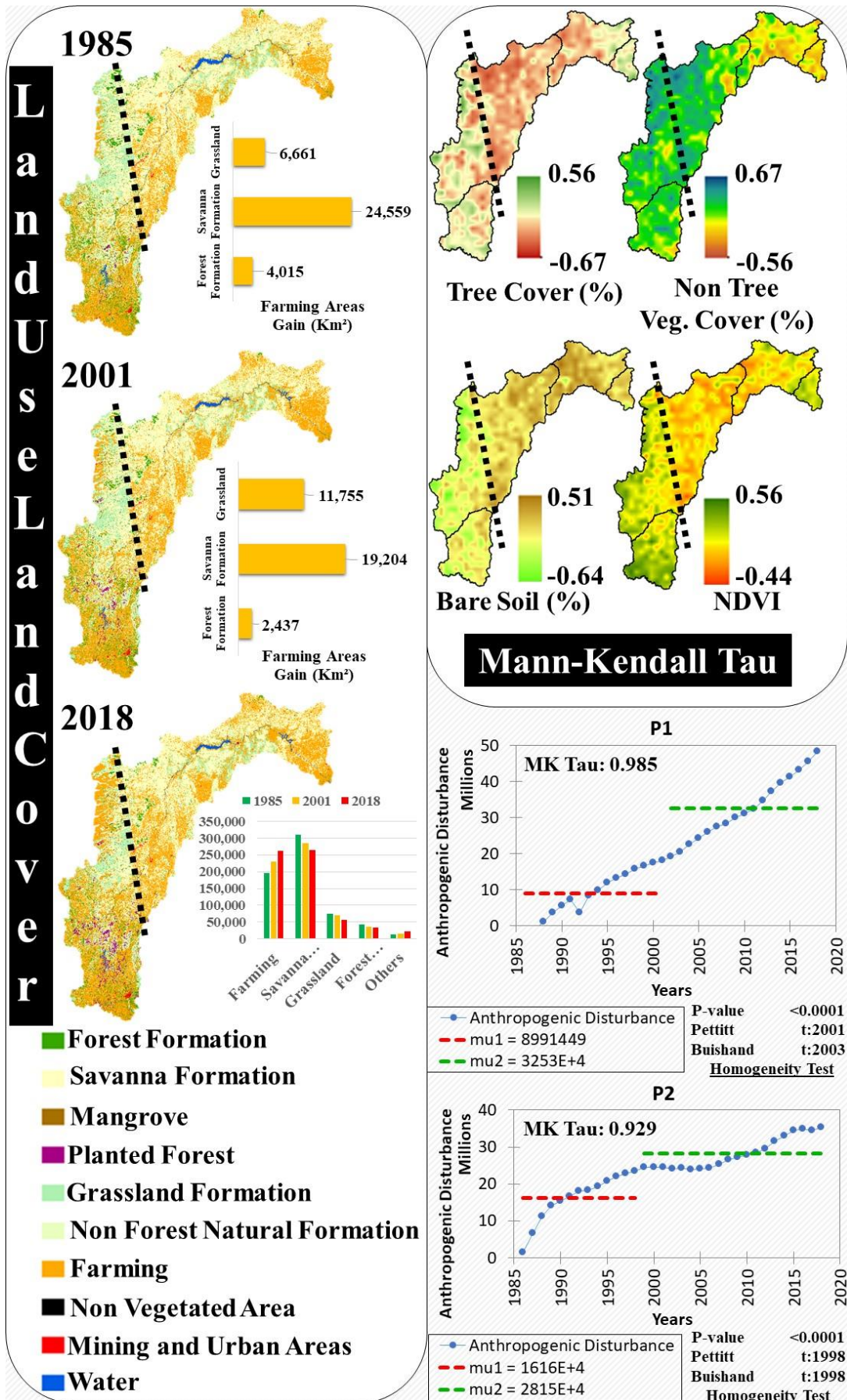


Figure 6.5 – Changes in land use and land cover in SFB and its effects on the presence of tree and non-tree vegetation cover and bare soil.

**Table 6.5** - Changes in tree and non-tree vegetable coverings and bare soil in the SFB.

<b>Tree Cover (%)</b>			<b>Non-Tree Cover (%)</b>			<b>Bare Soil (%)</b>		
<b>MK Statistics</b>	<b>P1</b>	<b>P2</b>	<b>MK Statistics</b>	<b>P1</b>	<b>P2</b>	<b>MK Statistics</b>	<b>P1</b>	<b>P2</b>
Average	-0.06	-0.2	Average	0.2	0.1	Average	-0.13	0.1
Min.	-0.56	-0.58	Min.	-0.28	-0.44	Min.	-0.6	-0.58
Max.	0.56	0.56	Max.	0.67	0.67	Max.	0.51	0.51
Std. Dev.	0.21	0.18	Std. Dev.	0.18	0.23	Std. Dev.	0.21	0.17
<b>MK Range (P1)</b>	<b>Area (%)</b>		<b>MK Range (P1)</b>	<b>Area (%)</b>		<b>MK Range (P1)</b>	<b>Area (%)</b>	
-0.56 to 0	60		-0.28 to 0	15		-0.6 to 0	73	
0 to 0.56	40		0 to 0.67	85		0 to 0.51	27	
<b>MK Range (P2)</b>	<b>Area (%)</b>		<b>MK Range (P2)</b>	<b>Area (%)</b>		<b>MK Range (P2)</b>	<b>Area (%)</b>	
-0.58 to 0	87		-0.44 to 0	36		-0.58 to 0	30	
0 to 0.56	13		0 to 0.67	64		0 to 0.51	70	

Concerning the NDVI (Table 6), even with drop in tree cover in P1, there was mostly an increase, which on average rose 0.06, from 0.50 to 0.56. In P2, in general, it remained stable, with a drop of 0.01, from 0.52 to 0.51, approximately half of the area falling and the remainder rising.

**Table 6.6** - Changes in NDVI in SFB.

<b>MK Statistics</b>	<b>P1</b>	<b>MK Statistics</b>	<b>P2</b>
Average	0.18	Average	0
Min.	-0.32	Min.	-0.35
Max.	0.56	Max.	0.56
Std. Dev.	0.17	Std. Dev.	0.13
<b>MK Range (P1)</b>	<b>Area (%)</b>	<b>MK Range (P2)</b>	<b>Area (%)</b>
-0.32 to 0	18	-0.35 to 0	57
0 to 0.56	82	0 to 0.56	43

Arboreal vegetation has a greater capacity to retain rainwater in its canopies, favors infiltration and retention of moisture in the soil (Ebling et al., 2021; Patidar and Behera, 2018). It also reduces the incidence of radiation and, consequently, the heat flux close to the ground, ensuring less evaporation (Borges et al., 2020; Dugdale et al., 2018). So, the increase in vegetation transpiration across the SFB and the concomitant reduction in water evaporation directly from the vegetation canopy is likely due to the replacement of native vegetation by crops resulted in an increase in the areas occupied by non-tree vegetation at the same time that arboreal vegetation was reduced. The increase in crop areas exposes the soil to greater radiation and

heat fluxes, consequently causing greater potential evaporation, in addition to the plants themselves needing water for their development, which results in greater plant transpiration, especially in irrigated crops.

The growth of bare soil in P2 is linked to the fact that rainfed agriculture is predominant in the region (Kemp-Benedict et al., 2011; Zeri et al., 2018), being practiced for three to four months of the year, approximately the same time that the typical vegetation of the region blooms (Barbosa et al., 2019; Barbosa and Lakshmi Kumar, 2016; Cunha et al., 2015), to which loses its leaves in the dry period (8 to 9 months) as an adaptation to the semi-arid climate to miss less water to the environment. The stability in evaporation directly from the bare soil is due to the occurrence of less precipitation in P2 in relation to P1 and its stable trend over time, resulting in lower humidity in the environment, even with greater potential evapotranspiration.

The energy flow and water cycle variables (GLDAS data) that showed a trend, positive or negative, with significant p-values, obtained results in Pettitt and Buishand tests that showed a break in homogeneity mainly in the 1990s, varying between 1995 and 2000 in P1, and between 1986 and 2000 in P2 (Figure 4). The variables latent heat, precipitation, evapotranspiration, direct water evaporation from bare soil and subsurface runoff, whether in P1 and P2 or one of them, were those that obtained meanings that were more distant from zero, being exactly those that showed a break in homogeneity in different years to the rest of variables. This means that there was no break in their series, as the results in Mann-Kendall and KPSS tests showed that the variables with most distant values of significance were exactly those with no defined trend, that is, tending to stationarity.

The tests by Pettitt and Buishand for anthropogenic disturbance (LCLU data) (Figure 5), show that the break in homogeneity in historical series of occurred in the late 1990s for P1 and early 2000s for P2, very close to the results achieved for variables from the GLDAS database.

### **6.3.2. Impacts and changes in São Francisco river' flow rate dynamics**

Although the drop in rainfall index in P1 was small, 5% between 1948 and 2019, the drought events of the last decade (2010-2019) affected the permanence flow curve of São Francisco river ( $Q_{95}$  and  $Q_{50}$ ) (Figure 6). It is also noteworthy that these flows were influenced by the temporal behavior of rainfall, increasing when

rainfall increases (between 1950 and 1989) and decreasing when rainfall drops (between 1990 and 2019).

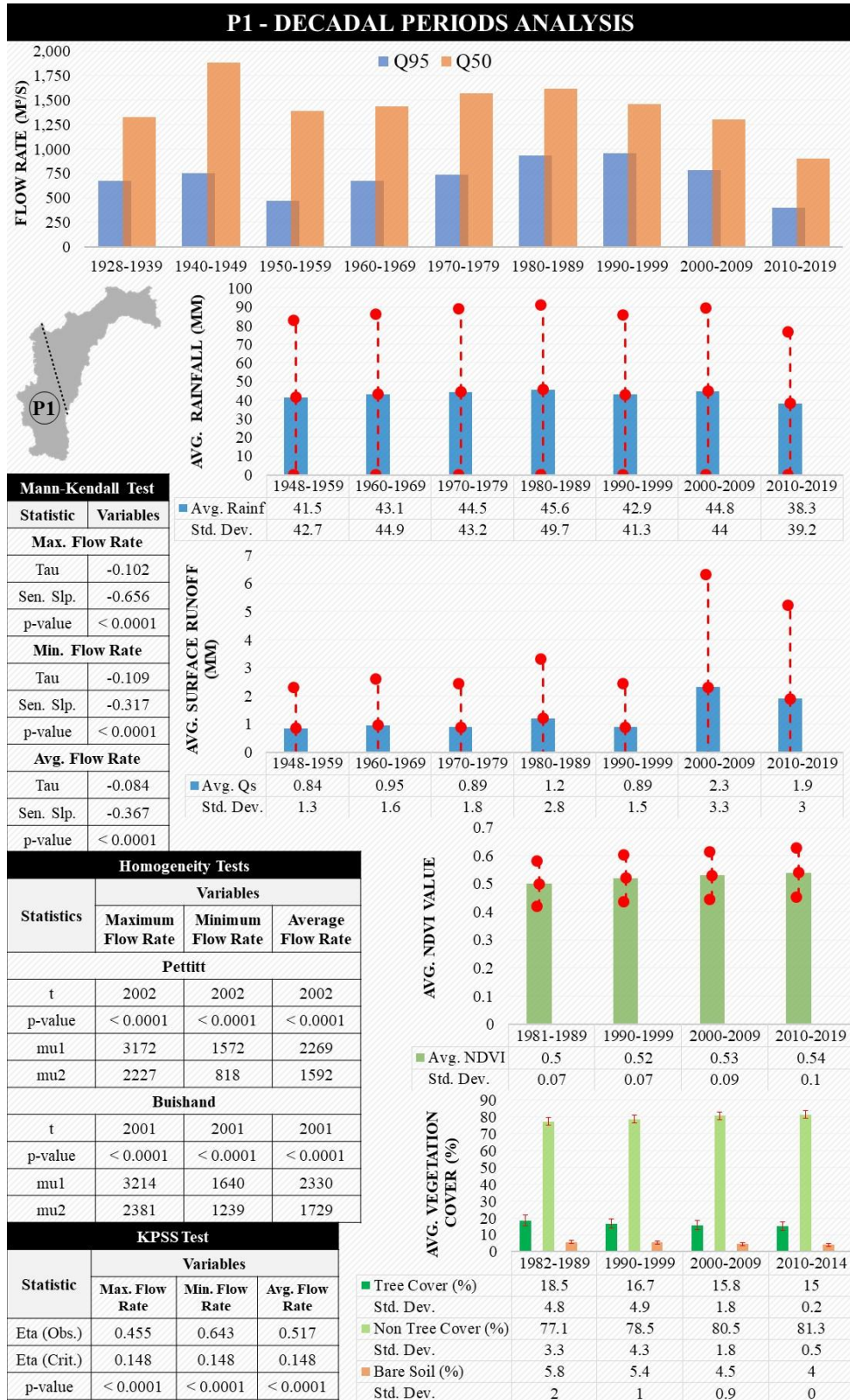


Figure 6.6 – Influence of rain dynamics and changes in land cover on the behavior of SFB flow rate in P1.

Another relevant factor is the land cover changes caused by the expansion of activities and land uses, mainly linked to agriculture and livestock. Even though in P1 there was a fall in bare soils, this was accompanied by a reduction in tree vegetation cover and an increase in the non-tree vegetation cover, due exactly to increase in pastures and crops areas. This fact has implications for other variables related to energy flow and water cycle, such as the greater radiation flux and, consequently, of heat flux, causing a greater evapotranspiration process, in addition to reduction in tree cover contribute to increase in surface runoff and reduction of water soil infiltration, reducing subsurface runoff and soil moisture in plants root zone.

Even with the reduction in rainfall during the 2000s and 2010s, surface runoff was greater than in previous decades, when there were similar or higher rainfall levels. This has an impact on the long-term flow rate of São Francisco river, given the precipitated water that drains superficially is reaching the watercourses faster due to reduction of friction caused by the replacement of the land cover. Thus, water soil infiltration reduced and caused less subsurface runoff, impairing the recharge of groundwater that supplies tributaries and the main river itself. This supply is even more important in drought periods.

In P2 (Figure 7), the situation is similar to P1, although there was a greater drop in tree cover and a greater increase in bare soil. The exception is the behavior of rainfall over the decades, which is not similar to that of flows rate (Figure 7). This occurs because in P2 the flow rate also follows the behavior of P1 rains, which are responsible for 65% of the water entering basin on average.

The impacts are even clearer when the statistical results referring to the maximum, average and minimum flows rate are revealed, which show downward trends (MK) with values of -0.102, -0.109 and -0.084 respectively, in P1 (Figure 6), and P2 (Figure 7) with values of -0.151, -0.062 and -0.115. KPSS tests for all flows rate show that the critical levels have been reached, reporting non-stationarity in the series. The tests by Pettitt and Buishand reveal that the break in historical series homogeneity occurred in the early 2000s, in agreement with years obtained for data on LULC and very close to energy fluxes and water cycle variables. This fact is a strong indication that changes in LULC in SFB have resulted in changes in the natural cycles of energy and water in the basin.

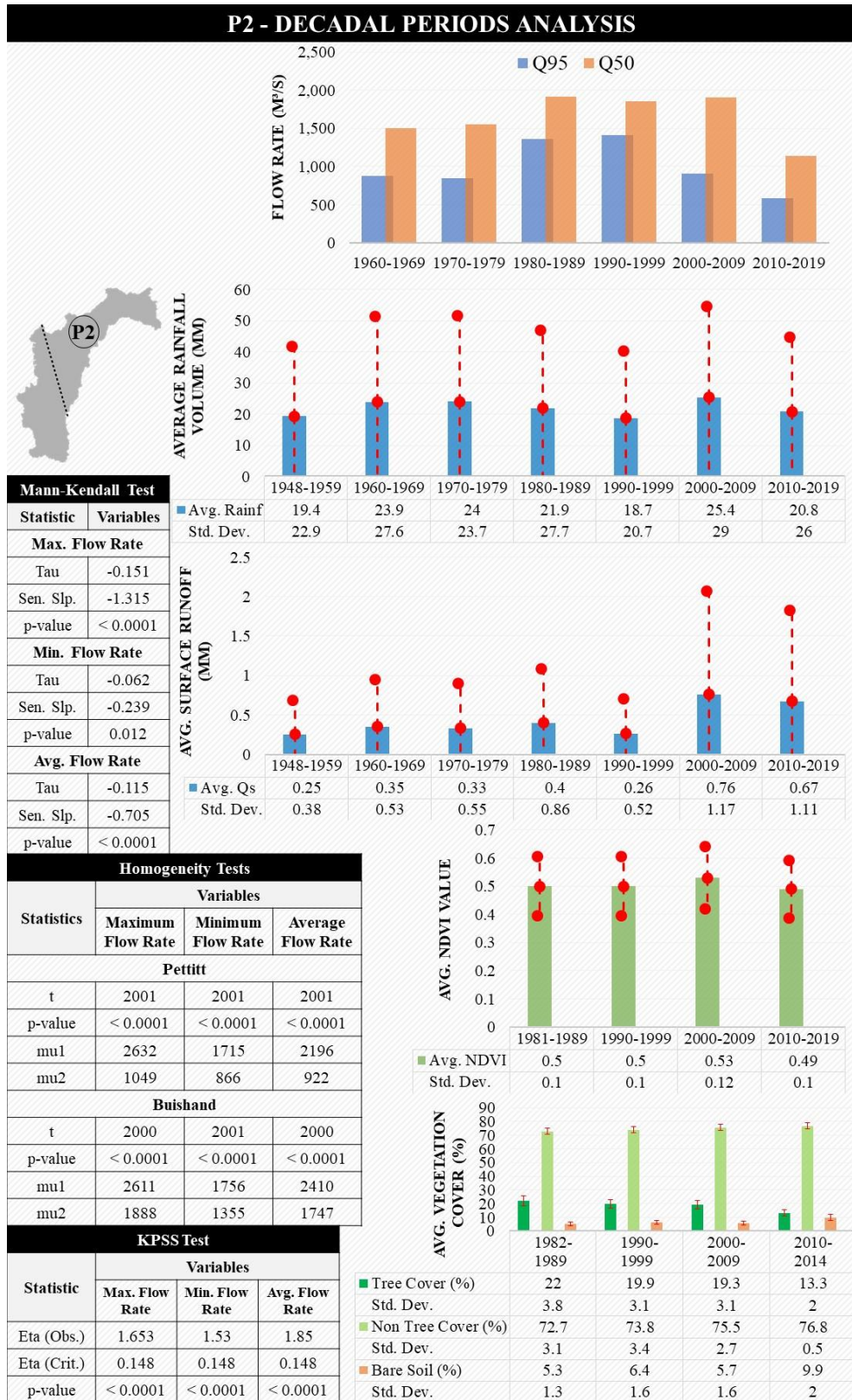


**Figure 6.7** – Influence of rain dynamics and changes in land cover on the behavior of SFB flow rate in P2.

It is also worth mentioning another factor that influenced the flows rate, which is the construction of the Sobradinho dam, in the state of Bahia. Inaugurated in 1982,

from then on the dam contributed to regularization of the São Francisco flow rate. Between 1959 and 1980, in rainy season, maximum and minimum flows rate reached values close to 4,600 and 2,800 m<sup>3</sup>/s, respectively, and 1,200 and 1,100 m<sup>3</sup>/s, respectively, in drought period. From the 1980s to 2000s, even with a certain increase in rainfall, maximum and minimum flows rate did not reach 3,600 and 2,400 m<sup>3</sup>/s, respectively, in rainy season, and exceeded 1,900 and 1,500 m<sup>3</sup>/s, respectively, in drought period, showing a control of increase in flows rate when the rains occur with greater frequency and intensity, and release when the drought occurs (Figure 8).

The flow rate regularization shown in the fluviometric station located in P2 does not occur in the one located in P1, which reveals that there was a clear drop in the maximum and minimum flows rate over the three periods evaluated, except for some similar values that occur between the periods, notably in dry season. Comparing P2 to P1, the amplitude of maximum and minimum flows rate between rainy and drought periods in 2001-2019, shows how the dams can help to regulate water flow rate in watercourses and keep their availability even higher in drought periods.

In P2, despite the reduction in rainfall between 2001 and 2019, there was an average drop of 28% and 8% in maximum and minimum flows rate, respectively. In P1, the fall was 82% and 63%, respectively. This fact shows that without the construction of the dam, the situation in P2, regarding water availability in São Francisco river, could have been more serious in drought periods.

In 2001-2019 period, in addition to a small reduction in rainfall in P1 and a stable situation in P2, there was also an increase in average evapotranspiration in rainy season and a reduction in drought in both areas (Table 7). There was an increase in average surface runoff practically throughout the year, notably in greatest rainfall period, and average subsurface runoff decreased, mainly in rainy season in P1. The presence of moisture in plants' root zone also dropped in the period 2001-2019, in both areas. The average reduction of 5% of rainfall in P1 is one of the factors related to the reduction of water present in basin, but the increase in evapotranspiration and surface runoff, caused by changes in land cover, had a greater impact on water maintenance.

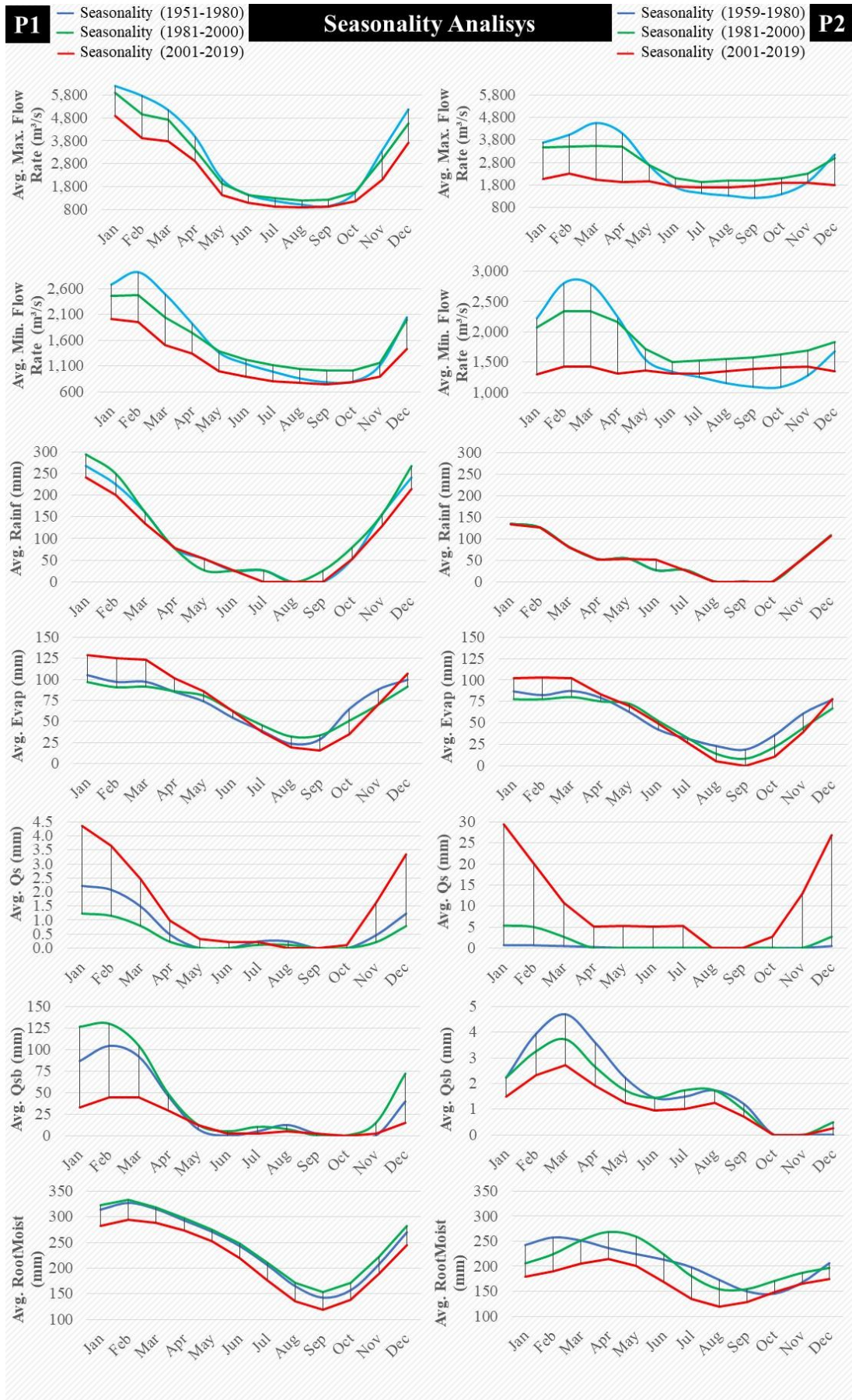


**Figure 6.8** – Seasonal analysis of variables related to water cycle in the SFB.

**Table 6.7** - Seasonal variation of water flow in SFB between 1951-1980 and 2001-2019.

Variable	Average Variation (P1)			
	Rainy Season		Dry Season	
	Absolute	Relative	Absolute	Relative
Rainf	-131 mm	-11%	-27 mm	-11%
Evap	+81 mm	+14%	-29 mm	-10%
Qs	+8.4 mm	+105%	+0.4 mm	+80%
Qsb	-201 mm	-55%	-2 mm	-7%
RootMoist	-152 mm	-9%	-146 mm	-12%
Variable	Average Variation (P2)			
	Rainy Season		Dry Season	
	Absolute	Relative	Absolute	Relative
Rainf	0 mm	0%	+26 mm	+16%
Evap	+33 mm	+7%	-47 mm	-19%
Qs	+102 mm	+3,792%	+24 mm	+2,380%
Qsb	-5 mm	-36%	-3 mm	-38%
RootMoist	-230 mm	-17%	-203 mm	-18%

The correlation (R) between the monthly data from January 1981 to December 2019 of NDVI with those of rain, evapotranspiration, root zone soil moisture of the plants, surface and subsurface runoff, shows, to a certain extent, the influence of vegetation maintaining humidity in basin.

Figure 9 shows how the NDVI has a higher correlation with rain, evapotranspiration and soil moisture in root zone. In other words, it shows how the seasonality of rainfall influences the seasonality of vegetation, with vegetation increasing its vigor in the rainy seasons and decreasing in the dry seasons, expect for some areas, probably influenced by local factors, such as relief, irrigation, among others.

The same occurs with soil moisture in root zone and with evapotranspiration, as in the rainy seasons it tends to have a greater water accumulation in the soil, increasing its humidity, and consequently a greater plant development, which also increases evapotranspiration processes. In the dry seasons, the lower occurrence of rain decreases inlet of water into basin, and with increase in energy fluxes (radiation and heat), it tends to increase potential evapotranspiration, removing more water from the system by this process.

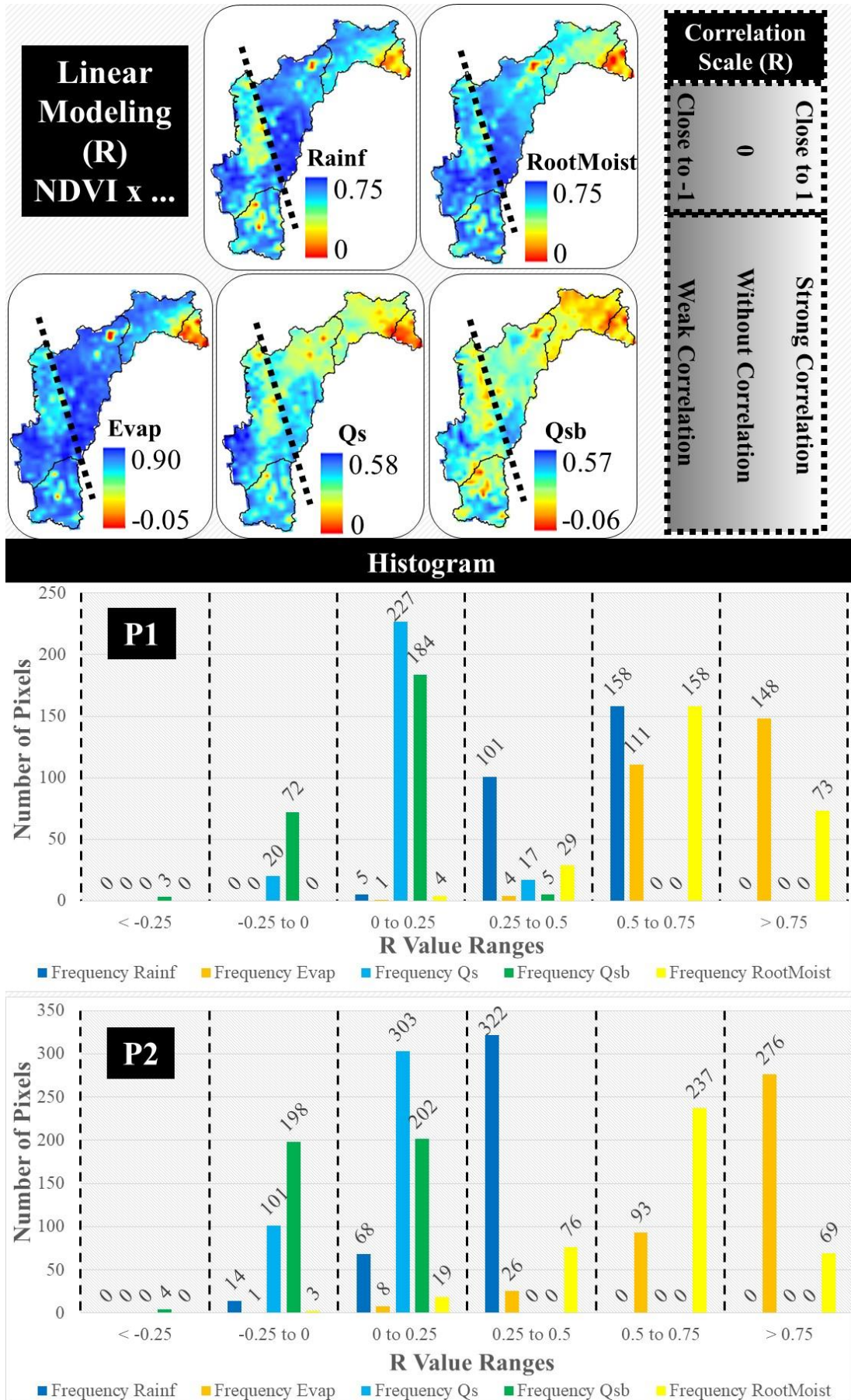


**Figure 6.9 – Correlations between NDVI and water cycle variables in SFB.**

Although NDVI shows the vigor and health status of vegetation with some success, there is some difficulty in defining its size, as there is no direct relationship between this and the values of this index, depending a lot on the type of vegetation evaluated, in which biome and climatic characteristics is located. For this reason, this index obtained lower correlations with surface and subsurface runoff, which will vary according to the occurrence of precipitation. It also depends on the relief and obstacles that favor or not water infiltration in soil and flow speed on the surface, with plant sizes as important factors in this case. Land covers (bare soil, arboreal and non-arboreal vegetation) were not used in this correlation because their information is of annual frequency, and it is not possible to assess the seasonality of the process, which is important in assessing the correlations, mainly due to the differences in the rainy and dry seasons.

Correlating average monthly flow rate of the fluviometric stations located in P1 and P2, with variables of rainfall, surface and subsurface runoff (Figure 10), it is clear their importance in the flow rate dynamics over time. However, notably, as subsurface runoff is vital for maintaining flow rate, especially in droughts. This shows how the recharge of groundwater is essential during rainy periods, and this process has been hampered by changes in land cover (Figure 11).

As seen earlier, Buishand and Pettitt tests show that the break in homogeneity for energy flows, water cycle and LULC variables, occurred in the late 1990s and early 2000s, similar, too, the result for these tests in the cases of flows rate in P1 and P2, which were between 2000 and 2002. Thus, concerning the pre and post-1990s periods, for the entire SFB, the average reduction in rainfall volume was 2%, from 958.9 to 940.5 mm per year, down 18.4 mm. While rainfall is stable, average evapotranspiration increased by 5% (+38.1 mm), surface runoff increased by 225% (+36 mm) and water infiltration in the soil decreased by 52% (-92.5 mm) (Figure 11).

This means that in the period before the 1990s, from 100% of the water volume that entered the basin (precipitation), 79% returned to the atmosphere through evapotranspiration. In the current period, after the 1990s, this ratio is 85%. The loss through surface runoff was 2% and became 6%. In other words, there was a reduction in the water infiltration into the soil, which corresponded to 19% of the water volume, which entered the basin due to rains. This ratio has now dropped to 9% (Figure 11).

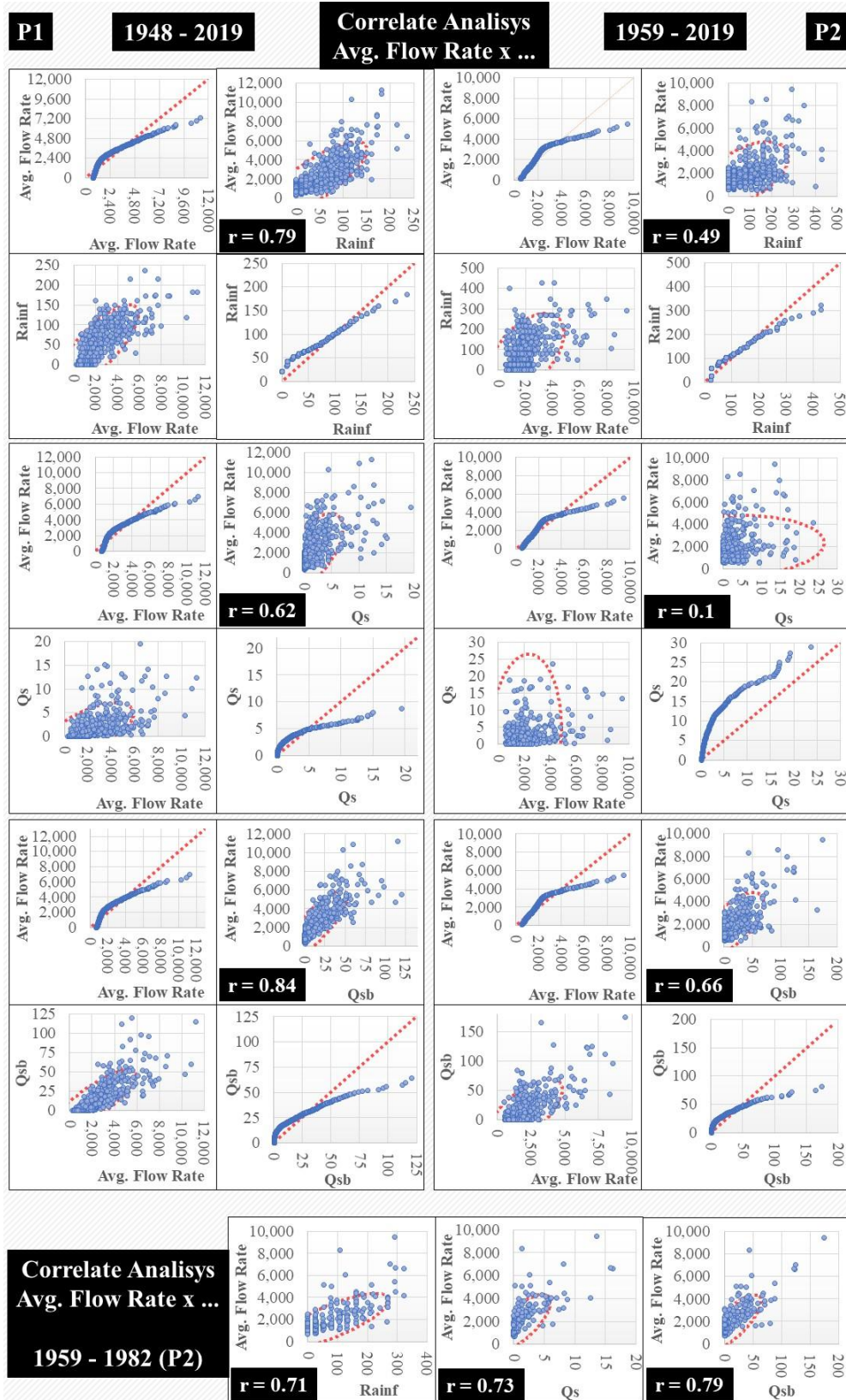


**Figure 6.10** – Correlations between average monthly flow rate with rainfall, surface and subsurface runoff data in SFB. Note: the construction of Sobradinho dam influenced the correlation values at the fluviometric station located in P2, due to flow rate regularization in São Francisco river, which significantly changed its behavior compared to other variables natural dynamics.

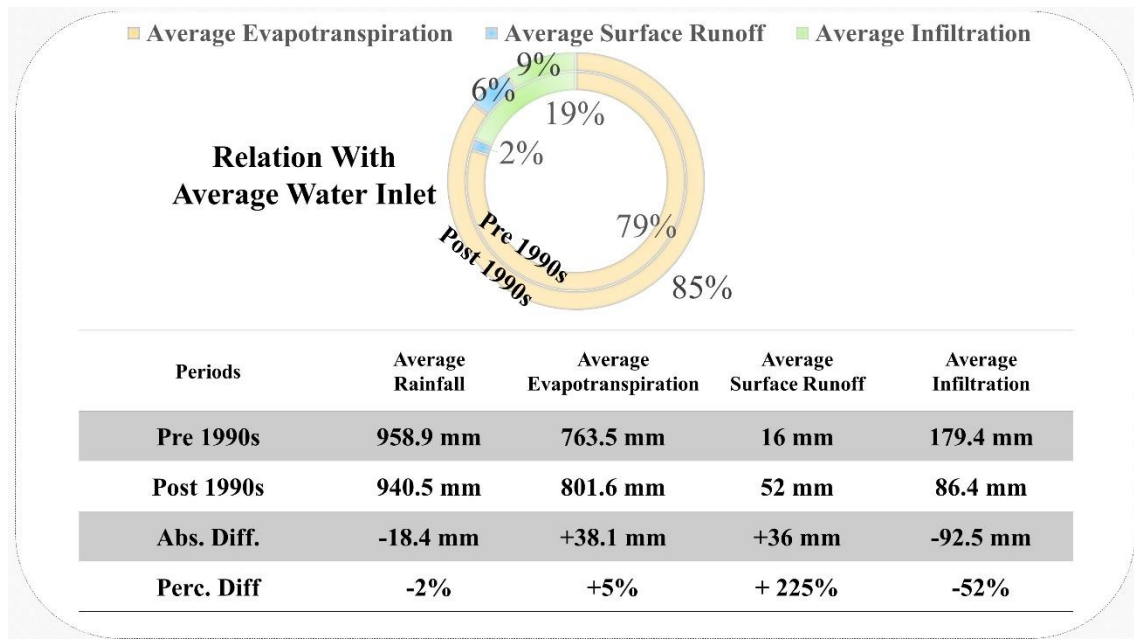


**Figure 6.11** – Simplified water balance for the pre and post-1990s periods at SFB.

In line with what was found in this research, other studies identified drops in the São Francisco river flow rate and in the groundwater volume present in the basin (de Jong et al., 2018; Gonçalves et al., 2020; Paredes-Trejo et al., 2021; Silva et al., 2021; Sun et al., 2016), caused by the decrease in rainfall over the last three decades (Cunha et al., 2019; de Jong et al., 2018; Gonçalves et al., 2020; Marengo et al., 2017, 2020) and intensified by changes in LULC (de Andrade et al., 2021; Pousa et al., 2019), especially for agropastoral activities and the intensive water withdrawal for irrigation, in addition to the increase in evaporative demand (de Andrade et al., 2021).

Such occurrences had consequences in the electric energy generation in the dams on the São Francisco river (Três Marias, Sobradinho, Itaparica, Moxotó, Paulo Afonso Complex and Xingó) to supply the Northeast region of Brazil, in which hydroelectricity generation has fallen from 50% before 2012 to 18% in 2017, being gradually replaced by thermal and wind generation, in addition to the import of energy from other regions by the integrated Brazilian grid (de Jong et al., 2018; Silva et al., 2021).

In addition to hydroelectric power generation impacts, there were consequences for the São Francisco' waters quality after the Xingó dam, the most downstream of this river. Flow rate reductions allowed greater intrusion of saline water from the Atlantic Ocean. Between 2008 and 2010 salinity levels, both at the

surface and at greater depths, were below 0.1‰, within the limit established by CONAMA Resolution 357 of 0.5‰ to consider water as fresh. After successive reductions in flow rates, between 2013 and 2017, salinity increased from 8 to 64 times, ranging from 1.4 ‰ for flow rates of 1105 m<sup>3</sup>/s in October 2014, and 15.4‰ for flow rates of 741 m<sup>3</sup>/s (Fonseca et al., 2020). The saline intrusion was observed 16 km from the mouth, which caused the replacement of agricultural activities for carcinoculture by the riverside population, in addition to a reduction in water quality, which reached turbidity levels 15.6 times higher than recommended by the World Health Organization (WHO) (Soares et al., 2020; Vital Filho et al., 2020).

Such consequences already evidenced on the São Francisco river, in view of climate alterations and LULC changes in its basin, cast doubt on the sustainability of this river since the climate predictions for the region in which it is located project an increase in temperature and reduction in rainfall, in addition to a tendency towards greater frequency of drought events, increasing the potential for evaporation from reservoirs and a drop in soil moisture (Marengo et al., 2017). All these factors favor the occurrence of aridification in the region, causing the replacement of Caatinga vegetation by others adapted to arid conditions (Marengo et al., 2020). However, there are other estimates that the decrease in rainfall volumes can be faster, in which in the SFB there is at least 35% chance of occurrence in the reduction of rainfall to values below 440 mm by the 2030s (de Jong et al., 2018).

In addition to climate change, changes in LULC are another factor of concern, with predictions of a 250% increase in water withdrawal by 2025 (Bezerra et al., 2019), especially for irrigation, which would account for 75% of this increase, with 282 m<sup>3</sup>/s already being removed in the basin to carry out activities in various sectors (77% for irrigation only) (ANA, 2019). The São Francisco transposition is one of the factors that increase the river pressure, since maximum, average and minimum pumped flows rate of 127 m<sup>3</sup>/s, 65 m<sup>3</sup>/s and 26.4 m<sup>3</sup>/s are expected to serve 399 municipalities in the Northeast Septentrional Brazilian (ENGEORPS/HARZA, 2000; Molinas, 2019).

Since the axes inauguration, the maximum transposed flow rate has been a maximum of 22.98 m<sup>3</sup>/s in the North and 14.05 m<sup>3</sup>/s in the East (PISF, 2021), and it is not possible to use the channels full capacity due to scarcity of water that occurred since 2012 and that affected the São Francisco river. The projections materialization of rainfall reduction together with the river overexploitation, can cause the total

dryness of its waters in its low course or have very low flows rate with a high level of salinity (de Jong et al., 2018). Similar situations already occur in several rivers on the planet, such as Colorado, which runs dry before reaching its mouth (Teclé, 2017; Waterman, 2014), and hydroelectric power generation is threatened by reductions in reservoir levels (Huckleberry and Potts, 2019). Other major rivers in the world have also suffered declines in their flows due to the overexploitation of their waters, concomitant with climate change, such as the Nile and the Yellow (Brown, 2011; Omer et al., 2020).

#### **6.4. Conclusions**

In this research, the following conclusions were reached:

- Between 1985 and 2018, the SFB lost 68,631 km<sup>2</sup> of native vegetation, equivalent to 10.8% of the basin area;
- These LULC changes that contributed to the increase in radiation and heat fluxes close to the ground, consequently increasing the potential evapotranspiration, in addition to the surface runoff increase, subsurface runoff reduction and decreases in humidity of the plants' root zone;
- The flow rate of São Francisco River has been impacted by such changes, since the water contribution of subsurface runoff has decreased in both P1 and P2, notably in the first, an area that represents 65% of the water entering SFB due to rain;
- The São Francisco River flow rate have been impacted mainly by the drop in the contribution of P1 in the maintenance of basin's water resources, notably by the reduction in subsurface runoff of the last two decades, caused by the greater loss of water in surface runoff and evapotranspiration;
- In summary, the very activities that depend on greater water maintenance in the basin are those that promote water loss through surface runoff and evapotranspiration, reducing flow rates of São Francisco River, by decreasing the recharge of aquifers and soil moisture.

#### **6.5. Acknowledgments, Samples, and Data**

This research was supported in part by a grant from the Coordenação de Aperfeiçoamento de Pessoal de Nível Superior (CAPES) – Finance Code 001,

belonging to the Education Ministry of Brazil. The entire database was obtained from secondary sources, on the websites indicated in subtopic 2.2, and duly referenced. The authors have no conflicts of interest to declare.

## 6.6. References

Ala-aho, P., Soulsby, C., Wang, H., Tetzlaff, D., 2017. Integrated surface-subsurface model to investigate the role of groundwater in headwater catchment runoff generation: A minimalist approach to parameterisation. *J. Hydrol.* 547, 664–677. <https://doi.org/10.1016/j.jhydrol.2017.02.023>

Alcoforado de Moraes, M.M.G., Biewald, A., Carneiro, A.C.G., Souza da Silva, G.N., Popp, A., Lotze-Campen, H., 2018. The impact of global change on economic values of water for Public Irrigation Schemes at the São Francisco River Basin in Brazil. *Reg. Environ. Chang.* 18, 1943–1955. <https://doi.org/10.1007/s10113-018-1291-0>

ANA, 2019. Manual de Usos Consuntivos da Água no Brasil, 1º. ed. Agência Nacional de Águas, Brasília, DF.

Barber, C., Lamontagne, J.R., Vogel, R.M., 2020. Improved estimators of correlation and  $R^2$  for skewed hydrologic data. *Hydrol. Sci. J.* 65, 87–101. <https://doi.org/10.1080/02626667.2019.1686639>

Barbosa, H.A., Lakshmi Kumar, T. V., 2016. Influence of rainfall variability on the vegetation dynamics over Northeastern Brazil. *J. Arid Environ.* <https://doi.org/10.1016/j.jaridenv.2015.08.015>

Barbosa, H.A., Lakshmi Kumar, T. V., Paredes, F., Elliott, S., Ayuga, J.G., 2019. Assessment of Caatinga response to drought using Meteosat-SEVIRI Normalized Difference Vegetation Index (2008–2016). *ISPRS J. Photogramm. Remote Sens.* 148, 235–252. <https://doi.org/10.1016/J.ISPRSJPRS.2018.12.014>

Beaudoin, H., Rodell, M., 2019. GLDAS Noah Land Surface Model L4 monthly 0.25 x 0.25 degree V2.0, Greenbelt, Maryland, USA, Goddard Earth Sciences Data and Information Services Center (GES DISC) [WWW Document]. NASA/GSFC/HSL. <https://doi.org/10.5067/9SQ1B3ZXP2C5>

Bezerra, B.G., Silva, L.L., Santos e Silva, C.M., de Carvalho, G.G., 2019.

Changes of precipitation extremes indices in São Francisco River Basin, Brazil from 1947 to 2012. *Theor. Appl. Climatol.* 135, 565–576. <https://doi.org/10.1007/s00704-018-2396-6>

Bickici Arıkan, B., Kahya, E., 2019. Homogeneity revisited: analysis of updated precipitation series in Turkey. *Theor. Appl. Climatol.* 135, 211–220. <https://doi.org/10.1007/s00704-018-2368-x>

Borges, C.K., dos Santos, C.A.C., Carneiro, R.G., da Silva, L.L., de Oliveira, G., Mariano, D., Silva, M.T., da Silva, B.B., Bezerra, B.G., Perez-Marin, A.M., de S. Medeiros, S., 2020. Seasonal variation of surface radiation and energy balances over two contrasting areas of the seasonally dry tropical forest (Caatinga) in the Brazilian semi-arid. *Environ. Monit. Assess.* 2020 1928 192, 1–18. <https://doi.org/10.1007/S10661-020-08484-Y>

Brown, L.R., 2011. When the Nile Runs Dry [WWW Document]. New York Times. URL [https://www.nytimes.com/2011/06/02/opinion/02Brown.html?\\_r=1&ref=contributors](https://www.nytimes.com/2011/06/02/opinion/02Brown.html?_r=1&ref=contributors) (accessed 8.23.21).

Buishand, T.A., 1982. Some methods for testing the homogeneity of rainfall records. *J. Hydrol.* 58, 11–27. [https://doi.org/10.1016/0022-1694\(82\)90066-X](https://doi.org/10.1016/0022-1694(82)90066-X)

CBHSF, 2016. Resumo Executivo do Plano de Recursos Hídricos da Bacia Hidrográfica do Rio São Francisco 2016-2025. Alagoas.

Correia, R.C., Araújo, J.L.P., Cavalcanti, E. de B., 2001. A fruticultura como vetor de desenvolvimento: o caso dos municípios de Petrolina (PE) e Juazeiro (BA). - Portal Embrapa, in: Correia, R.C. (Embrapa S.-C., Araujo, J.L.P. (Embrapa S.-C. (Eds.), CONGRESSO BRASILEIRO DE ECONOMIA E SOCIOLOGIA RURAL. SOBER/ESALQ/EMBRAPA/UFPE/URFPE, Recife, Brasil, p. 8.

Creech, C.T., Siqueira, R.B., Selegean, J.P., Miller, C., 2015. Anthropogenic impacts to the sediment budget of São Francisco River navigation channel using SWAT. *Int. J. Agric. Biol. Eng.* 8, 1–20. <https://doi.org/10.3965/j.ijabe.20150803.1372>

Cunha, A.P.M., Alvalá, R.C., Nobre, C.A., Carvalho, M.A., 2015. Monitoring vegetative drought dynamics in the Brazilian semiarid region. *Agric. For. Meteorol.* 214–215, 494–505. <https://doi.org/10.1016/j.agrformet.2015.09.010>

Cunha, A.P.M.A., Zeri, M., Leal, K.D., Costa, L., Cuartas, L.A., Marengo, J.A., Tomasella, J., Vieira, R.M., Barbosa, A.A., Cunningham, C., Cal Garcia, J.V., Broedel, E., Alvalá, R., Ribeiro-Neto, G., 2019. Extreme drought events over Brazil from 2011 to 2019. *Atmosphere (Basel)*. 10, 642.

<https://doi.org/10.3390/atmos10110642>

Das, P., Behera, M.D., Patidar, N., Sahoo, B., Tripathi, P., Behera, P.R., Srivastava, S.K., Roy, P.S., Thakur, P., Agrawal, S.P., Krishnamurthy, Y.V.N., 2018. Impact of LULC change on the runoff, base flow and evapotranspiration dynamics in eastern Indian river basins during 1985–2005 using variable infiltration capacity approach. *J. Earth Syst. Sci.* 127, 19. <https://doi.org/10.1007/s12040-018-0921-8>

de Andrade, B.C.C., de Andrade Pinto, E.J., Ruhoff, A., Senay, G.B., 2021. Remote sensing-based actual evapotranspiration assessment in a data-scarce area of Brazil: A case study of the Urucuia Aquifer System. *Int. J. Appl. Earth Obs. Geoinf.* 98, 102298. <https://doi.org/10.1016/J.JAG.2021.102298>

de Jong, P., Tanajura, C.A.S., Sánchez, A.S., Dargaville, R., Kiperstok, A., Torres, E.A., 2018. Hydroelectric production from Brazil's São Francisco River could cease due to climate change and inter-annual variability. *Sci. Total Environ.* 634, 1540–1553. <https://doi.org/10.1016/j.scitotenv.2018.03.256>

Didan, K., Barreto, A., 2016. NASA MEaSURES Vegetation Index and Phenology (VIP) Vegetation Indices Monthly Global 0.05Deg CMG [Data set] [WWW Document]. NASA EOSDIS L. Process. DAAC.

<https://doi.org/10.5067/MEaSURES/VIP/VIP30.004>

Donzé, F.-V., Truche, L., Namin, P.S., Lefeuvre, N., Bazarkina, E.F., 2020. Migration of Natural Hydrogen from Deep-Seated Sources in the São Francisco Basin, Brazil. *Geosci.* 2020, Vol. 10, Page 346 10, 346.

<https://doi.org/10.3390/GEOSCIENCES10090346>

Dugdale, S.J., Malcolm, I.A., Kantola, K., Hannah, D.M., 2018. Stream temperature under contrasting riparian forest cover: Understanding thermal dynamics and heat exchange processes. *Sci. Total Environ.* 610–611, 1375–1389.

<https://doi.org/10.1016/J.SCITOTENV.2017.08.198>

Eastman, J.R., 2016. *Terrset: Geospatial Monitoring and Modeling System Manual* [WWW Document]. Clark Univ. URL <https://clarklabs.org/wp->

content/uploads/2016/10/Terrset-Manual.pdf (accessed 9.10.20).

Ebling, É.D., Reichert, J.M., Zuluaga Peláez, J.J., Rodrigues, M.F., Valente, M.L., Lopes Cavalcante, R.B., Reggiani, P., Srinivasan, R., 2021. Event-based hydrology and sedimentation in paired watersheds under commercial eucalyptus and grasslands in the Brazilian Pampa biome. *Int. Soil Water Conserv. Res.* 9, 180–194. <https://doi.org/10.1016/J.ISWCR.2020.10.008>

ENGEORPS/HARZA, 2000. R32 - Relatório síntese de viabilidade técnico-econômica e ambiental. São Paulo.

Fonseca, S.L.M., Magalhães, A.A. de J., Campos, V.P., Medeiros, Y.D.P., 2020. Effect of the reduction of the outflow restriction discharge from the Xingó dam in water salinity in the lower stretch of the São Francisco River. *RBRH* 25. <https://doi.org/10.1590/2318-0331.252020180093>

Gonçalves, R.D., Stollberg, R., Weiss, H., Chang, H.K., 2020. Using GRACE to quantify the depletion of terrestrial water storage in Northeastern Brazil: The Urucuia Aquifer System. *Sci. Total Environ.* 705, 135845. <https://doi.org/10.1016/J.SCITOTENV.2019.135845>

Hansen, M., Song, X.P., 2018. Vegetation Continuous Fields (VCF) Yearly Global 0.05 Deg [Data set] [WWW Document]. NASA EOSDIS L. Process. DAAC. <https://doi.org/10.5067/MEaSURES/VCF/VCF5KYR.001>

Hirsch, R.M., Slack, J.R., 1984. A Nonparametric Trend Test for Seasonal Data With Serial Dependence. *Water Resour. Res.* 20, 727–732. <https://doi.org/10.1029/WR020i006p00727>

Hirsch, R.M., Slack, J.R., Smith, R.A., 1982. Techniques of trend analysis for monthly water quality data. *Water Resour. Res.* 18, 107–121. <https://doi.org/10.1029/WR018i001p00107>

Huckleberry, J.K., Potts, M.D., 2019. Constraints to implementing the food-energy-water nexus concept: Governance in the Lower Colorado River Basin. *Environ. Sci. Policy* 92, 289–298. <https://doi.org/10.1016/J.ENVSCI.2018.11.027>

Jiang, S., Wei, L., Ren, L., Xu, C.Y., Zhong, F., Wang, M., Zhang, L., Yuan, F., Liu, Y., 2021. Utility of integrated IMERG precipitation and GLEAM potential evapotranspiration products for drought monitoring over mainland China. *Atmos.*

Res. 247, 105141. <https://doi.org/10.1016/j.atmosres.2020.105141>

Kemp-Benedict, E., Cook, S., Allen, S.L., Vosti, S., Lemoalle, J., Giordano, M., Ward, J., Kaczan, D., 2011. Connections between poverty, water and agriculture: evidence from 10 river basins. <https://doi.org/10.1080/02508060.2011.541015> 36, 125–140. <https://doi.org/10.1080/02508060.2011.541015>

Kendall, M., 1975. *Multivariate analysis*. Charles Griffim & Company Ltd., London.

Koch, H., Biewald, A., Liersch, S., Azevedo, J.R.G. de, Silva, G.N.S. da, Kölling, K., Fischer, P., Koch, R., Hattermann, F.F., 2015. Scenarios of climate and land-use change, water demand and water availability for the São Francisco River basin. *Rev. Bras. Ciências Ambient.* 96–114. <https://doi.org/10.5327/z2176-947820151007>

Kwiatkowski, D., Phillips, P.C.B., Schmidt, P., Shin, Y., 1992. Testing the null hypothesis of stationarity against the alternative of a unit root. How sure are we that economic time series have a unit root? *J. Econom.* 54, 159–178. [https://doi.org/10.1016/0304-4076\(92\)90104-Y](https://doi.org/10.1016/0304-4076(92)90104-Y)

Lindsey, R., 2009. *Climate and Earth's Energy Budget*.

Mann, H.B., 1945. Nonparametric Tests Against Trend. *Econometrica* 13, 245. <https://doi.org/10.2307/1907187>

Marengo, J.A., Cunha, A.P.M.A., Nobre, C.A., Ribeiro Neto, G.G., Magalhaes, A.R., Torres, R.R., Sampaio, G., Alexandre, F., Alves, L.M., Cuartas, L.A., Deusdará, K.R.L., Álvala, R.C.S., 2020. Assessing drought in the drylands of northeast Brazil under regional warming exceeding 4 °C. *Nat. Hazards* 103, 2589–2611. <https://doi.org/10.1007/s11069-020-04097-3>

Marengo, J.A., Torres, R.R., Alves, L.M., 2017. Drought in Northeast Brazil—past, present, and future. *Theor. Appl. Climatol.* 129, 1189–1200. <https://doi.org/10.1007/s00704-016-1840-8>

Mokhtari, A., Noory, H., Vazifedoust, M., 2018. Performance of Different Surface Incoming Solar Radiation Models and Their Impacts on Reference Evapotranspiration. *Water Resour. Manag.* 32, 3053–3070. <https://doi.org/10.1007/s11269-018-1974-9>

Molinas, P.A., 2019. Gestão e operação do Projeto de Integração do Rio São Francisco com bacias hidrográficas do Nordeste Setentrional.

Omer, A., Elagib, N.A., Zhuguo, M., Saleem, F., Mohammed, A., 2020. Water scarcity in the Yellow River Basin under future climate change and human activities. *Sci. Total Environ.* 749, 141446. <https://doi.org/10.1016/J.SCITOTENV.2020.141446>

Paredes-Trejo, F., Barbosa, H.A., Giovannettone, J., Kumar, T.V.L., Thakur, M.K., Buriti, C. de O., Uzcátegui-Briceño, C., 2021. Drought Assessment in the São Francisco River Basin Using Satellite-Based and Ground-Based Indices. *Remote Sens.* 2021, Vol. 13, Page 3921 13, 3921. <https://doi.org/10.3390/RS13193921>

Patidar, N., Behera, M.D., 2018. How Significantly do Land Use and Land Cover (LULC) Changes Influence the Water Balance of a River Basin? A Study in Ganga River Basin, India. *Proc. Natl. Acad. Sci. India Sect. A Phys. Sci.* 2018 892 89, 353–365. <https://doi.org/10.1007/S40010-017-0426-X>

Pereira, S.B., Pruski, F.F., Da Silva, D.D., Ramos, M.M., 2007. Study of the hydrological behavior of São Francisco River and its main tributaries. *Rev. Bras. Eng. Agric. e Ambient.* 11, 615–622. <https://doi.org/10.1590/S1415-43662007000600010>

Pettitt, A.N., 1979. A Non-Parametric Approach to the Change-Point Problem. *Appl. Stat.* 28, 126. <https://doi.org/10.2307/2346729>

PISF, 2021. Tarifa de Adução de Água Bruta (R\$/m<sup>3</sup>) e Vazões [WWW Document]. Painel PISF. URL <https://www.gov.br/ana/pt-br/assuntos/seguranca-hidrica/pisf/paineis> (accessed 8.23.21).

Pousa, R., Costa, M.H., Pimenta, F.M., Fontes, V.C., Brito, V.F.A. de, Castro, M., 2019. Climate Change and Intense Irrigation Growth in Western Bahia, Brazil: The Urgent Need for Hydroclimatic Monitoring. *Water* 11, 933. <https://doi.org/10.3390/W11050933>

Pruski, F.F., Pereira, S.B., Novaes, L.F. de, Silva, D.D. da, Ramos, M.M., 2004. Specific yield discharge and mean precipitation in São Francisco Basin. *Rev. Bras. Eng. Agrícola e Ambient.* 8, 247–253. <https://doi.org/10.1590/s1415-43662004000200013>

Rodell, M., Houser, P.R., Jambor, U., Gottschalck, J., Mitchell, K., Meng, C.J., Arsenault, K., Cosgrove, B., Radakovich, J., Bosilovich, M., Entin, J.K., Walker, J.P.,

Lohmann, D., Toll, D., 2004. The Global Land Data Assimilation System. *Bull. Am. Meteorol. Soc.* 85, 381–394. <https://doi.org/10.1175/BAMS-85-3-381>

Rougé, C., Ge, Y., Cai, X., 2013. Detecting gradual and abrupt changes in hydrological records. *Adv. Water Resour.* 53, 33–44. <https://doi.org/10.1016/j.advwatres.2012.09.008>

Serinaldi, F., Kilsby, C.G., 2015. Stationarity is undead: Uncertainty dominates the distribution of extremes. *Adv. Water Resour.* 77, 17–36. <https://doi.org/10.1016/j.advwatres.2014.12.013>

Serinaldi, F., Kilsby, C.G., Lombardo, F., 2018. Untenable nonstationarity: An assessment of the fitness for purpose of trend tests in hydrology. *Adv. Water Resour.* 111, 132–155. <https://doi.org/10.1016/j.advwatres.2017.10.015>

Seyoum, W.M., Milewski, A.M., 2017. Improved methods for estimating local terrestrial water dynamics from GRACE in the Northern High Plains. *Adv. Water Resour.* 110, 279–290. <https://doi.org/10.1016/j.advwatres.2017.10.021>

Silva, M.V.M. da, Silveira, C. da S., Costa, J.M.F. da, Martins, E.S.P.R., Júnior, F. das C.V., 2021. Projection of Climate Change and Consumptive Demands Projections Impacts on Hydropower Generation in the São Francisco River Basin, Brazil. *Water* 2021, Vol. 13, Page 332 13, 332. <https://doi.org/10.3390/W13030332>

Soares, E.C., Silva, C.A., Cruz, M.A.S., Santos, E.L., Oliveira, T.R., Silva, T. de J., Rial, E.P., Silva, R.N., Silva, J.V., 2020. Expedition on the Lower São Francisco: An X-ray of fisheries and agriculture, pollution, silting and saline intrusion. *Brazilian J. Dev.* 6, 3047–3064. <https://doi.org/10.34117/BJDV6N1-221>

Souza, C.M., Z. Shimbo, J., Rosa, M.R., Parente, L.L., A. Alencar, A., Rudorff, B.F.T., Hasenack, H., Matsumoto, M., G. Ferreira, L., Souza-Filho, P.W.M., de Oliveira, S.W., Rocha, W.F., Fonseca, A. V., Marques, C.B., Diniz, C.G., Costa, D., Monteiro, D., Rosa, E.R., Vélez-Martin, E., Weber, E.J., Lenti, F.E.B., Paternost, F.F., Pareyn, F.G.C., Siqueira, J. V., Viera, J.L., Neto, L.C.F., Saraiva, M.M., Sales, M.H., Salgado, M.P.G., Vasconcelos, R., Galano, S., Mesquita, V. V., Azevedo, T., 2020. Reconstructing Three Decades of Land Use and Land Cover Changes in Brazilian Biomes with Landsat Archive and Earth Engine. *Remote Sens.* 12, 2735. <https://doi.org/10.3390/rs12172735>

Sun, T., Ferreira, V., He, X., Andam-Akorful, S., 2016. Water Availability of São Francisco River Basin Based on a Space-Borne Geodetic Sensor. *Water* 8, 213. <https://doi.org/10.3390/w8050213>

Teclé, A., 2017. Downstream Effects of Damming the Colorado River. *Int. J. Lakes Rivers* 10, 7–33.

Torres, M.D.O., Maneta, M., Howitt, R., Vosti, S.A., Wallender, W.W., Basso, L.H., Rodrigues, L.N., 2012. Economic impacts of regional water scarcity in the São Francisco river Basin, Brazil: An application of a linked hydro-economic model. *Environ. Dev. Econ.* 17, 227–248. <https://doi.org/10.1017/S1355770X11000362>

Umair, M., Kim, D., Choi, M., 2019. Impacts of land use/land cover on runoff and energy budgets in an East Asia ecosystem from remotely sensed data in a community land model. *Sci. Total Environ.* 684, 641–656. <https://doi.org/10.1016/j.scitotenv.2019.05.244>

Vital Filho, J.L., Santos, D.S., Martins, C.M.C., Silva, R.B., Martins, G.M.C., 2020. Salinization at the mouth of the São Francisco River: impacts on the Potengi community, Alagoas, Brazil. *Rev. AGRO@MBIENTE ON-LINE* 14. <https://doi.org/10.18227/1982-8470RAGRO.V14I0.6455>

Waterman, J., 2014. Where the Colorado Runs Dry [WWW Document]. *New York Times*. URL [https://www.nytimes.com/2012/02/15/opinion/where-the-colorado-river-runs-dry.html?\\_r=1&pagewanted=print](https://www.nytimes.com/2012/02/15/opinion/where-the-colorado-river-runs-dry.html?_r=1&pagewanted=print) (accessed 8.23.21).

Yan, G., Jiao, Z.H., Wang, T., Mu, X., 2020. Modeling surface longwave radiation over high-relief terrain. *Remote Sens. Environ.* 237, 111556. <https://doi.org/10.1016/j.rse.2019.111556>

Yang, F., Lu, H., Yang, K., He, J., Wang, W., Wright, J.S., Li, C., Han, M., Li, Y., 2017. Evaluation of multiple forcing data sets for precipitation and shortwave radiation over major land areas of China. *Hydrol. Earth Syst. Sci.* 21, 5805–5821. <https://doi.org/10.5194/hess-21-5805-2017>

Yin, L., Feng, X., Fu, B., Chen, Y., Wang, X., Tao, F., 2020. Irrigation water consumption of irrigated cropland and its dominant factor in China from 1982 to 2015. *Adv. Water Resour.* 143, 103661. <https://doi.org/10.1016/j.advwatres.2020.103661>

Yozgatligil, C., Yazici, C., 2016. Comparison of homogeneity tests for

temperature using a simulation study. *Int. J. Climatol.* 36, 62–81.  
<https://doi.org/10.1002/joc.4329>

Yuan, R.Q., Chang, L.L., Gupta, H., Niu, G.Y., 2019. Climatic forcing for recent significant terrestrial drying and wetting. *Adv. Water Resour.* 133, 103425.  
<https://doi.org/10.1016/j.advwatres.2019.103425>

Zeri, M., Alvalá, R.C.S., Carneiro, R., Cunha-Zeri, G., Costa, J.M., Spatafora, L.R., Urbano, D., Vall-Llossera, M., Marengo, J., 2018. Tools for Communicating Agricultural Drought over the Brazilian Semiarid Using the Soil Moisture Index. *Water* 2018, Vol. 10, Page 1421 10, 1421. <https://doi.org/10.3390/W10101421>

## 7. GENERAL CONCLUSIONS

In this research, it was found, in the first paper, that, in general, CHIRPS had the best performance in estimating rainfall volumes when compared to data from field stations used as a test for product evaluation. From the results obtained, there is evidence that the best performance is due to the incorporation of different data sources from field stations, estimates from infrared sensors from geostationary satellites and physiographic predictors. Information not fully present in other products. Thus, CHIRPS, for studies that use long-term monthly data, would be the best choice for information on rainfall volumes for the Brazilian semiarid region, although more studies are needed to assess other data and scales. All methods had the worst performance in the eastern range of the BSOL, an area that receives moisture from the Atlantic Ocean and has complex terrain, due to the set of mountains located in the topographical complex of the northeast coast of Brazil.

In the environmental context, evaluated in paper two, it was found that the São Francisco basin has undergone relevant changes in its land cover over the last four decades, with the deforestation of native vegetation replacing pasture and agricultural crops, and that these changes have significant relationships with the reduction of water infiltration into the soil and subsurface runoff, in addition to the increase in surface runoff and evapotranspiration. Altogether, rainfall volumes have been decreasing since the 1990s, accompanied by reductions in the São Francisco River flows. The fall has been more intense since the last decade, in a strong event of drought that hit the São Francisco basin and the Brazilian Semiarid Region

between 2012 and 2018. In this event, the long-term flows of the São Francisco River were the lowest in the whole historical record, impacting the generation of hydroelectric energy in plants located in the sub-middle and lower São Francisco hydrographic sub-regions, and enabling the intrusion of saline water from the Atlantic Ocean, reducing water quality kilometers inland from the continent in the São Francisco River gutter.

## 8. REFERENCES

ALVALÁ, R. C. D. S. et al. Drought monitoring in the Brazilian semiarid region. *Anais da Academia Brasileira de Ciências*, v. 91, p. 91, 16 out. 2019.

BARBOSA, H. A.; LAKSHMI KUMAR, T. V. Influence of rainfall variability on the vegetation dynamics over Northeastern Brazil *Journal of Arid Environments* Academic Press, , 1 jan. 2016.

BRITO, S. S. B. et al. Frequency, duration and severity of drought in the Semiarid Northeast Brazil region *International Journal of Climatology* John Wiley and Sons Ltd, , 1 fev. 2018. Disponível em: <[http://www.star.nesdis.noaa.gov/smcd/emb/vci/VH/vh\\_](http://www.star.nesdis.noaa.gov/smcd/emb/vci/VH/vh_)>. Acesso em: 23 jun. 2021.

CREECH, C. T. et al. Anthropogenic impacts to the sediment budget of São Francisco River navigation channel using SWAT. *International Journal of Agricultural and Biological Engineering*, v. 8, n. 3, p. 1–20, 3 abr. 2015.

DANTAS, J. C.; SILVA, R. M. DA; SANTOS, C. A. G. Drought impacts, social organization, and public policies in northeastern Brazil: a case study of the upper Paraíba River basin. *Environmental Monitoring and Assessment*, v. 192, n. 5, p. 1–21, 28 abr. 2020.

FREITAS, M. A. DE S. The Piencó-Piranhas-Açu Hydrographic Basin Face to the 2012-2020 Drought Event. *Brazilian Journal of Animal and Environmental Research*, v. 4, n. 1, p. 1033–1046, 22 fev. 2021.

LINDOSO, D. P. et al. Integrated assessment of smallholder farming's vulnerability to drought in the Brazilian Semi-arid: a case study in Ceará. *Climatic Change*, v. 127, n. 1, p. 93–105, 21 out. 2014.

LIRA AZEVÊDO, E. DE et al. How do people gain access to water resources in the Brazilian semiarid (Caatinga) in times of climate change? *Environmental Monitoring and Assessment*, v. 189, n. 8, p. 1–17, 1 ago. 2017.

MARENGO, J. A. et al. Assessing drought in the drylands of northeast Brazil under regional warming exceeding 4 °C. *Natural Hazards*, v. 103, n. 2, p. 2589–2611, 1 set. 2020.

MARENGO, J. A.; BERNASCONI, M. Regional differences in aridity/drought conditions over Northeast Brazil: present state and future projections. *Climatic Change*, v. 129, n. 1–2, p. 103–115, 1 mar. 2015.

MARENGO, J. A.; TORRES, R. R.; ALVES, L. M. Drought in Northeast Brazil—past, present, and future. *Theoretical and Applied Climatology*, v. 129, n. 3–4, p. 1189–1200, 1 ago. 2017.

ROSSATO, L. et al. Impact of soil moisture on crop yields over Brazilian semiarid. *Frontiers in Environmental Science*, v. 5, n. NOV, p. 73, 7 nov. 2017.

SILVA, M. V. M. DA et al. Projection of Climate Change and Consumptive Demands Projections Impacts on Hydropower Generation in the São Francisco River Basin, Brazil. *Water* 2021, Vol. 13, Page 332, v. 13, n. 3, p. 332, 29 jan. 2021.

TOMASELLA, J. et al. Desertification trends in the Northeast of Brazil over the period 2000–2016. *International Journal of Applied Earth Observation and Geoinformation*, v. 73, p. 197–206, 1 dez. 2018.